STATE OF CALIFORNIA • DEPARTMENT OF TRANSPORTATION
TECHNICAL REPORT DOCUMENTATION PAGE
TR0003 (REV 10/98)

1. REPORT NUMBER	2. GOVERNMENT ASSOCIATION NUMBER	3. RECIPIENT'S CATALOG NUMBER
CA13-2221A		

4. TITLE AND SUBTITLE
Warm-Mix Asphalt Study: Test Track Construction and First-Level Analysis of Phase 3a HVS and Laboratory Testing. (Mix Design #1)

5. REPORT DATE
June 2011

6. PERFORMING ORGANIZATION CODE

7. AUTHOR
David Jones, Rongzong Wu, Bor-Wen Tsai, and John T. Harvey

8. PERFORMING ORGANIZATION REPORT NO.
UCPRC-RR-2011-02

9. PERFORMING ORGANIZATION NAME AND ADDRESS
University of California Pavement Research Center
Civil and Environmental Engineering
University of California, Davis
One Shields Avenue
Davis, CA 95616

10. WORK UNIT NUMBER

11. CONTRACT OR GRANT NUMBER
65A0272

12. SPONSORING AGENCY AND ADDRESS
California Department of Transportation
Division of Research, Innovation and System Information, (MS-83)
P.O. Box 942873
Sacramento, CA 94273-0001

13. TYPE OF REPORT AND PERIOD COVERED
Research Report
April 2010 - June 2011

14. SPONSORING AGENCY CODE

15. SUPPLEMENTARY NOTES

16. ABSTRACT
This is one of two first-level reports describing the third phase of a warm-mix asphalt study that compares the performance of two rubberized asphalt control mixes with that of seven mixes produced with warm-mix technologies. The control mixes were produced and compacted at conventional hot-mix asphalt temperatures (>300 F [150°C]), while the warm-mixes were produced and compacted at temperatures between 36°F (20°C) and 60°F (35°C) lower than the controls. This report discusses the mixes produced at the Granite Bradshaw Plant and covers the Cecabase®, Evotherm DATTM and Gencor Ultrafoam GX® warm-mix technologies. The test track layout and design, mix design and production, and test track construction are discussed, as well as the results of Heavy Vehicle Simulator (HVS) and laboratory testing. Key findings from the study include:
- Adequate compaction can be achieved on rubberized warm-mixes at lower temperatures. Roller operators should, however, be aware of differences in roller response between warm-mix and conventional hot mixes, and that rolling operations and patterns may need to be adjusted to ensure that optimal compaction is achieved.
- Optimal compaction temperatures will differ among the different warm-mix technologies. However, a temperature reduction of at least 60°F (35°C) is possible for some technologies.
- Equal and potentially better rutting performance compared to hot mix can be achieved from warm-mix asphalt
provided that standard specified construction and performance limits for hot-mix asphalt are met.

17. KEY WORDS
Warm-mix asphalt, WMA, rubberized asphalt, accelerated pavement testing, Heavy Vehicle Simulator

18. DISTRIBUTION STATEMENT
No restrictions. This document is available to the public through the National Technical Information Service, Spingfield, Virginia, 22161

19. SECURITY CLASSIFICATION (of this report)
Unclassified

20. NUMBER OF PAGES
152

21. COST OF REPORT CHARGED

Reproduction of completed page authorized.

Contract: 65A0272
Task ID: 2221

- Laboratory test results indicate that use of the warm-mix technologies assessed in this study did not significantly influence performance when compared to control specimens. However, the mixes produced with chemical surfactant technologies did appear to be influenced in part by the lower mix production and construction temperatures, which would have resulted in less oxidation of the binder and consequent lower stiffness of the mix. Rutting performance under accelerated load testing did not appear to be affected, however, nor did fatigue performance or moisture sensitivity. The warm mix produced using water injection technology appeared to have lower moisture resistance compared to the other three mixes in all the laboratory moisture sensitivity tests, but still met Caltrans-specified performance requirements in most instances. This mix was produced at a higher temperature than the other two warm mixes and contained no moisture.

- Smoke and odors are significantly reduced on warm mixes compared to hot mixes, while workability is considerably better on warm mixes compared to hot mixes. The HVS and laboratory testing completed in this phase have provided no results to suggest that warm-mix technologies should not be used in rubberized asphalt in California.

Warm-Mix Asphalt Study: Test Track Construction and First-Level Analysis of Phase 3a HVS and Laboratory Testing (Rubberized Asphalt, Mix Design #1)

Authors:
D. Jones, R. Wu, B.-W. Tsai, and J.T. Harvey

DISCLAIMER STATEMENT

This document is disseminated in the interest of information exchange. The contents of this report reflect the views of the authors who are responsible for the facts and accuracy of the data presented herein. The contents do not necessarily reflect the official views or policies of the State of California or the Federal Highway Administration. This publication does not constitute a standard, specification or regulation. This report does not constitute an endorsement by the Department of any product described herein.

For individuals with sensory disabilities, this document is available in Braille, large print, audiocassette, or compact disk. To obtain a copy of this document in one of these alternate formats, please contact: the Division of Research and Innovation, MS-83, California Department of Transportation, P.O. Box 942873, Sacramento, CA 94273-0001.

PROJECT OBJECTIVES

The objective of this warm-mix asphalt study is to determine whether the use of additives to reduce the production and construction temperatures of hot-mix asphalt will influence the performance of the mix. This will be achieved through the following tasks:

1. Preparation of a workplan to guide the research;
2. Monitoring the construction of Heavy Vehicle Simulator (HVS) and in-service test sections;
3. Sampling of mix and mix components during asphalt concrete production and construction;
4. Trafficking of demarcated sections with the HVS in a series of tests to assess performance;
5. Conducting laboratory tests to identify comparable laboratory performance measures;
6. Monitoring the performance of in-service pilot test sections; and
7. Preparation of first- and second-level analysis reports and a summary report detailing the experiment and the findings.

This report covers Tasks 2, 3, 4, 5, and 7.

ACKNOWLEDGEMENTS

EXECUTIVE SUMMARY

The third phase of a comprehensive study into the use of warm-mix asphalt has been completed for the California Department of Transportation (Caltrans) by the University of California Pavement Research Center (UCPRC). This phase of the study, which investigated gap-graded rubberized asphalt concrete, was based on a workplan approved by Caltrans and included the design and construction of a test track, accelerated load testing using a Heavy Vehicle Simulator (HVS) to assess rutting behavior, and a series of laboratory tests on specimens sampled from the test track to assess rutting and fatigue cracking performance and moisture sensitivity. The objective of the study is to determine whether the use of technologies that reduce the production and construction temperatures of asphalt concrete influences performance of the mix. The study compared the performance of two rubberized asphalt control mixes, which were produced and constructed at conventional hot-mix asphalt temperatures (320°F [160°C]), with seven warm-mixes, produced and compacted at between 36°F (20°C) and 60°F (35°C) lower than the control. The mixes were produced at two different asphalt plants. The first part of the study, covered in this report, included mixes produced at Granite Construction's Bradshaw Plant using *Cecabase RT®, Evotherm DAT™*, and *Gencor Ultrafoam GX™* warm-mix technologies. The second part of the study, discussed in a separate report (UCPRC-RR-2011-03) included mixes produced at the George Reed Marysville Plant using *Astec Double Barrel Green®, Advera WMA®*, *Rediset™*, and *Sasobit®* technologies.

The test track is located at the University of California Pavement Research Center in Davis, California. The design and construction of the test track was a cooperative effort between Caltrans, the UCPRC, Granite Construction, George Reed Construction, Teichert Construction, and the seven warm-mix technology suppliers. The test track is 360 ft. by 50 ft. (110 m by 15 m) divided into nine test sections (two controls and seven warm-mixes). The pavement structure consists of the ripped and recompacted subgrade, 1.3 ft. (400 mm) of imported aggregate base, one 0.2 ft. (60 mm) lift of dense-graded hot-mix asphalt, and one 0.2 ft. (60 mm) lift of gap-graded rubberized hot-mix (RHMA-G) or warm-mix (RWMA-G) asphalt concrete. Each asphalt plant prepared a mix design. No adjustments were made to these mix designs to accommodate the warm-mix technologies. Target production temperatures were not set; instead the warm-mix technology suppliers set their own temperatures based on experience, ambient temperatures, and haul distance.

The production temperature for the Granite Bradshaw RHMA-G control mix was 320°F (160°C) and 266°F (130°C), 248°F (125°C), and 284°F (140°C) for the Cecabase, Evotherm, and Gencor warm-mixes, respectively.

The rubberized asphalt sections were placed in April 2010. Specimens were removed from the test track for laboratory testing approximately six weeks after construction.

Heavy Vehicle Simulator (HVS) testing commenced in June 2010 after a six-week curing period and was completed in December 2010. This testing compared early rutting performance at elevated temperatures (pavement temperature of 122°F at 2.0 in. [50°C at 50 mm]), starting with a 9,000 lb (40 kN) load on a standard dual-wheel configuration and a unidirectional trafficking mode. Laboratory testing also commenced in June 2010 and was completed in July 2011. The test program included shear testing, wet and dry fatigue testing, Hamburg Wheel-Track testing, and determination of the wet-to-dry tensile strength ratio.

Key findings from the study include:

- A consistent subgrade was prepared and consistent base-course and underlying dense-graded hot-mix asphalt concrete layers were constructed on the test track using materials sourced from a nearby quarry and asphalt plant. Thickness and compaction of the base and bottom layer of asphalt were consistent across the test track.
- Minimal asphalt plant modifications were required to accommodate the warm-mix technologies and the delivery systems were approved under the Caltrans Material Plant Quality Program.
- No problems were noted with producing the asphalt mixes at the lower temperatures. Target mix production temperatures (320°F, 284°F, 248°F, and 266°F [160°C, 125°C, 140°C, and 130°C] for the Control, Gencor, Evotherm, and Cecabase mixes, respectively), set by the warm-mix technology providers, were all achieved. There was very little variation in mix properties between the four mixes. Hveem stabilities, determined at three different curing regimes, exceeded the minimum requirement by a considerable margin. Curing did not appear to influence the stability. No moisture was measured in the mixes after production.
- Compaction temperatures differed considerably between the mixes and were consistent with production temperatures. The Evotherm and Cecabase mixes, produced at 248°F and 266°F (140°C and 130°C), respectively, lost heat during transport and placement at a slower rate that the Control and Gencor mixes, which were produced at higher temperatures. The lower temperatures in the three warm-mixes did not appear to influence the paving or compaction operations and interviews with the paving crew after construction revealed that no problems were experienced at the lower temperatures. Improved working conditions were identified as an advantage.
- Smoke and odors were significantly more severe on the Control section compared to the Gencor section. No smoke or odors were noted on the Evotherm and Cecabase sections.
- Mix workability, determined through observation of and interviews with the paving crew, was considerably better on the warm-mix sections compared to the Control.
- Average thicknesses of the top (rubberized) and bottom asphalt layers across the four sections were 0.22 ft. (66 mm) and 0.23 ft. (74 mm), respectively. The average thickness of the combined two layers was 0.45 ft. (137 mm), 0.05 ft. (17 mm) thicker than the design thickness of 0.4 ft. (120 mm). General consistency of thickness across the track was considered satisfactory and representative of typical construction projects.

- Nuclear gauge–determined density measurements were inconsistent with core determined air-void contents. The core determined air-void contents indicated that slightly higher density was achieved on the Control section (95 percent of the RICE specific gravity) compared to the warm-mix sections (94 percent). Compaction across the test track appeared to be consistent, confirming that adequate compaction can be achieved on rubberized warm-mixes at lower temperatures. Based on observations from the test track construction and interviews with roller operators, optimal compaction temperatures and rolling patterns will differ between the different warm-mix technologies, but it was shown that adequate compaction can be achieved on warm-mixes at the lower temperatures. Roller operators will, however, need to consider that there might be differences in roller response between warm-mix and conventional hot mixes, and that rolling operations and patterns may need to be adjusted to ensure that optimal compaction is always achieved.
- HVS trafficking on each of the four sections revealed that the duration of the embedment phases on all sections were similar; however, the depth of the ruts at the end of the embedment phases differed slightly between sections, with the Gencor (0.26 in. [6.5 mm]) and Cecabase (0.22 in. [5.5 mm]) having less embedment than the Control and Evotherm sections, which had similar embedment (0.31 in. [7.9 mm]). This is opposite to the early rutting performance in the Phase 1 study.
- Rut rate (rutting per load repetition) after the embedment phase on the Control and Evotherm sections was almost identical. On the Gencor and Cecabase sections, rut rate was considerably slower than the Control after the embedment phase. The difference in performance between the three warm-mix sections is attributed in part to the lower production and paving temperatures of the Evotherm mix compared to the other warm mixes, as well as to the thickness of the asphalt layers (the Evotherm section had thinner asphalt layers than the Control and Cecabase sections).
- The laboratory test results indicate that use of the warm-mix technologies assessed in this study, which were produced and compacted at lower temperatures, did not significantly influence the performance of the asphalt concrete when compared to control specimens produced and compacted at conventional hot-mix asphalt temperatures. Specific observations include:
  + Shear performance of the Evotherm and Cecabase mixes did appear to be influenced in part by the lower mix production and construction temperatures, which would have resulted in less oxidation of the binder and consequent lower stiffness of the mix. Rutting performance under accelerated load testing did not appear to be affected, however. Fatigue performance and moisture sensitivity also did not appear to be affected.
  + The Gencor (water injection technology) mix appeared to have lower moisture resistance compared to the other three mixes in all the moisture sensitivity tests, but still met Caltrans-specified performance requirements in most instances. This mix was produced at a higher temperature than the other two warm-mixes and contained no moisture.
  + Laboratory test results were influenced by mix production temperatures, actual binder content, specimen air-void content, actual stress and strain levels, and actual test temperature. These parameters need to be taken into consideration when comparing performance between the different mixes.

The HVS and laboratory testing completed in this phase have provided no results to suggest that warm-mix technologies should not be used in gap-graded rubberized mixes in California, provided that standard specified construction and performance limits for hot-mix asphalt are met. Significant reductions in smoke and odors and improved workability of the warm mixes also support wider use of these

technologies. Consideration should be given to further study into the effects of warm-mix asphalt technologies and production and placement of warm-mixes at lower temperatures on binder oxidation/aging rates. The effects that these may have on performance over the life of the asphalt surfacing should also be investigated. Research in this study has shown differences in early rutting performance between conventional and rubber mixes, between mixes tested after different curing periods, and between pavements subjected to mostly shade and mostly sun, respectively.

TABLE OF CONTENTS

LIST OF TABLES

LIST OF FIGURES

LIST OF ABBREVIATIONS

AASHTO	American Association of State Highway and Transportation Officials
ASTM	American Society for Testing and Materials
Caltrans	California Department of Transportation
DCP	Dynamic cone penetrometer
DGAC	Dense-graded asphalt concrete
ESAL	Equivalent standard axle load
FHWA	Federal Highway Administration
FWD	Falling weight deflectometer
HMA	Hot-mix asphalt
HVS	Heavy Vehicle Simulator
HWTT	Hamburg Wheel-Track Test
MDD	Multi-depth deflectometer
MPD	Mean profile depth
PPRC	Partnered Pavement Research Center
RHMA-G	Gap-graded rubberized hot-mix asphalt
RWMA-G	Gap-graded rubberized warm-mix asphalt
SPE	Strategic Plan Element
TSR	Tensile strength retained
UCPRC	University of California Pavement Research Center
WMA	Warm-mix asphalt

CONVERSION FACTORS

SI* (MODERN METRIC) CONVERSION FACTORS				
APPROXIMATE CONVERSIONS TO SI UNITS				
Symbol	**When You Know**	**Multiply By**	**To Find**	**Symbol**
LENGTH				
in	inches	25.4	Millimeters	mm
ft	feet	0.305	Meters	m
yd	yards	0.914	Meters	m
mi	miles	1.61	Kilometers	Km
AREA				
in^2	square inches	645.2	Square millimeters	mm^2
ft^2	square feet	0.093	Square meters	m^2
yd^2	square yard	0.836	Square meters	m^2
ac	acres	0.405	Hectares	ha
mi^2	square miles	2.59	Square kilometers	km^2
VOLUME				
fl oz	fluid ounces	29.57	Milliliters	mL
gal	gallons	3.785	Liters	L
ft^3	cubic feet	0.028	cubic meters	m^3
yd^3	cubic yards	0.765	cubic meters	m^3
NOTE: volumes greater than 1000 L shall be shown in m^3				
MASS				
oz	ounces	28.35	Grams	g
lb	pounds	0.454	Kilograms	kg
T	short tons (2000 lb)	0.907	megagrams (or "metric ton")	Mg (or "t")
TEMPERATURE (exact degrees)				
°F	Fahrenheit	5 (F-32)/9 or (F-32)/1.8	Celsius	°C
ILLUMINATION				
fc	foot-candles	10.76	Lux	lx
fl	foot-Lamberts	3.426	candela/m^2	cd/m^2
FORCE and PRESSURE or STRESS				
lbf	poundforce	4.45	Newtons	N
lbf/in^2	poundforce per square inch	6.89	Kilopascals	kPa
APPROXIMATE CONVERSIONS FROM SI UNITS				
Symbol	**When You Know**	**Multiply By**	**To Find**	**Symbol**
LENGTH				
mm	millimeters	0.039	Inches	in
m	meters	3.28	Feet	ft
m	meters	1.09	Yards	yd
km	kilometers	0.621	Miles	mi
AREA				
mm^2	square millimeters	0.0016	square inches	in^2
m^2	square meters	10.764	square feet	ft^2
m^2	square meters	1.195	square yards	yd^2
ha	Hectares	2.47	Acres	ac
km^2	square kilometers	0.386	square miles	mi^2
VOLUME				
mL	Milliliters	0.034	fluid ounces	fl oz
L	liters	0.264	Gallons	gal
m^3	cubic meters	35.314	cubic feet	ft^3
m^3	cubic meters	1.307	cubic yards	yd^3
MASS				
g	grams	0.035	Ounces	oz
kg	kilograms	2.202	Pounds	lb
Mg (or "t")	megagrams (or "metric ton")	1.103	short tons (2000 lb)	T
TEMPERATURE (exact degrees)				
°C	Celsius	1.8C+32	Fahrenheit	°F
ILLUMINATION				
lx	lux	0.0929	foot-candles	fc
cd/m^2	candela/m^2	0.2919	foot-Lamberts	fl
FORCE and PRESSURE or STRESS				
N	newtons	0.225	Poundforce	lbf
kPa	kilopascals	0.145	poundforce per square inch	lbf/in^2

*SI is the symbol for the International System of Units. Appropriate rounding should be made to comply with Section 4 of ASTM E380 (Revised March 2003)

1. INTRODUCTION

1.1 Background

Warm-mix asphalt is a relatively new technology. It has been developed in response to needs for reduced energy consumption and stack emissions during the production of asphalt concrete, long hauls, lower placement temperatures, improved workability, and better working conditions for plant and paving crews. Studies in the United States and Europe indicate that significant reductions in production and placement temperatures are possible.

Research initiatives on warm-mix asphalt are currently being conducted in a number of states, as well as by the Federal Highway Administration and the National Center for Asphalt Technology (NCAT). Accelerated pavement testing experiments are being carried out at NCAT.

The California Department of Transportation (Caltrans) has expressed interest in warm-mix asphalt with a view to reducing stack emissions at plants, to allow longer haul distances between asphalt plants and construction projects, to improve construction quality (especially during nighttime closures), and to extend the annual period for paving. However, the use of warm-mix asphalt technologies requires incorporating an additive into the mix, and/or changes in production and construction procedures, specifically related to temperature, which could influence the short- and long-term performance of the pavement. Consequently, the need for research was identified by Caltrans to address a range of concerns related to these changes before statewide implementation of the technology is approved.

1.2 Project Objectives

The research presented in this report is part of Partnered Pavement Research Center Strategic Plan Element 4.18 (PPRC SPE 4.18), titled "Warm-Mix Asphalt Study," undertaken for Caltrans by the University of California Pavement Research Center (UCPRC). The objective of this multi-phase project is to determine whether the use of additives intended to reduce the production and construction temperatures of asphalt concrete influence mix production processes, construction procedures, and the short-, medium-, and/or long-term performance of hot-mix asphalt. The potential benefits of using the additives will also be quantified. This is to be achieved through the following tasks:

- Develop a detailed workplan *(1)* for Heavy Vehicle Simulator (HVS) and laboratory testing *(Completed in September 2007)*.
- Construct test tracks (subgrade preparation, aggregate base-course, tack coat, and asphalt wearing course) at the Graniterock A.R. Wilson quarry near Aromas, California *(completed in September*

2007 for the Phase 1 and Phase 2 studies), and at the UCPRC facility in Davis, California *(completed in April 2010 for the Phase 3 study)*.

- Undertake HVS testing in separate phases, with later phases dependent on the outcome of earlier phases and laboratory tests *(Phase 1 [rutting on HMA/WMA] was completed in April 2008, Phase 2 [moisture sensitivity on HMA/WMA] was completed in July 2009, and Phase 3 [rutting on RHMA-G/RWMA-G] was completed in July 2011)*.
- Carry out a series of laboratory tests to assess rutting and fatigue behavior *(Phase 1 [plant-mixed, field-compacted] completed in August 2008, Phase 2a [plant-mixed, laboratory-compacted] completed in August 2009, Phase 2b [laboratory-mixed, laboratory-compacted] was completed in June 2010, and Phase 3 [plant-mixed, field-compacted] was completed in June 2011)*.
- Prepare a series of reports describing the research.
- Prepare recommendations for implementation.

Selected pilot studies with warm-mix technologies on in-service pavements will also be monitored as part of the study.

1.3   Overall Project Organization

This UCPRC project has been planned as a comprehensive study to be carried out in a series of phases, with later phases dependent on the results of the initial phase. The planned testing phases include *(1)*:

- Phase 1 compared early rutting potential at elevated temperatures (pavement temperature of 122°F at 2.0 in. [50°C at 50 mm]). HVS trafficking began approximately 45 days after construction. Cores and beams sawn from the sections immediately after construction were subjected to rutting, fatigue, cracking, and moisture sensitivity testing in the laboratory. The workplan dictated that moisture sensitivity, additional rutting, and fatigue testing with the HVS would be considered if the warm-mix asphalt concrete mixes performed differently than the conventional mixes. The results from this phase are discussed in a report entitled *Warm-Mix Asphalt Study: Test Track Construction and First-Level Analysis of Phase 1 HVS and Laboratory Testing (2)*.
- Depending on the outcome of laboratory testing for moisture sensitivity, a testing phase, if deemed necessary, would assess general performance under dry and wet conditions with special emphasis on moisture sensitivity. Phase 1 laboratory testing indicated a potential for moisture damage, prompting initiation of a second phase. Phase 2 compared rutting potential at elevated temperatures (pavement temperature of 122°F at 2.0 in. [50°C at 50 mm] pavement depth) and under wet conditions. HVS trafficking started approximately 90 days after completion of the Phase 1 HVS testing (12 months after construction). The results from Phase 2 are discussed in two reports entitled *Warm-Mix Asphalt Study: First-Level Analysis of Phase 2 HVS and Laboratory Testing, and Phase 1 and Phase 2 Forensic Assessments (3)* and *Warm-Mix Asphalt Study: First-Level Analysis of Phase 2b Laboratory Testing on Laboratory Prepared Specimens (4)*.
- Depending on the outcome of laboratory testing for rutting, a testing phase, if deemed necessary, would assess rutting performance on artificially aged test sections at elevated temperatures (122°F at 2.0 in. [50°C at 50 mm]). The actual process used to artificially age the sections was not finalized, but it would probably follow a protocol developed by the Florida Department of

Transport Accelerated Pavement Testing program, which uses a combination of infrared and ultraviolet radiation. Phase 1 laboratory testing results and Phase 2 HVS testing results provided no indication of increased rutting on aged sections and consequently this phase was not undertaken.

- Depending on the outcome of the laboratory study for fatigue, a testing phase, if deemed necessary, would assess fatigue performance at low temperatures (59°F at 2.0 in. [15°C at 50 mm]). Phase 1 laboratory testing did not indicate that the warm-mix asphalt technologies tested would influence fatigue performance and consequently this phase was not undertaken.

- Depending on the outcome of the above testing phases and if agreed upon by the stakeholders (Caltrans, warm-mix technology suppliers), the sequence listed above or a subset of the sequence would be repeated for gap-graded rubberized asphalt concrete (RHMA-G), and again for open-graded mixes. The testing of gap-graded rubberized mixes was undertaken in two subphases and is discussed in this report and in a companion report entitled *Warm-Mix Asphalt Study: Test Track Construction and First-Level Analysis of Phase 3b HVS and Laboratory Testing (Rubberized Asphalt, Mix Design #2) (5)*.

- Periodic assessment of the performance of gap-graded mixes in full-scale field experiments. This work is discussed in a separate report on that study entitled *Warm-Mix Asphalt Study: Field Test Performance Evaluation (6)*.

This test plan is designed to evaluate short-, medium-, and long-term performance of the mixes.

- Short-term performance is defined as failure by rutting of the asphalt-bound materials.
- Medium-term performance is defined as failure caused by moisture and/or construction-related issues.
- Long-term performance is defined as failure from fatigue cracking, reflective cracking, and/or rutting of the asphalt-bound and/or unbound pavement layers.

The following questions, raised by Caltrans staff in a pre-study meeting, will be answered during the various phases of the study *(1)*:

- What is the approximate comparative energy usage between HMA and WMA during mix preparation? This will be determined from asphalt plant records/observations in pilot studies where sufficient tonnages of HMA and WMA are produced to undertake an assessment.
- Can satisfactory compaction be achieved at lower temperatures? This will be established from construction monitoring and subsequent laboratory tests.
- What is the optimal temperature range for achieving compaction requirements? This will be established from construction monitoring and subsequent laboratory tests.
- What are the cost implications? These will be determined with basic cost analyses from pilot studies where sufficient tonnages of HMA and WMA are produced to undertake an assessment.
- Does the use of warm-mix asphalt technologies influence the rutting performance of the mix? This will be determined from all HVS and laboratory tests.
- Is the treated mix more susceptible to moisture sensitivity given that the aggregate is heated to lower temperatures? This will be determined from Phase 1 laboratory tests and Phase 2 HVS testing.

- Does the use of warm-mix asphalt technologies influence fatigue performance? This will be determined from Phase 1 and Phase 2 laboratory tests and potential additional laboratory and HVS testing.
- Does the use of warm-mix asphalt technologies influence the performance of the mix in any other way? This will be determined from HVS and laboratory tests, and from field observations (all phases).
- If the experiment is extended to rubberized gap-graded and standard, rubberized, and polymer-modified open-graded mixes, are the impacts of using the warm-mix technologies in these mixes the same as for conventional dense-graded mixes?

1.3.1 Project Deliverables

Deliverables from the study will include:

- A detailed workplan for the entire study *(1)*;
- A report detailing construction, first-level data analysis of the Phase 1 HVS testing, first-level data analysis of the Phase 1 laboratory testing, and preliminary recommendations *(2)*;
- A report detailing first-level data analysis of the Phase 2 HVS testing, first-level data analysis of the Phase 2a laboratory testing, Phase 1 and Phase 2 forensic investigations, and preliminary recommendations *(3)*;
- A report detailing first-level analysis of the Phase 2b laboratory testing on laboratory-mixed, laboratory-compacted specimens *(4)*;
- A report detailing first-level data analysis of the Phase 3a (mixes produced at Granite Construction's Bradshaw plant) HVS testing, first-level data analysis of the Phase 3a laboratory testing, Phase 3a forensic investigation, and preliminary recommendations (this report);
- A report detailing first-level data analysis of the Phase 3b (mixes produced at George Reed's Marysville plant) HVS testing, first-level data analysis of the Phase 3b laboratory testing, Phase 3b forensic investigation, and preliminary recommendations *(5)*;
- A report summarizing periodic observations from test sections on in-service pavements *(6)*; and
- A summary report for the entire study.

A series of conference and journal papers documenting various components of the study will also be prepared.

1.4 Structure and Content of this Report

1.4.1 Warm-Mix Technologies Tested

In the Phase 1 and Phase 2 studies, the three most prominent warm mix technologies (*Advera WMA*®, *Evotherm DAT*™, and *Sasobit*®) were assessed. During that testing phase numerous other technologies were developed and consequently additional technologies, specifically those based on water injection (or mechanical foam), were considered for the Phase 3 study. The technologies assessed were selected based on participation of warm-mix technology providers in the Caltrans Warm-mix Asphalt Technical Working Group. Given that two different water injection technologies would be tested and that these technologies are asphalt plant-specific (i.e., they are integral components of the asphalt plant), the Phase 3 study tested

mixes from two different asphalt plants. Since two different aggregate sources and consequently two different mix designs were used, testing and reporting has been undertaken in two subphases to limit inappropriate performance comparisons, as follows:

- Phase 3a: Mix Design #1 using mixes produced at the Granite Construction Bradshaw Plant (this report)
  + Hot-mix control
  + *Gencor Ultrafoam GX^{TM}*, water injection technology, referred to as Gencor in this report
  + *Evotherm DAT^{TM}*, chemical surfactant technology, referred to as Evotherm in this report
  + *Cecabase RT$^{®}$*, chemical surfactant technology, referred to as Cecabase in this report
- Phase 3b: Mix Design #2 using mixes produced at the George Reed Construction Marysville Plant (companion report *[5]*)
  + Hot-mix control
  + *Astec Double Barrel Green$^{®}$*, water injection technology, referred to as Astec in this report
  + *Sasobit$^{®}$*, organic wax technology, referred to as Sasobit in this report
  + *Advera WMA$^{®}$*, chemical water foaming technology, referred to as Advera in this report
  + *Rediset^{TM}*, chemical surfactant technology, referred to as Rediset in this report.

1.4.2   Report Layout

This report presents an overview of the work carried out in Phase 3a to continue meeting the objectives of the study, and is organized as follows:

- Chapter 2 summarizes the HVS test track location, design, and construction.
- Chapter 3 details the HVS test section layout and HVS test criteria.
- Chapter 4 provides a summary of the Phase 3a HVS test data collected from each test.
- Chapter 5 details the forensic investigations undertaken on each HVS test section after testing.
- Chapter 6 discusses the Phase 3a laboratory testing on specimens sampled from the test track.
- Chapter 7 provides conclusions and preliminary recommendations.

1.5   Measurement Units

Although Caltrans has recently returned to the use of U.S. standard measurement units, metric units have always been used by the UCPRC in the design and layout of HVS test tracks, and for laboratory and field measurements and data storage. In this report, both English and metric units (provided in parentheses after the English units) are provided in general discussion. In keeping with convention, only metric units are used in HVS and laboratory data analyses and reporting. A conversion table is provided on page xix of this report.

1.6   Terminology

The term "asphalt concrete" is used in this report as a general descriptor for the surfacing on the test track. The terms "hot-mix asphalt (HMA)" and "warm-mix asphalt (WMA)" are used as descriptors to differentiate between the control and warm-mixes discussed in this study.

2. TEST TRACK LOCATION, DESIGN, AND CONSTRUCTION

2.1 Experiment Location

The Phase 3 warm-mix asphalt experiment is located on the North Test Track at the University of California Pavement Research Center facility in Davis, California. An aerial view of the site is shown in Figure 2.1. This was the first test undertaken on this test track.

Figure 2.1: Aerial view of the UCPRC research facility.

2.2 Test Track Layout

The North Test Track is 361 ft. (110 m) long and 49.2 ft (15 m) wide. It has a two percent crossfall in a north-south direction. For the study, the track was divided into nine equal cells, 120.4 ft. (36.7 m) long and 16.4 ft. (5.0 m) wide. Its lay out is shown in Figure 2.2, with Cells 1 through 4 used in the Phase 3a study (Control, Gencor, Evotherm, and Cecabase, respectively) and Cells 5 through 9 (Sasobit, Advera, Control, Astec, and Rediset, respectively) used in the Phase 3b study *(5)*. All test track measurements and locations discussed in this report are based on this layout.
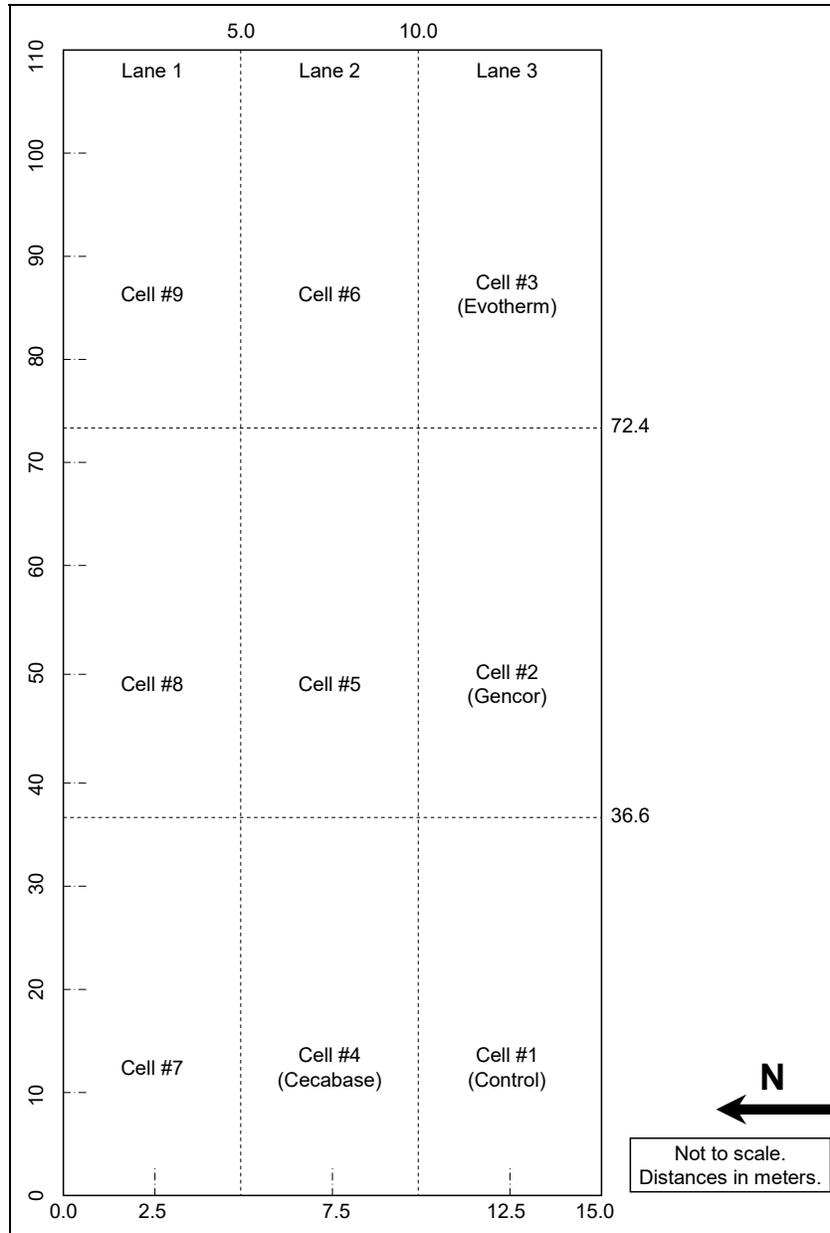
Figure 2.2: Test track layout.

2.3   Pavement Design

Dynamic cone penetrometer (DCP) tests were performed along the center lines of each lane over the length and width of the test track (Figure 2.3) prior to any construction to obtain an indication of the in situ subgrade strength. Results are summarized in Table 2.1. Penetration rates varied between 11 mm per blow and 30 mm per blow, with the weakest areas in the middle of the track spanning Cells 5 and 6. Variation was attributed to the degree of soil mixing, temporary stockpiling of lime-treated soils (lime treatment was used to dry the soil in some areas of the site), to compaction from equipment during construction of the facility, and to varying subgrade moisture contents.
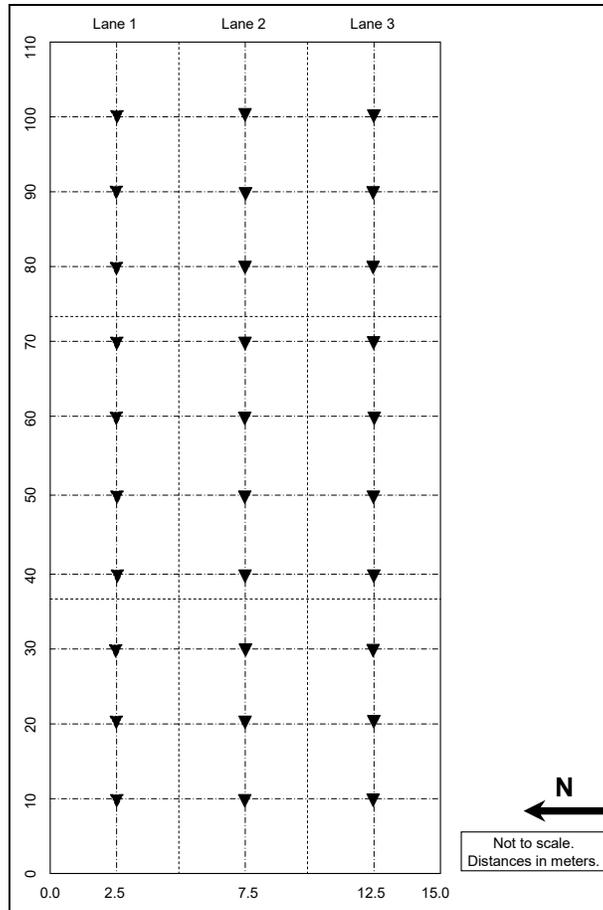
Figure 2.3: DCP test locations.

Table 2.1: Summary of DCP Survey on Subgrade Material

Test Location[1] (m)	Penetration Rate (mm/blow)			Estimated California Bearing Ratio[2]			Estimated Stiffness (MPa)[2]		
	Lane #1	Lane #2	Lane #3	Lane #1	Lane #2	Lane #3	Lane #1	Lane #2	Lane #3
10	17	21	19	11	9	9	56	41	44
20	16	18	15	12	10	13	60	46	63
30	14	16	13	14	12	15	66	60	71
40	13	22	16	15	8	12	71	40	60
50	13	26	15	15	6	13	71	36	63
60	12	25	16	17	6	12	77	37	60
70	15	30	15	13	5	13	63	30	63
80	14	28	15	14	5	13	66	34	63
90	12	26	14	17	6	14	77	36	66
100	11	20	15	19	9	13	85	42	63

[1] Measured from southwest corner of the track. [2] Estimated from DCP software tool.

A sensitivity analysis of potential pavement designs using layer elastic theory models was carried out using the DCP results obtained during the site investigation and estimates, based on previous experience, of the moduli of a representative aggregate base-course and asphalt concrete surfacing. Components of the sensitivity analysis included the following 24 cells:

- Three asphalt concrete thicknesses (100 mm, 125 mm, and 150 mm)
- Three asphalt concrete moduli (600 MPa, 1,000 MPa, and 3,000 MPa)
- Two base-course thicknesses (300 mm and 400 mm)
- Two base-course moduli (150 MPa and 300 MPa)
- One subgrade (existing soil with modulus of 60 MPa).

A test pavement design was selected to maximize the information that would be collected about the performance of warm-mix asphalt, taking into consideration that a very strong pavement would lengthen the testing time before results (and an understanding of the behavior) could be obtained, while a very weak pavement could fail before any useful data was collected. The pavement design shown in **Error! Reference source not found.** was considered appropriate for the study.

Layer: RHMA-G/RWMA-G
Thickness: 60 mm (0.2 ft.),   Modulus: 460 MPa @ 50°C (66.7 ksi @ 122°F)
Layer: HMA
Thickness: 60 mm (0.2 ft.),   Modulus: 615 MPa @ 50°C (89.2 ksi @ 122°F)

Layer: Imported Class 2 Aggregate Base-Course
Thickness: 400 mm (1.3 ft.), Modulus: 300 MPa (43.5 ksi)

Layer: Prepared Subgrade
Thickness: Semi-infinite, Modulus: 60 MPa (8.7 ksi)
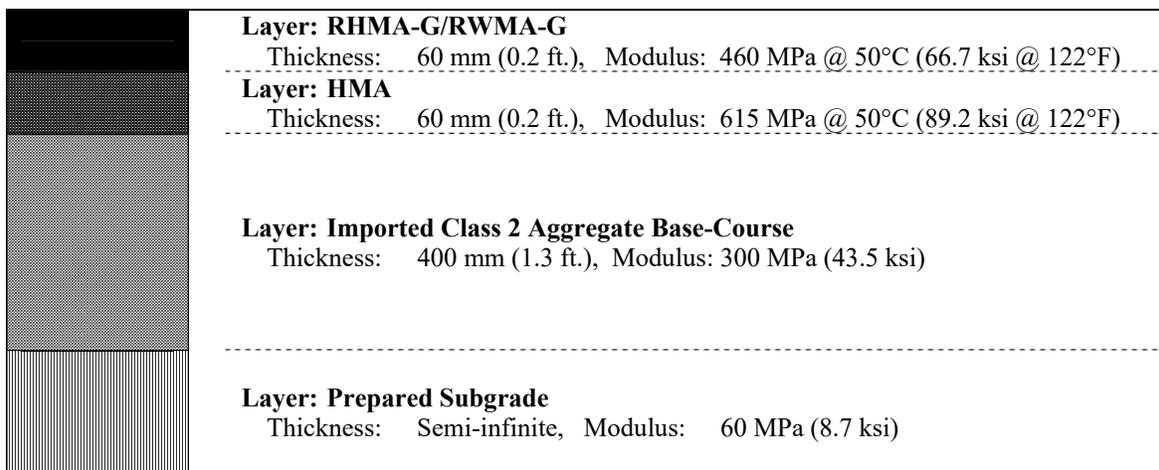
Figure 2.4: Pavement structure for rubberized warm-mix asphalt test sections.

2.4   Subgrade Preparation

2.4.1   Equipment
The following equipment was used for preparation of the subgrade:
- Water tanker (4,000 gal. [15,000 L])
- Caterpillar 163H grader
- Caterpillar 623F scraper
- Caterpillar 815F padfoot roller
- Ingersoll Rand SD-115-D vibrating steel drum roller

2.4.2   Preparation
The subgrade was prepared on September 22, 2009. Preparation included vegetation removal, preliminary leveling, ripping, watering and mixing, compaction, and final leveling to include a two percent north–south crossfall as follows:

- Removing vegetation with a grader, windrowing of the deleterious material toward the center of the track, collecting this material with a scraper and dumping it in a temporary stockpile for removal (Figure 2.5).
- Preliminary leveling with a grader followed by watering (Figure 2.6).
- Ripping to a depth of 12 in. (300 mm) (Figure 2.7).
- Watering and mixing using both the scraper and grader (Figure 2.8). Pockets of high clay content soils were observed during this process, which required additional working with the grader and scraper to break up the clods (Figure 2.9).
- Initial compaction with a padfoot roller (Figure 2.10). Despite extensive mixing, some clay pockets were still observed after completion of the initial compaction, with padfoot impressions clearly visible (Figure 2.11). Clay pockets appeared to predominate on the eastern half of the track.
- Final compaction with a vibrating smooth drum roller (Figure 2.12).
- Final leveling with a grader.
- Density checks on the finished surface (Figure 2.13) with a nuclear density gauge.

Figure 2.5: Vegetation removal.

Figure 2.6: Preliminary leveling.

Figure 2.7: Ripping.

Figure 2.8: Watering and mixing.

Figure 2.9: Breaking up of clay clods.

Figure 2.10: Initial compaction.

Figure 2.11: Padfoot impressions in clay pockets.

Figure 2.12: Final compaction.

Figure 2.13: Final subgrade surface.

2.4.3 Quality Control

Quality control of the subgrade preparation was limited to density checks with a nuclear gauge following Caltrans Test Method CT 231 and comparison of the results against a laboratory maximum density of 134.2 lb/ft³ (2,150 kg/m³) determined according to Caltrans Test Method CT 216. Nuclear gauge measurements were taken at 10 different locations selected according to a nonbiased plan shown in Figure 2.14. Samples for laboratory density determination were taken at locations 1, 2 and 3. Results are summarized in Table 2.2 and indicate that the subgrade density was generally consistent across the test track. Relative compaction varied between 95.4 percent and 99.2 percent with an average of 97.0 percent, two percent above the Caltrans-specified minimum density of 95 percent for subgrade compaction *(7)*. No location had a relative compaction lower than this minimum.
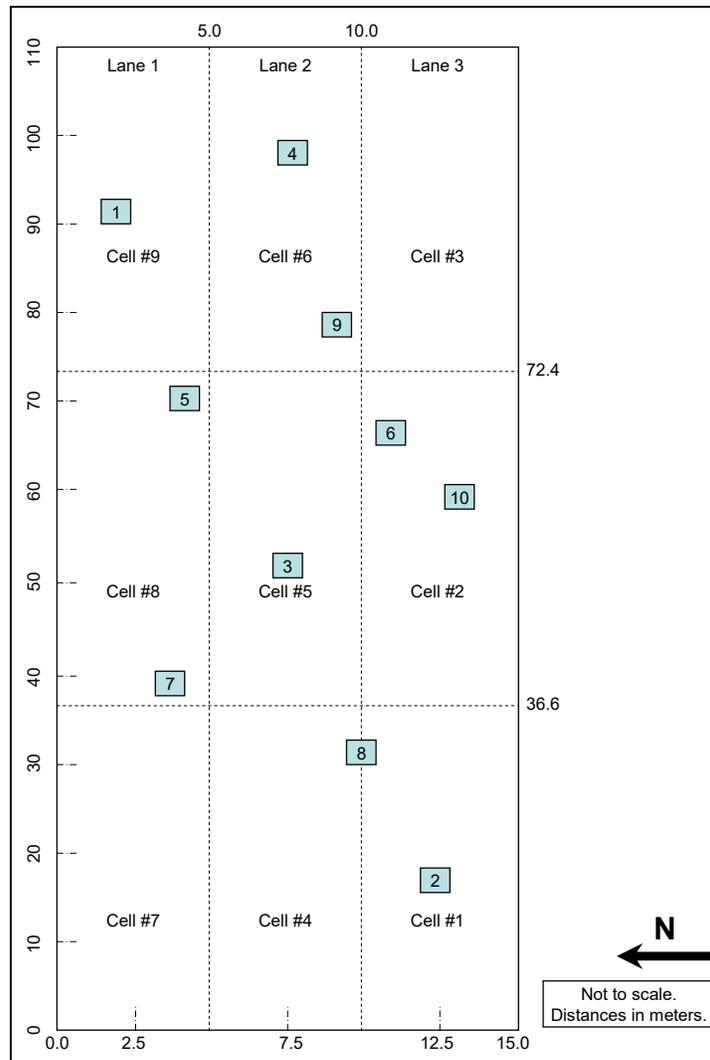
Figure 2.14: Location of subgrade density measurements.

Table 2.2: Summary of Subgrade Density Measurements

Location	Wet Density		Moisture Content	Dry Density		Relative Compaction
	(lb/ft^3)	(kg/m^3)	(%)	(lb/ft^3)	(kg/m^3)	(%)
1	130.5	2,091	15.6	112.6	1,804	97.3
2	132.6	2,124	17.3	113.1	1,811	98.8
3	131.3	2,103	16.8	112.4	1,801	97.8
4	130.2	2,086	16.2	112.1	1,796	97.0
5	133.2	2,133	15.2	115.6	1,852	99.2
6	128.9	2,065	17.8	109.5	1,754	96.0
7	132.2	2,117	17.9	112.1	1,795	98.5
8	128.1	2,052	18.7	107.9	1,728	95.4
9	132.3	2,120	16.5	113.6	1,820	98.6
10	128.7	2,062	15.0	111.9	1,793	95.9
Average	130.8	2,095	17.0	112.1	1,795	97.0
Std. Dev.	1.8	29	1.2	2.1	34	1.3

2.5   Base-Course Construction

2.5.1   Material Properties

Base-course aggregates were sourced from Teichert's Cache Creek quarry. Key material properties are summarized in Table 2.3. The material met Caltrans specifications, except for the percent passing the #200 sieve, which exceeded the specification operating range by 3.0 percent, and just met the contract compliance limits.

Table 2.3: Base-Course Material Properties

Property			Result	Operating Range	Contract Compliance
Grading:	1"	(25 mm)	100	100	100
	3/4"	(19 mm)	99.1	90 – 100	87 – 100
	1/2"	(12.5 mm)	90.1	–	–
	3/8"	(9.5 mm)	83.5	–	–
	#4	(4.75 mm)	63.3	35 – 60	30 – 65
	#8	(2.36 mm)	48.8	–	–
	#16	(1.18 mm)	39.2	–	–
	#30	(600 μm)	30.8	10 – 30	5 – 35
	#50	(300 μm)	21.6	–	–
	#100	(150 μm)	15.6	–	–
	#200	(75 μm)	12.3	2 – 9	0 – 12
Liquid Limit				–	–
Plastic Limit			Non-plastic	–	–
Plasticity Index				–	–
Maximum Dry Density (lbs/ft^3/kg/m^3)			140.6 (2,252)	–	–
Optimum Moisture Content			6.0	–	–
R-Value			79	–	>78
Sand equivalent			30	25	>22
Durability index – course			78	–	>35
Durability index – fine			52	–	>35

2.5.2   Equipment

The following equipment was used during the construction of the base-course:

- Water tanker (4,000 gal. [15,000 L])

- Caterpillar 163H grader
- Caterpillar 623F scraper
- Ingersoll Rand SD-115-D vibrating steel drum roller

2.5.3 Construction

The test track base-course was constructed on September 24, 2009, two days after the subgrade preparation. The construction process included aggregate spreading, watering, compaction, and final leveling to include a two percent north-south crossfall as follows:

- Transporting crushed base-course material (alluvial) that complied with Caltrans Class 2 aggregate base-course specifications from Teichert's Cache Creek aggregate source to the test track with a fleet of bottom-dump trucks and trailers.
- Dumping the aggregate in windrows (Figure 2.15).
- Spreading the aggregate with a grader (Figure 2.16) to a thickness of approximately 4.0 in. (100 mm).
- Adding water to bring the aggregate to the optimum moisture content and re-mixing with the grader to ensure even distribution of the moisture throughout the material (Figure 2.17).
- Initial compaction of the spread material with a vibrating steel wheel roller (Figure 2.18).
- Repeating the process until the design thickness of 1.3 ft. (400 mm) was achieved.
- Applying a generous application of water (Figure 2.19) followed by compaction to pump fines to the surface to provide good aggregate interlock (slushing).
- Final leveling with a grader (Figure 2.20). Final levels were checked with a total station to ensure that a consistent base-course thickness had been achieved.
- Removal of excess material with a scraper followed by final compaction (Figure 2.21).
- Density checks on the finished surface with a nuclear density gauge.

Figure 2.15: Dumping material in windrows.

Figure 2.16: Material spreading.

Figure 2.17: Watering.

Figure 2.18: Initial compaction.

Figure 2.19: Heavy watering prior to pre-final compaction.

Figure 2.20: Final leveling with a grader.

Figure 2.21: Removing excess material and final compaction.

2.5.4 Quality Control

Quality control of the base-course construction was limited to density checks with a nuclear gauge following Caltrans Test Method CT 231 and comparison of the results against a laboratory maximum wet density of 150.5 lb/ft^3 (2,410 kg/m^3) determined according to Caltrans Test Method CT 216. Nuclear gauge measurements were taken at 10 different locations selected according to a nonbiased plan shown in Figure 2.22. A sample for laboratory density determination was taken at Location #1. Results are summarized in Table 2.4 and indicate that the base-course density properties were generally consistent across the test track, but that the material was relatively wet compared to the laboratory-determined optimum moisture content. Relative compaction varied between 96.7 percent and 99.4 percent with an average of 98.0 percent, three percent above the Caltrans specified minimum density of 95 percent for base compaction *(7)*. No location had a relative compaction lower than this minimum.
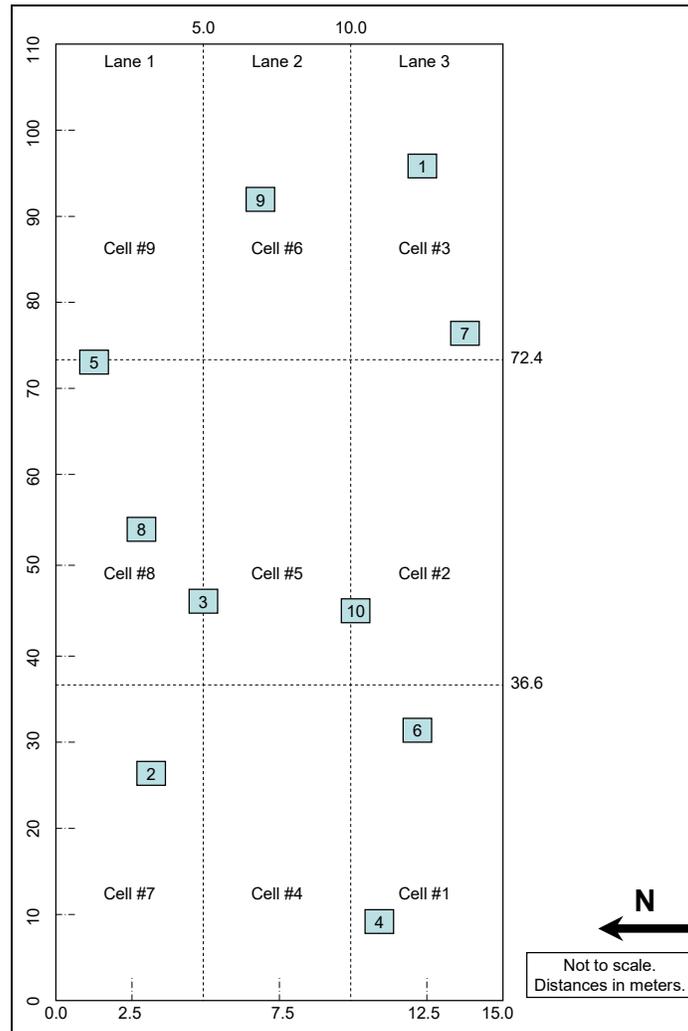
Figure 2.22: Location of base density measurements.

Table 2.4: Summary of Nuclear Gauge Base-Course Density Measurements

Location	Wet Density		Moisture Content	Dry Density		Relative Compaction
	(lb/ft^3)	(kg/m^3)	(%)	(lb/ft^3)	(kg/m^3)	(%)
1	146.5	2,346	6.6	137.4	2,201	97.3
2	148.5	2,379	7.0	138.8	2,223	98.7
3	148.0	2,371	8.0	137.0	2,195	98.4
4	147.1	2,356	7.8	136.5	2,186	97.8
5	148.7	2,382	6.3	139.9	2,241	98.8
6	145.5	2,330	6.8	136.2	2,182	96.7
7	149.0	2,387	8.2	137.7	2,206	99.0
8	145.6	2,332	7.7	135.2	2,165	96.8
9	149.5	2,395	6.9	139.8	2,240	99.4
10	145.7	2,334	7.8	135.2	2,165	96.8
Average	147.4	2,361	7.3	137.3	2,200	98.0
Std. Dev.	1.5	25	0.7	1.7	27.6	1.0

2.5.5 Follow-Up Testing Prior to Paving

Paving of the first lift of asphalt concrete was scheduled for October 7, 2009. However, contractor scheduling and then rainfall on four days (October 13, 14, 15, and 19) delayed priming of the surface until October 23, 2009, and paving until October 30, 2009. Rainfall measured over the four days totaled 3.1 in. (78 mm). Some ponding of water in Cells #1 and #2 on the western end of the test track was observed during these rainfall events (Figure 2.23).

Figure 2.23: Ponding of water on base.

Dynamic cone penetrometer (DCP) measurements were undertaken on the base at the same locations as the original subgrade DCP survey (Figure 2.3) to assess whether the rainfall had weakened the base on any parts of the track. The results are summarized in Table 2.5 and indicate that although average penetration rates (mm/blow) were consistent across the track, there was considerable difference in the average calculated stiffness of the base from the redefined layers based on actual penetration. Consequently, the contractor was requested to recompact the track with a static steel drum roller prior to priming to consolidate the base layer and accelerate movement of infiltrated water to the surface.

A significant improvement in subgrade stiffness attributed to the subgrade preparation and confinement by the base was also noted.

Table 2.5: Summary of DCP Survey on Base and Subgrade Material

Test Location (m)[1]	Penetration Rate (mm/blow)						Estimated Stiffness (MPa [ksi])[2]					
	Base			Subgrade			Base			Subgrade		
	Lane			Lane			Lane			Lane		
	#1	#2	#3	#1	#2	#3	#1	#2	#3	#1	#2	#3
10	3	-	-	9	-	-	430 (62)	-	-	111 (16)	-	-
20	-	3	-	-	8	-	-	395 (57)	-	-	119 (17)	-
30	-	-	3	-	-	7	-	-	320 (46)	-	-	139 (20)
40	4	-	-	9	-	-	332 (48)	-	-	114 (17)	-	-
50	-	4	-	-	9	-	-	299 (43)	-	-	107 (16)	-
60	-	-	4	-	-	9	-	-	279 (41)	-	-	137 (20)
70	4	-	-	10	-	-	255 (37)	-	-	99 (14)	-	-
80	-	4	-	-	10	-	-	260 (38)	-	-	105 (15)	-
90	-	-	4	-	-	7	-	-	273 (40)	-	-	148 (22)
100	4	-	-	11	-	-	259 (38)	-	-	116 (17)	-	-

[1] Measured from southwest corner of the track. [2] Estimated from DCP software tool.

2.6 Bottom Lift Asphalt Concrete Construction

2.6.1 Material Properties

Dense-graded asphalt concrete for the bottom lift was sourced from Teichert's Woodland Asphalt Plant. Key material properties are summarized in Table 2.6. The material met Caltrans specifications.

Table 2.6: Key Bottom Lift HMA Mix Design Parameters

Parameter			Wearing Course			
			Actual	Target	Specification	Compliance
Grading:	1"	(25 mm)	100	100	100	100
	3/4"	(19 mm)	98	100	100	100
	1/2"	(12.5 mm)	84	98	90 – 100	90 – 100
	3/8"	(9.5 mm)	75	83	77 – 89	76 – 90
	#4	(4.75 mm)	52	40	33 – 47	30 – 44
	#8	(2.36 mm)	34	23	18 – 28	6 – 26
	#16	(1.18 mm)	22	–	–	–
	#30	(600 μm)	15	12	–	–
	#50	(300 μm)	9	–	–	–
	#100	(150 μm)	6	–	–	–
	#200	(75 μm)	4	5	3 – 7	0 – 8
Asphalt binder grade			PG 64-16	-	–	-
Asphalt binder content (% by aggregate mass)			5.0	–	–	–
Hveem stability at optimum bitumen content			41.0	-	>37	-
Air-void content (%)			4.0	-	2 – 6	-
Dust proportion			0.9	-	0.6 – 1.3	-
Voids in mineral aggregate (LP-2) (%)			13.0	-	>13	-
Voids filled with asphalt (LP-3) (%)			69.0	-	65 – 75	-
Crushed particles (1 face) (%)			92	-	>90	-
Sand equivalent (%)			71.0	-	>47	-
Fine aggregate angularity (%)			54.0	-	>47	-
Los Angeles Abrasion at 100 repetitions (%)			5.0	-	<12	-
Los Angeles Abrasion at 500 repetitions (%)			21.3	-	<45	

2.6.2 Equipment

The following equipment was used during the construction of the bottom lift of asphalt concrete:

- Terex Cedar Rapids CR552 paver and material transfer device
- Caterpillar CB-534D vibrating steel twin-drum roller (two)
- Ingersoll Rand PT-240R pneumatic tire roller

2.6.3 Prime Coat Application

On the day before the prime coat application (October 22, 2009), the test track was compacted with a twin-drum steel roller to consolidate the base layer and accelerate movement of infiltrated water to the surface. An SS-1 asphalt emulsion prime coat was applied to the surface at a rate of 0.25 gal./yd^2 (1.0 L/m^2). The time of application was 1:00 p.m., ambient temperature was 88°F (35°C), and relative humidity was 28 percent. A consistent application was achieved (Figure 2.24); however, differential penetration was observed, which was attributed to patches of near-surface moisture (Figure 2.25).

Figure 2.24: Prime coat application.

Figure 2.25: Differential penetration of prime coat.

2.6.4 Asphalt Placement

The bottom lift of asphalt concrete was placed on October 30, 2009. Construction started at approximately 8:30 a.m. Ambient air temperature was 50°F (10°C) and the relative humidity was 45 percent. Construction was completed at approximately 11:00 a.m. when ambient temperature was 61°F (16°C) and the relative humidity was 40 percent.

Mix was transported using bottom-dump trucks and placed in a windrow on the surface. Paving started in Lane #1, followed by Lanes #2 and #3, and was carried out in a west-east direction. A pickup machine connected to the paver collected the material and fed it into the paver hopper. Paving followed conventional procedures. The breakdown roller closely followed the paver applying about four passes. A

single pass was made with the intermediate rubber-tired roller, followed by another four passes with the finish roller. The construction process is summarized in Figure 2.26.

Placing asphalt in windrow

Paving and breakdown rolling

Intermediate rolling

Final rolling

Figure 2.26: Construction of bottom lift asphalt concrete layer.

2.6.5   Construction Quality Control

Compaction was measured by the UCPRC using a nuclear gauge on the day after construction using the mix design specific gravity values. Measurements were taken at 33 ft. (10 m) intervals along the center line of each lane, with a focus on checking densities in the areas that would be used for HVS testing. A summary of the results is provided in Table 2.7. The results indicate that there was very little variability in the measurements and that satisfactory compaction had been achieved.

Table 2.7: Summary of Bottom Layer Asphalt Concrete Density Measurements

Position	Lane #1			Lane #2			Lane #3		
	Gauge		Relative	Gauge		Relative	Gauge		Relative
	lb/ft³	kg/m³	(%)	lb/ft³	kg/m³	(%)	lb/ft³	kg/m³	(%)
1	146.0	2,339	93	148.3	2,376	95	146.0	2,338	93
2	145.3	2,328	93	148.3	2,375	95	145.5	2,330	93
3	147.8	2,367	95	148.6	2,380	95	145.3	2,327	93
4	149.2	2,390	95	147.1	2,357	94	146.5	2,346	94
5	146.1	2,341	93	145.6	2,333	93	147.8	2,367	95
6	146.5	2,346	94	148.7	2,382	95	146.1	2,341	93
7	145.2	2,326	93	145.8	2,336	93	147.7	2,366	94
8	147.7	2,366	94	146.2	2,342	94	148.3	2,376	95
9	147.0	2,355	94	144.9	2,321	93	147.1	2,357	94
10	145.9	2,337	93	146.8	2,351	94	144.9	2,321	93
Average	146.7	2,350	94	146.5	2,347	94	146.5	2,347	94
Std. Dev.	1.3	0.020	0.8	1.4	0.019	0.8	1.2	0.019	0.8
RICE	2.504								

2.7 Rubberized Gap-Graded Asphalt Concrete Construction

2.7.1 Plant Modifications

No plant modifications were required to incorporate the warm-mix technologies. The Gencor Ultrafoam apparatus is integral to the asphalt plant. The Cecabase and Evotherm technologies were added via the liquid anti-strip system, which is also integral to the asphalt plant. All delivery systems were approved under the Caltrans Material Plant Quality Program.

2.7.2 Material Properties

A Caltrans-approved mix design, prepared by Granite Construction Company's Bradshaw Plant to meet Caltrans specifications for 1/2 in. (12.5 mm) gap-graded rubberized hot-mix asphalt (RHMA-G), was used for the experiment (Appendix A). Key parameters for the mix design are summarized in Table 2.8. The mix design was not adjusted for accommodation of the warm-mix technologies.

2.7.3 Warm-Mix Technology Application Rates

The warm-mix additive application rates were determined by the additive suppliers and were as follows:

- Cecabase: 0.5 percent by mass of binder
- Evotherm: 0.5 percent by mass of binder
- Gencor (water): 1.5 percent by mass of binder

2.7.4 Mix Production Temperatures

Mix production and paving temperatures were not set for the project. Instead, each technology provider was requested to select their own production temperatures based on ambient temperatures, haul distance, and discussions with the plant manager. Production temperatures were set as follows:

- Control: 320°F (160°C)
- Cecabase: 266°F (130°C)
- Evotherm: 248°F (125°C)
- Gencor: 284°F (140°C)

Table 2.8: Key RHMA-G Mix Design Parameters

Parameter		Wearing Course		
		Target	**Specification**	**Compliance**
Grading: 3/4" (19 mm)		100	100	100
1/2" (12.5 mm)		98	90 – 100	90 – 100
3/8" (9.5 mm)		83	77 – 89	76 – 90
#4 (4.75 mm)		40	33 – 47	30 – 44
#8 (2.36 mm)		23	18 – 28	6 – 26
#16 (1.18 mm)		–	–	–
#30 (600 µm)		12	–	–
#50 (300 µm)		–	–	–
#100 (150 µm)		–	–	–
#200 (75 µm)		5	3 – 7	0 – 8
Asphalt binder grade		PG 64-16	–	-
Asphalt binder source		Paramount	–	–
Asphalt binder content (% by mass of aggregate)		7.0	–	–
Rubber content (% by mass of binder)		18.0	–	-
Scrap tire rubber (%)		75.0	–	-
High natural rubber (%)		25.0	–	-
Extender oil (Raffex 120/Tricor, % by mass of binder)		2.5	–	-
Hveem stability at recommended bitumen content		35.0	23	-
Air-void content (%)		4.5	4 ± 2	-
Voids in mineral aggregate (LP-2) (%)		18.9	>18	-
Voids filled with asphalt (LP-3) (%)		76.5	65 – 75	-
Crushed particles (1 face) (%)		100	>90	-
Sand equivalent (%)		71.0	>47	-
Fine aggregate angularity (%)		46.0	>45	-
Los Angeles Abrasion at 100 repetitions (%)		3.0	<10	-
Los Angeles Abrasion at 500 repetitions (%)		15.0	<45	-

2.7.5   Mix Production

Mix production was overseen by technical representatives from each of the additive suppliers.

The control and warm mixes were produced and placed on April 7, 2010. The start of asphalt production was delayed until approximately 9:00 a.m. because of cold ambient air temperatures. Production began with the Control mix, followed by the Gencor, Evotherm, and Cecabase mixes. Approximately 150 tonnes of each mix were produced. Mix was stored in insulated silos for a limited time before load out and transport. The first approximately 20 tonnes of each mix was "wasted" to ensure that a consistent mix was used on the test track. The drum plant was also run for a short period with no warm-mix technology at the end of each production run to prevent any contamination of the next mix. This material was also wasted.

Plant emissions were not monitored due to the small volume of each mix produced.

2.7.6 Mix Production Quality Control

Asphalt Binder

A certificate of compliance was provided by the binder supplier with the delivery prior to modification with the rubber at the Granite Bradshaw plant. Rubber was added to the binder in an initial reaction time of 45 minutes at 375°F (190°C). Quality control data is provided in Table 2.9.

Table 2.9: Summary of Rubberized Binder Test Results

Parameter	Result
Binder content (%)	79.9
Extender content (%)	2.1
Crumb rubber (tire) (%)	13.5
Crumb rubber (natural) (%)	4.5
Total	100

	Minutes of Reaction Time							
	45	60	90	120	240	360	1,440	Limits
Cone penetration @ 77°F	25				27		55	25 – 70
Resilience @ 77°F	39				31		29	> 18
Field softening (°F)	148				148		152	125 – 165
Viscosity (Centipoises)	2,300	2,900	3,300	3,500	2,700	2,800	3,000	1,500 – 4,000

Asphalt Mix

Quality control of the mixes produced for the test track was undertaken by Granite Construction Company on mix sampled from the trucks at the silos. Hveem stabilities were determined at three different intervals on mix sampled from the paver during construction of the test track. The results are summarized in Table 2.10.

The following observations were made:

- The aggregate gradation generally met the target and was within the required ranges. The material passing the #4 (4.75 mm) sieve was slightly below (0.7%) the specified range.
- The binder contents of all mixes were slightly above the high limit of the target (between 0.2 and 0.4 percent). These differences were taken into consideration in performance discussions in Chapter 4 and Chapter 6.
- The maximum and bulk specific gravities of the four mixes were within a very close range and the differences were unlikely to influence performance in any way.
- Hveem stabilities were similar for all mixes and well above the minimum specified requirement of 23. The stabilities increased slightly for the samples that were cured before testing.
- There was essentially no moisture measured in any of the samples after mix production.

2.7.7 Paving Equipment

The following equipment was used during placement of the rubberized asphalt layer:

- Terex Cedar Rapids CR552 paver and material transfer device
- Caterpillar CB-534D vibrating steel twin drum roller (two)

Table 2.10: Quality Control of Mix After Production

Parameter	Specification/ Target	Control	Gencor	Evotherm	Cecabase
Grading[1]					
3/4" (19 mm)	100	100.0	Not tested	Not tested	Not tested
1/2" (12.5 mm)	90 – 100	99.4			
3/8" (9.5 mm)	78 – 88	78.3			
#4 (4.75 mm)	32 – 42	<u>31.3</u>			
#8 (2.36 mm)	17 – 25	19.2			
#16 (1.18 mm)	–	13.2			
#30 (0.6 mm)	7 – 15	9.8			
#50 (0.3 mm)	–	7.4			
#100 (0.15 mm)	–	5.6			
#200 (0.075 mm	2 – 7	4.1			
Sand equivalent[2]		68	Not tested	Not tested	Not tested
AC Binder Content (%)[3]	6.55 – 7.45	<u>7.73</u>	<u>7.86</u>	<u>7.69</u>	<u>7.67</u>
Max. Specific Gravity[4]					
AC plant	–	2.483	2.489	2.482	2.493
Bulk Specific Gravity					
Paver, immediate	–	2.458	2.456	2.442	2.442
Paver, 3 hour cure	–	2.449	2.449	2.446	2.445
Paver, cool + reheat + cure	–	2.452	2.450	2.433	2.444
Unit Weight (lb/f^3 [kg/m^3]					
AC plant	–	154.6 (2,482)	154.9 (2,482)	154.5 (2,475)	155.2 (2,486)
Hveem stability[5]					
Paver, immediate	–	27	28	27	27
Paver, 3-hour cure	–	30	30	28	29
Paver, cool + reheat + cure	–	31	29	30	29
Moisture (before plant) (%)	–	Not tested	Not tested	Not tested	Not tested
Moisture[6] (after silo) (%)	1.0	0.00	0.00	0.04	0.02

[1] CT 202   [2] CT 217   [3] CT 382   [4] CT 308   [5] CT 366   [6] CT 370
Underlined entries indicate that specification/target were not met

2.7.8 Tack Coat Application

The test track was broomed to remove dust and organic matter from the surface prior to any work undertaken. Tack coat was applied to Lane #1 in a single pass at 8:25 a.m., and to the Cecabase section (Cell #4 in Lane #2) at 10:50 a.m. (Figure 2.27). A diluted SS-1 emulsion (70:30) was applied with a distributor at an application rate of approximately 0.08 gal./yd^2 (0.36 L/m^2). Some steam was observed during application. Weather conditions at the time of tack coat application were as follows:

- Air temperature: 46°F (8°C)
- Surface temperature: 54°F (12°C)
- Relative humidity: 68 percent

Figure 2.27: Tack coat application.

2.7.9 Asphalt Placement

<u>Control Section</u>

Placement of the asphalt concrete on the Control section started at 9:20 a.m. with the positioning of the paver at the start of the section. Three loads were used and the paver reached the end of the section eight minutes after starting. Considerable smoke was observed from the trucks during tipping and from the paver (Figure 2.28). A pungent odor, typical of rubberized asphalt construction projects, was also noted. The paving crew wore respirators to limit the effects of these odors (Figure 2.29). Breakdown rolling started as soon as the paver was moved off of the section. Density and temperature measurements were taken throughout (see Section 2.7.6). Seven passes were made with the breakdown roller with vibration over a period of approximately 15 minutes (Figure 2.30). Some cooling was allowed before final rolling, which consisted of five passes with no vibration (Figure 2.31). No significant tenderness was observed and the roller operator considered the exercise typical of normal rubberized asphalt projects. Paver spillage was removed from the end of the section to ensure a clean and regular surface and join for the Gencor section.

Figure 2.28: Control: Smoke from truck and paver.

Figure 2.29: Control: Paver operator wearing respirator.

Figure 2.30: Control: Breakdown rolling.

Figure 2.31: Control: Final rolling.

<u>Gencor Section</u>

The same process described above was followed for the placement of the Gencor mix, which started at 9:45 a.m. Some smoke was observed and odors noted, but the intensity was considerably less than that observed/noted on the Control section (Figure 2.32). Breakdown rolling was achieved with eight passes, followed by a further four passes after a short period of cooling (Figure 2.33). Final rolling was completed in ten passes. No problems were observed during any of the compaction phases and a tightly bound surface was achieved. When interviewed, the roller operator noted that the mat was a little tender and responded a little differently to typical rubberized asphalt projects in that the response of the roller did not relate to the density measurements with the nuclear gauge. The operator had considered compaction to be complete; however, the density gauge indicated that compaction levels were not the same as those measured on the Control section and consequently the additional roller passes were applied. The paving crew noted that workability of this mix in terms of raking and shoveling was better than the Control, which was stiff and adhered to tools.

Figure 2.32: Gencor: Smoke from truck and paver.

Figure 2.33: Gencor: Breakdown rolling.

Evotherm Section

The same process followed for the previous two sections was also followed for the Evotherm mix. Construction started at 10:35 a.m. No smoke or odors were observed/noted (Figure 2.34). Eight passes were made with the breakdown roller, followed by another four passes after a period of cooling (Figure 2.35). Ten passes were applied during final rolling. Some tenderness was observed during breakdown rolling and the roller operator noted similar "discrepancies" between roller response and density gauge readings discussed above, when compared to typical rubberized asphalt projects. The paving crew noted that the workability of the mix was better than the previous two mixes, especially with regard to raking and shoveling (Figure 2.36), and was comparable to nonrubberized mixes. The crew also removed their respirators during paving of this section given the absence of smoke and odors.

Figure 2.34: Evotherm: No smoke from truck and paver.

Figure 2.35: Evotherm: Breakdown rolling.

Figure 2.36: Evotherm: Improved workability.

Cecabase Section

The same process followed for the previous three sections was also followed for the Cecabase mix. Construction started at 11:45 a.m. No smoke or odors were observed/noted (Figure 2.37). Ten initial passes were made with the breakdown roller (Figure 2.38), followed by a further four passes after a period

of cooling. Final rolling consisted of 12 passes. Some tenderness was noted and the roller operator stated that the Evotherm and Cecabase mixes behaved in a similar way. The paving crew also noted similar good workability to that noted for the Evotherm mix (Figure 2.39).

Figure 2.37: Cecabase: No smoke from truck and paver.

Figure 2.38: Cecabase: Breakdown rolling.

Figure 2.39: Cecabase: Improved workability.

General

All construction was completed at 1:10 p.m. The surface of the completed cells appeared to have a uniform color and appearance (Figure 2.40).

2.7.10 Construction Quality Control

Quality control, both during and after construction, was undertaken jointly by Teichert Construction, the UCPRC, and an appointed contractor, and included:

- Placement and compaction temperatures
- Thickness
- Compaction density
- Deflection

Figure 2.40: Completed construction.

Placement and Compaction Temperatures

Temperatures were systematically measured throughout the placement of the asphalt concrete using infrared temperature guns, thermocouples, and an infrared camera. Measurements of the following were included:

- Surface prior to start of paving
- Mix as it was tipped into the paver
- Mix behind the paver
- Mat before and during compaction

A summary of the measurements is provided in Table 2.11 and in Figure 2.41 and Figure 2.42.

The following observations were made:

- Ambient and paving temperatures were considered representative of early- or late-season paving.
- Paving and compaction temperatures were consistent with production temperatures, as expected.
- There was no significant drop in temperature during the approximate 60 minute haul in covered trucks.
- Ambient temperatures at the start of paving increased slightly for each section, as expected.
- There was very little temperature difference between the material being tipped into the paver and the mat behind the paver before compaction.
- Mid-depth temperatures on the Evotherm and Cecabase sections decreased at a slower rate than the Control and Gencor sections, consistent with the differences in production temperatures.

Thermal camera images (*FLIR Systems ThermaCAM PM290*, recorded by T.J. Holland of Caltrans) of the mat behind the paver are shown in Figure 2.43. The images clearly show consistent temperature across the mat on all sections. (Note that temperature scales on the right side of the photographs differ between images.)

Table 2.11: Summary of Temperature Measurements

Measuring Point	Temperature (°F)[1]			
	Control	**Gencor**	**Evotherm**	**Cecabase**
Production	320	284	248	266
Ambient at start of paving	54	55	59	61
Surface before paving[2]	57	66	77	84
Truck[2]	266	257	248	264
Paver[2]	309	262	248	261
Mat before compaction[2]	293	234	219	232
Mat at end of compaction[2]	151	144	165	156
Mid-depth at start of compaction[3]	309	264	235	259
Mid-depth at end of compaction[3]	153	135	124	151
Ambient at end of compaction	57	58	61	63
Measuring Point	Temperature (°C)[1]			
	Control	**Gencor**	**Evotherm**	**Cecabase**
Production	160	140	125	130
Ambient at start of paving	12	13	15	16
Surface before paving[2]	14	19	25	29
Truck[2]	130	125	120	129
Paver[2]	154	128	120	127
Mat before compaction[2]	145	112	104	111
Mat at end of compaction[2]	66	62	74	69
Mid-depth at start of compaction[3]	154	129	113	126
Mid-depth at end of compaction[3]	67	57	51	66
Ambient at end of compaction	14	14	16	17

[1] Average of three sets of measurements   [2] Measured with a temperature gun   [3] Measured with a thermocouple
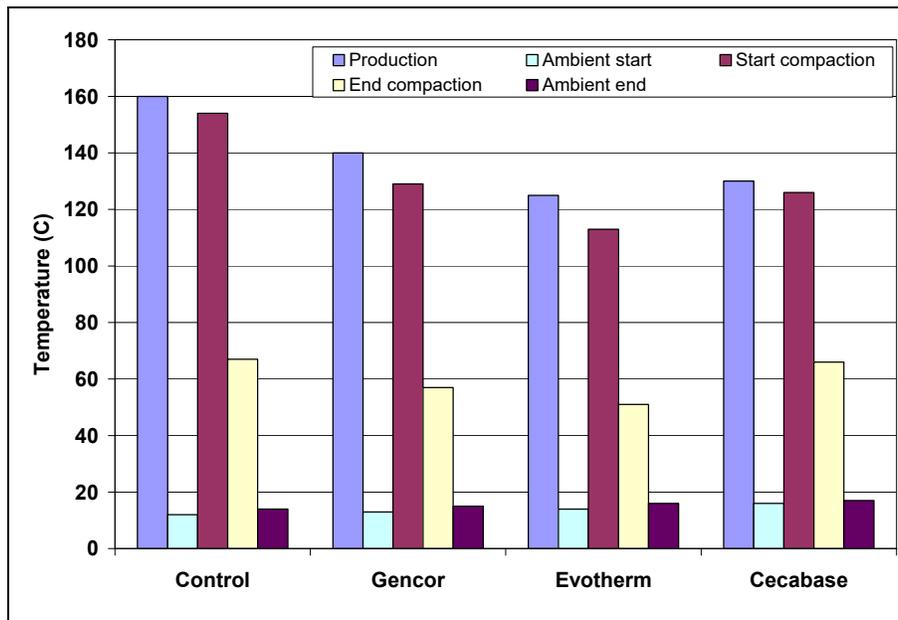
Figure 2.41: Summary of temperature measurements.
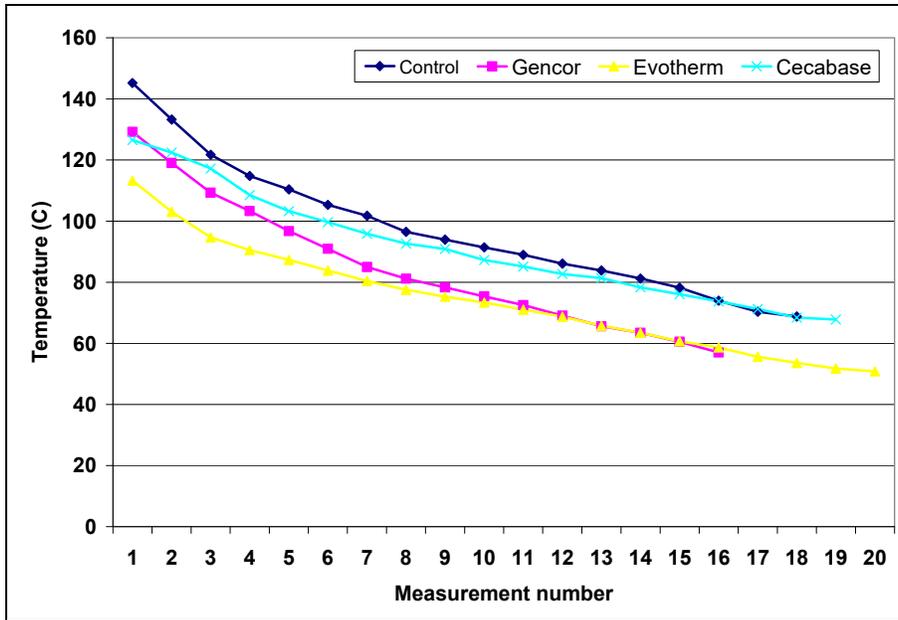
Figure 2.42: Summary of mid-depth temperatures over time.

Control

Gencor

Evotherm

Cecabase
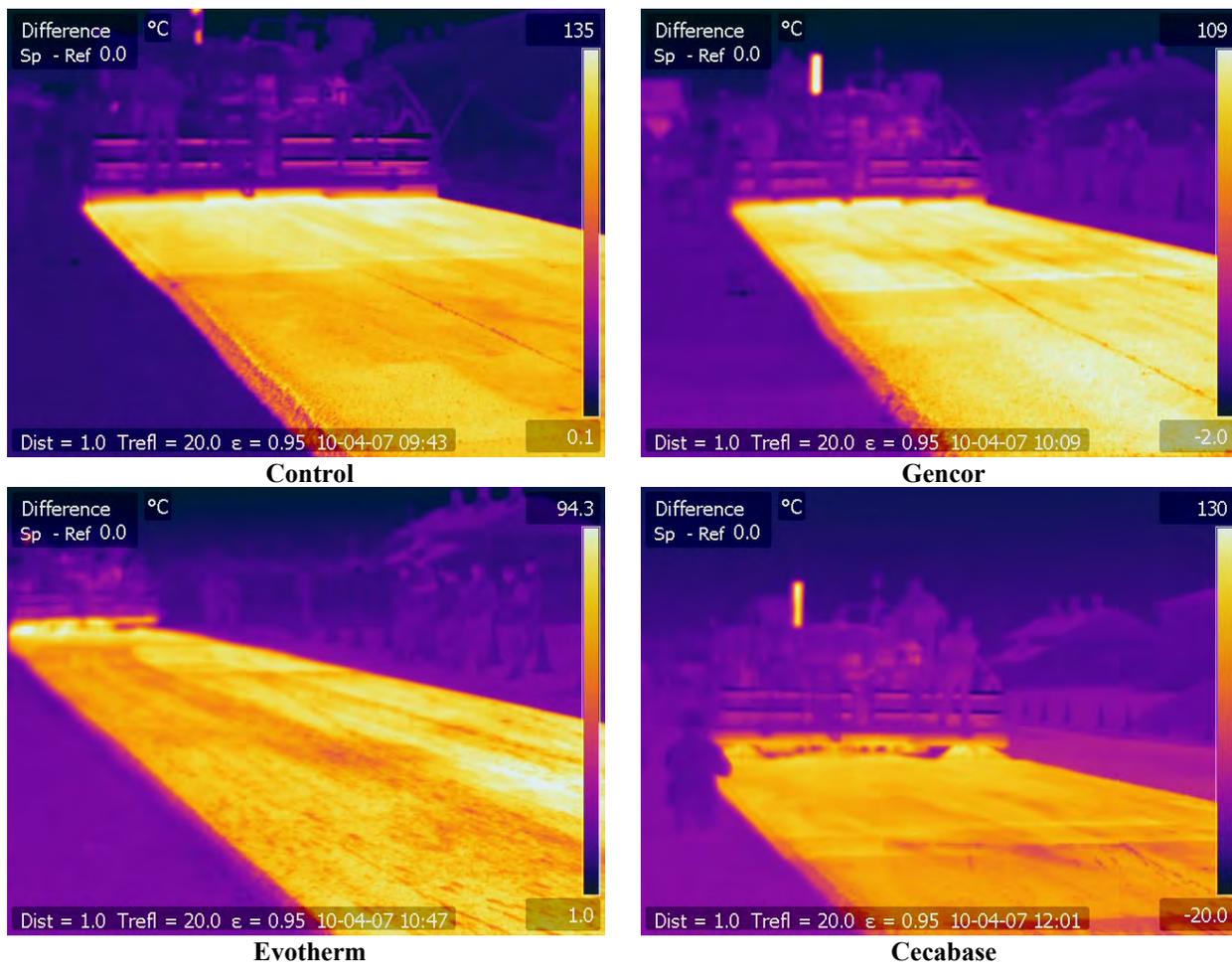
Figure 2.43: Thermal images of test track during construction.

Thickness

Thickness was monitored with probes by the paving crew throughout the construction process. The thickness of the slabs and cores removed for laboratory testing after construction (see Section 2.8) was measured for quality control purposes. The results of these measurements are summarized in Table 2.12. Layer thicknesses of actual Heavy Vehicle Simulator test sections were determined during forensic investigations after testing and are discussed in Section 5.7.

Table 2.12: Summary of Asphalt Layer Thickness

Measurement	Control		Gencor		Evotherm		Cecabase	
	(ft.)	(mm)	(ft.)	(mm)	(ft.)	(mm)	(ft.)	(mm)
Surface layer	0.22	65	0.22	65	0.22	65	0.22	67
Bottom layer	0.23	74	0.23	72	0.23	68	0.24	70
Total	0.45	139	0.45	137	0.45	133	0.46	137

The average thickness of the combined two layers was 0.45 ft. (137 mm), 0.05 ft. (17 mm) thicker than the design thickness of 0.4 ft. (120 mm). General consistency of thickness across the track was considered satisfactory and representative of typical construction projects.

Compaction Density

Compaction was monitored using nuclear gauges throughout the construction process using the mix design specific gravity values. Given the very small quantities of mix produced for each technology, actual mix specific gravities were not available before completion of construction of each section. The results were used to manage the number of roller passes and roller settings and were monitored but not recorded.

Final density measurements were taken on June 18, 2010, by an independent consultant using a calibrated nuclear gauge. Measurements were taken on each section according to the plan shown in Figure 2.44, which focused primarily on checking densities in the areas selected for HVS testing, but also to assess variability across each section. A summary of the results is provided in Table 2.13. The results indicate that there was very little variability across the sections and that slightly better densities were achieved on the Control section compared to the warm-mix sections, but that relatively poor compaction was achieved overall. This did not correspond to actual measurements taken on the day of construction, which indicated that acceptable densities had been achieved. A series of cores were therefore taken from positions 7 through 10 (Figure 2.44) to check these densities in the laboratory using the CoreLok method. The results are summarized in Table 2.14 and indicate that higher densities were actually achieved. Air-void contents were also determined on each specimen sampled from the test track for laboratory testing. The results for these tests, which are similar to the results shown in Table 2.14, are discussed in Chapter 6. It is not clear

why there was a considerable difference between the gauge- and core-determined densities. Core-determined densities were used for all analyses in this study.
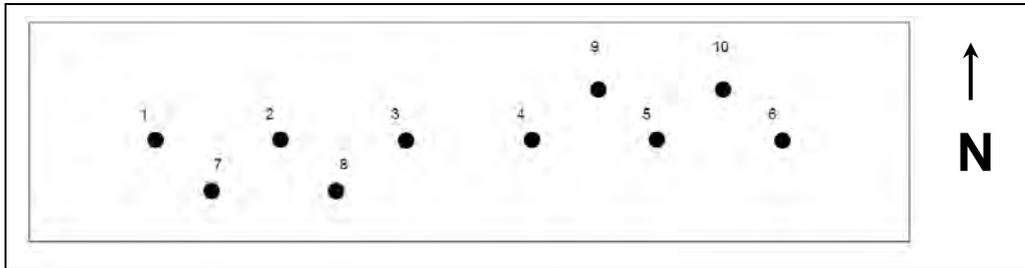
Figure 2.44: Asphalt concrete density measurement plan.

Table 2.13: Summary of Rubberized Asphalt Concrete Density Measurements

Position	Control		Gencor		Evotherm		Cecabase	
	Gauge (kg/m³)	Relative (%)	Gauge (kg/m³)	Relative (%)	Gauge (kg/m³)	Relative (%)	Gauge (kg/m³)	Relative (%)
1	2,221	89	2,194	88	2,150	87	2,234	90
2	2,204	89	2,125	85	2,213	89	2,188	88
3	2,228	90	2,173	87	2,219	89	2,280	91
4	2,236	90	2,169	87	2,148	87	2,185	88
5	2,234	90	2,223	89	2,164	87	2,155	86
6	2,257	91	2,171	87	2,123	86	2,195	88
7	2,243	90	2,273	91	2,202	89	2,213	89
8	2,300	93	2,247	90	2,234	90	2,274	91
9	2,280	92	2,224	89	2,239	90	2,238	90
10	2,259	91	2,300	92	2,224	90	2,263	91
Average	2,246	90	2,210	89	2,192	88	2,223	89
RICE	2.483		2.489		2.482		2.493	

Table 2.14: Summary of Asphalt Concrete Density Measurements from Cores

Position	Control		Gencor		Evotherm		Cecabase	
	Air-Void (%)	Relative (%)	Air-Void (%)	Relative (%)	Air-Void (%)	Relative (%)	Air-Void (%)	Relative (%)
7	5.2	95	6.5	93	6.5	93	6.4	94
8	5.1	95	6.7	93	6.4	94	6.2	94
9	4.6	95	6.0	94	5.9	94	6.5	93
10	4.5	95	5.8	94	5.9	94	6.6	93
Average	4.9	95	6.3	94	6.2	94	6.4	94

Deflection

Falling weight deflectometer (FWD) measurements were taken on May 27 and May 28, 2010, at 1.0 m intervals along the centerline of each lane to assess general variability across the test track. Average results of the second 40 kN load drop are summarized in Table 2.15 and in Figure 2.45 and Figure 2.46. The D1 sensor data were used to obtain an indication of overall pavement deflection. The D2 sensor data were used to obtain an indication of deflection in the asphalt layers. The D3 and D5 sensor data were used

to obtain an indication of deflection in the top and bottom of the base respectively, and the D6 sensor data were used to obtain an indication of deflection in the subgrade. All deflection measurements were normalized to 40 kN by proportioning at 20°C pavement temperature at 40 mm depth (i.e., one-third of the total asphalt concrete thickness) using the Bells Temperature calculated from actual air and surface temperatures.

There was no significant difference in the deflections measured on Lane #1 (Control, Gencor, and Evotherm sections). Deflections on the Cecabase section were lower than on the other three sections, indicating a marginally stiffer structure. Deflections were higher at the start and end of each section, but consistent in the middle 80 ft. (25 m) where the HVS test sections would be positioned.

Table 2.15: Summary of Average FWD Deflection Measurements

Section	Deflection (micron)							
	Control		Gencor		Evotherm		Cecabase	
	Mean	Std. Dev.	Mean	Std. Dev.	Mean	Std. Dev.	Mean	Std. Dev.
Sensor D1[1]	586	76	567	41	609	52	471	27
Sensor D2[2]	403	61	391	39	404	35	308	15
Sensor D3[3]	308	50	301	37	301	24	230	12
Sensor D5[4]	141	23	144	23	136	12	107	4
Sensor D6[5]	87	12	93	14	85	9	70	2
Section	Average Temperatures Measured							
Air	14.4	0.2	14.6	0.2	15.6	0.4	15.2	1.5
Surface	21.7	0.9	21.9	0.9	24.2	1.6	21.8	2.9
[1] Geophone D1, 0 mm offset [2] Geophone D2, 150 mm offset [3] Geophone D3, 315 mm offset [4] Geophone D5, 630 mm offset [5] Geophone D6, 925 mm offset								
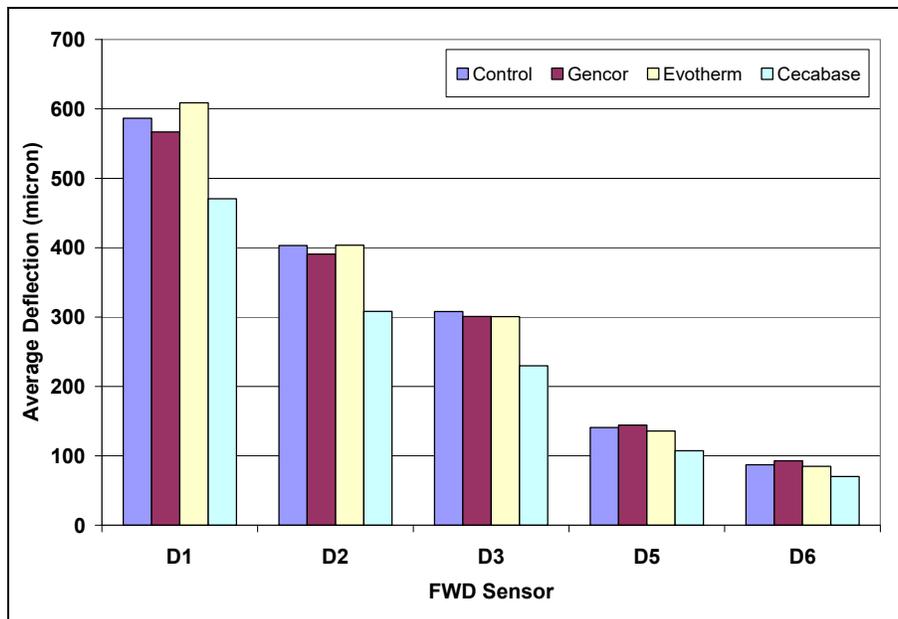
Figure 2.45: Summary of average deflection by section (40 kN load at 20°C).
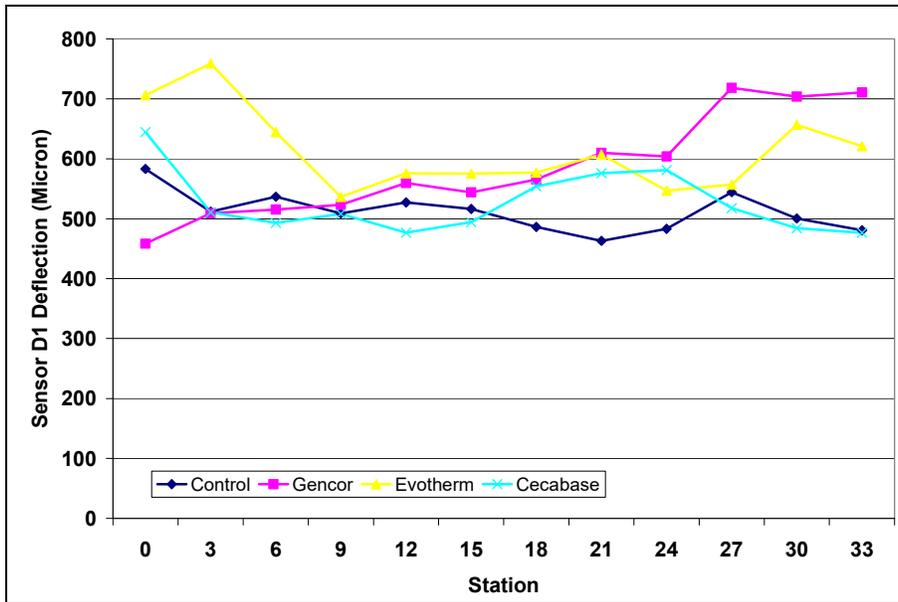
Figure 2.46: Summary of Sensor-1 deflection measurements.

2.8 Sampling

Specimens in the form of 6.0 in. (152 mm) diameter cores and 20 in. by 10 in. (500 mm by 250 mm) slabs were sawn from the middle of each section adjacent to the planned HVS test sections for laboratory testing, as shown in Figure 2.47. Slabs were sawn to the bottom of the combined asphalt concrete layers, extracted, stored on pallets, and then transported to the UCPRC Richmond Field Station laboratory. Inspection of the slabs indicated that the asphalt concrete was well bonded to the top of the base-course material, and that the two asphalt layers were well bonded to each other.
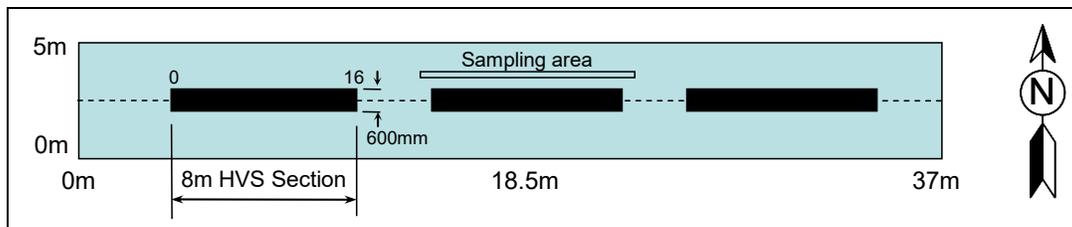
Figure 2.47: Sampling location for laboratory specimens.

2.9 Postconstruction Observations

A number of relatively heavy rainfall events occurred in the period between the end of construction and the commencement of HVS testing. After initial dryback of the sections, seepage of water from hairline cracks was noted on the Cecabase section (Figure 2.48), and from the longitudinal joint between the

Cecabase and Control sections (Figure 2.49). This was attributed to final compaction at low temperatures and would be taken into consideration in the analysis of HVS test results.

Figure 2.48: Water seepage from Cecabase section.

Figure 2.49: Water seepage from longitudinal joint between Cecabase and Control sections.

2.10 Construction Summary

Key observations from the test track construction process include the following:

- Preparation of the subgrade resulted in a generally consistent platform on which to construct the base. Density measurements taken after final compaction indicated an average relative compaction of 97 percent of the laboratory-determined value, with very little variation across the track.
- Construction of the base-course followed conventional procedures. Measurements after final compaction indicated that the average dry density was 98 percent of the laboratory-determined maximum dry density with very little variation across the track. The final surface was tightly bound and free of loose material. Heavy rainfall after construction resulted in some loosening of the surface, and the layer was consequently recompacted prior to paving the bottom lift of asphalt concrete.

- Placement of the bottom lift of hot-mix asphalt followed conventional procedures. Thickness and compaction appeared to be consistent across the test track.
- Minimal asphalt plant modifications were required to accommodate the warm-mix additives. These complied with the Caltrans Material Plant Quality Program requirements.
- No problems were noted with producing the asphalt mixes at the lower temperatures. Target mix production temperatures (320°F, 284°F, 248°F, and 266°F [160°C, 125°C, 140°C, and 130°C] for the Control, Gencor, Evotherm, and Cecabase mixes, respectively), set by the warm-mix technology providers, were all achieved.
- The rubberized binder, with 18 percent rubber content, complied with the specification requirements.
- All mixes met the project mix design requirements, with little variability between the mixes. Binder contents were 7.7, 7.9, 7.7, and 7.7 percent for the Control, Gencor, Evotherm, and Cecabase mixes, respectively. Hveem stabilities, determined at three different curing regimes, exceeded the minimum requirement by a considerable margin. Curing did not appear to influence the stability.
- No moisture was measured in the mixes after production.
- Compaction temperatures differed considerably between the mixes and were consistent with production temperatures. The Evotherm and Cecabase mixes, produced at 248°F and 266°F (140°C and 130°C), respectively, lost heat during transport and placement at a slower rate than the Control and Gencor mixes, which were produced at higher temperatures. The lower temperatures of the three warm-mixes did not appear to influence the paving or compaction operations, and interviews with the paving crew after construction revealed that no problems were experienced at the lower temperatures. Improved working conditions were identified as an advantage.
- Smoke and odors were significantly more severe during construction of the Control section compared to the Gencor section. No smoke or odors were noted during construction of the Evotherm and Cecabase sections.
- Mix workability, determined through observations of and interviews with the paving crew, was considerably better on the warm-mix sections compared to the Control.
- Average thicknesses of the top (rubberized) and bottom asphalt layers across the four sections were 0.22 ft. (66 mm) and 0.23 ft. (74 mm), respectively. The average thickness of the combined two layers was 0.45 ft. (137 mm), 0.5 ft. (17 mm) thicker than the design thickness of 0.4 ft. (120 mm). General consistency of thickness across the track was considered satisfactory and representative of typical construction projects.
- Nuclear gauge–determined density measurements were inconsistent with core-determined air-void contents. The core-determined air-void contents indicated that slightly higher density was achieved on the Control section (95 percent of the RICE specific gravity) compared to the warm-mix sections (94 percent). Compaction across the test track appeared to be consistent, showing that adequate compaction can be achieved on rubberized warm-mixes at lower temperatures. Based on observations from the test track construction and interviews with roller operators, optimal compaction temperatures will differ between the different warm-mix technologies. Therefore on projects where warm-mix technologies are used, roller operators will need to consider potential differences in roller response between warm-mix and conventional hot mixes, and may need to adjust rolling procedures to ensure that optimal compaction is always achieved.

- Deflection measurements showed that relatively consistent construction was achieved on the test track. Marginally lower deflection was recorded on the Cecabase section in Lane #2 compared to the other three sections.

The test track was considered satisfactorily uniform for the purposes of accelerated pavement testing and sampling for laboratory testing.

3. TEST TRACK LAYOUT AND HVS TEST CRITERIA

3.1 Protocols

Heavy Vehicle Simulator (HVS) test section layout, test setup, trafficking, and measurements followed standard University of California Pavement Research Center (UCPRC) protocols *(8)*.

3.2 Test Track Layout

The Phase 3 Warm-Mix Asphalt Study test track layout is shown in Figure 3.1. Four HVS test sections were demarcated for the first phase of HVS testing for early-age rutting at high temperatures, and testing was carried out in the same order as construction (i.e., Control followed by warm-mixes in order of production). The section numbers allocated were as follows (HA refers to the specific HVS equipment used for testing):

- Section 620HA: Control
- Section 621HA: Gencor
- Section 622HA: Evotherm
- Section 623HA: Cecabase

3.3 HVS Test Section Layout

The general test section layout for each of the rutting sections is shown in Figure 3.2. Station numbers (0 to 16) refer to fixed points on the test section and are used for measurements and as a reference for discussing performance.

3.4 Pavement Instrumentation and Monitoring Methods

Measurements were taken with the instruments listed below. Instrument positions are shown in Figure 3.2. Detailed descriptions of the instrumentation and measuring equipment are included in Reference *(8)*. Intervals between measurements, in terms of load repetitions, were selected to enable adequate characterization of the pavement as damage developed.

- A laser profilometer was used to measure surface profile; measurements were taken at each station.
- Thermocouples measured pavement temperature (at Stations 4 and 12) and ambient temperature at one-hour intervals during HVS operation.

Air temperatures were recorded by a weather station next to the test section at the same intervals as the thermocouples. Subgrade and base moisture contents were measured with two moisture sensors positioned in the middle of the test track.
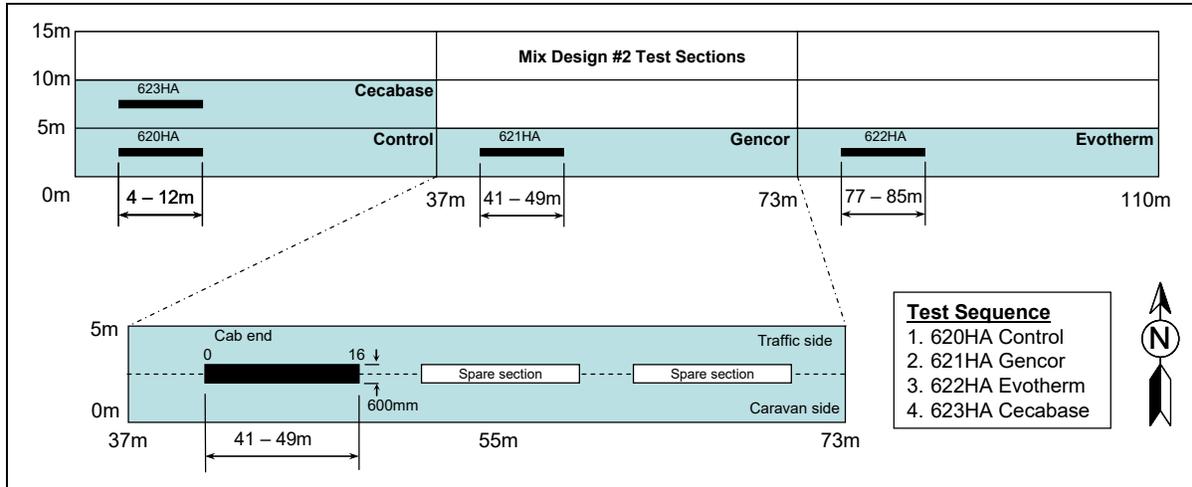

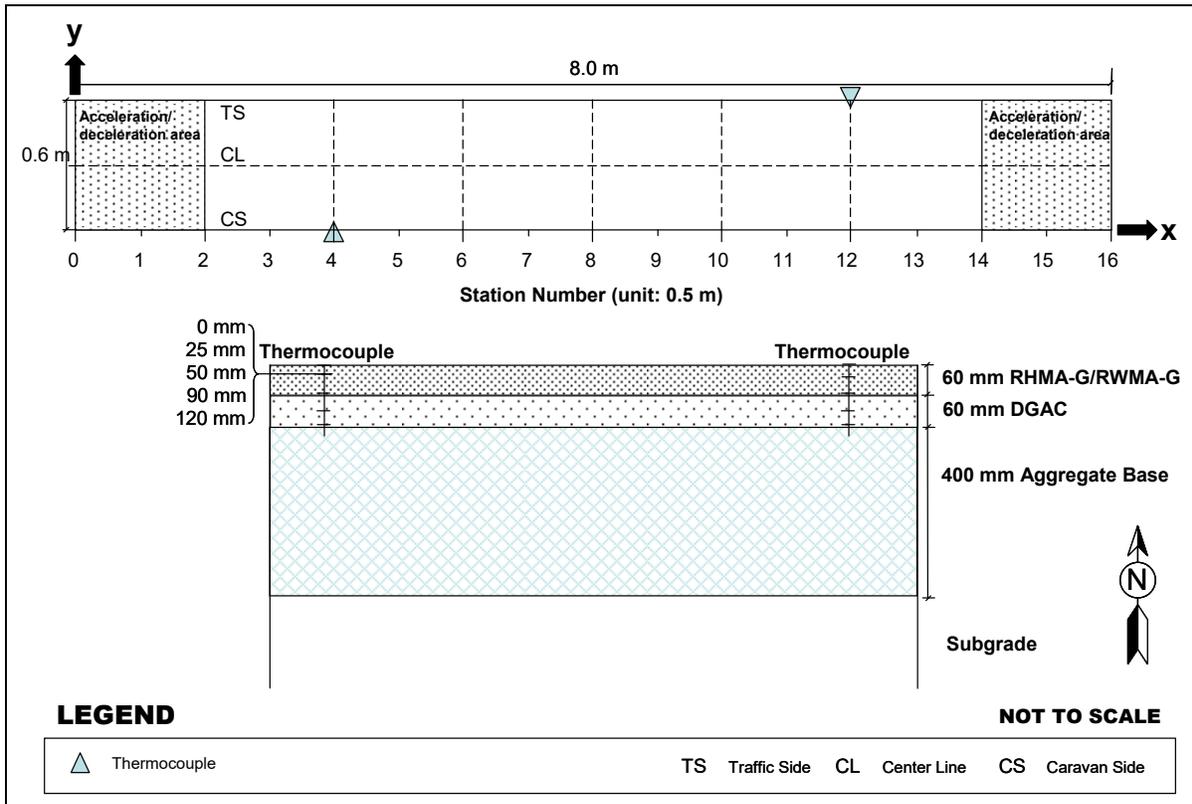**Figure 3.1: Layout of Phase 3 test track and Phase 3a HVS test sections.**

Figure 3.2: Location of thermocouples.

Surface and in-depth deflections were not measured. Surface deflection cannot be measured with the road surface deflectometer (RSD) on rutted pavements. In-depth deflection measured with multi-depth deflectometers (MDD) was not possible due to difficulties with installing and anchoring the instruments in the soft clay subgrade.

3.5 HVS Test Criteria

3.5.1 Test Section Failure Criteria
An average maximum rut depth of 12.5 mm (0.5 in.) over the full monitored section (Station 3 to Station 13) was set as the failure criterion for the experiment. However; in most instances, HVS trafficking was continued past this point to fully understand the rutting behavior of each mix.

3.5.2 Environmental Conditions
The pavement temperature at 50 mm (2.0 in.) was maintained at 50°C±4°C (122°F±7°F) to assess rutting potential under typical pavement conditions. Infrared heaters inside a temperature control chamber were used to maintain the pavement temperature. The test sections received no direct rainfall as they were protected by the temperature control chamber. The sections were tested predominantly during the dry season (June through December).

3.5.3 Test Duration
HVS trafficking on each section was initiated and completed as shown in Table 3.1.

Table 3.1: Test Duration for Phase 3a HVS Rutting Tests

Section	Overlay	Start Date	Finish Date	Repetitions
620HA	Control	06/25/2010	07/13/2010	74,000
621HA	Gencor	07/15/2010	08/03/2010	159,000
622HA	Evotherm	08/05/2010	09/03/2010	200,000
623HA	Cecabase	10/20/2010	12/07/2010	224,000

3.5.4 Loading Program
The HVS loading program for each section is summarized in Table 3.2. Equivalent Standard Axle Loads (ESALs) were determined using the following Caltrans conversion (Equation 3.1):

$$\text{ESALs} = (\text{axle load}/18,000)^{4.2} \tag{3.1}$$

All trafficking was carried out with a dual-wheel configuration, using radial truck tires (Goodyear G159 - 11R22.5- steel belt radial) inflated to a pressure of 720 kPa (104 psi), in a channelized, unidirectional loading mode. Load was checked with a portable weigh-in-motion pad at the beginning of each test, after each load change, and at the end of each test.

Table 3.2: Summary of HVS Loading Program

| Section	Overlay	Wheel Load[1] (kN)	Repetitions	ESALs[2]
620HA	Control	40	74,000	74,000
621HA	Gencor	40	159,000	159,000
622HA	Evotherm	40	160,000	160,000
		60	40,000	219,606
623HA	Cecabase	40	160,000	160,000
		60	64,000	351,369
		Total	**657,000**	**1,123,975**
[1] 40 kN = 9,000 lb.; 60 kN = 13,500 lb			[2] ESAL: Equivalent Standard Axle Load	

4. PHASE 3a HVS TEST DATA SUMMARY

4.1 Introduction

This chapter provides a summary of the data collected from the four HVS tests (Sections 620HA through 623HA) and a brief discussion of the first-level analysis. The data collected includes rainfall, air temperatures inside and outside the temperature control chamber, pavement temperatures, and surface permanent deformation (rutting).

Pavement temperatures were controlled using the temperature control chamber. Both air (inside and outside the temperature box) and pavement temperatures were monitored and recorded hourly during the entire loading period. In assessing rutting performance, the temperature at the bottom of the asphalt concrete and the temperature gradient are two important controlling temperature parameters influencing the stiffness of the asphalt concrete and are used to compute plastic strain. Permanent deformation at the pavement surface (rutting) was monitored with a laser profilometer. In-depth permanent deformation at various depths within the pavement was not monitored due to the soft subgrade clay and associated difficulties with the installation and anchoring of multi-depth deflectometers. The following rut parameters were determined from these measurements, as illustrated in Figure 4.1:

- Average maximum rut depth,
- Average deformation,
- Location and magnitude of the maximum rut depth, and
- Rate of rut development.
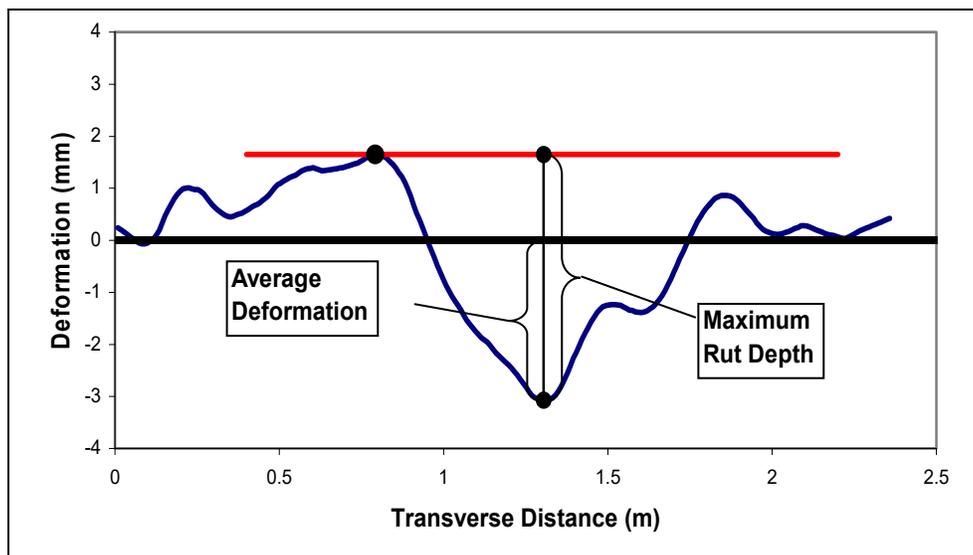
Figure 4.1: Illustration of maximum rut depth and average deformation of a leveled profile.

The laser profilometer provides sufficient information to evaluate the evolution of permanent surface deformation of the entire test section at various loading stages. The rut depth figures in this report show the average values over the entire section (Stations 3 through 13) as well as values for half sections between Stations 3 and 8 and Stations 9 and 13. These two additional data series were plotted to illustrate any differences along the length of the section. The precise nature of the permanent deformation was determined after the forensic investigation (test pits and cores) on each section and is discussed in Chapter 5.

The data from each HVS test is presented separately, with the presentation of each test following the same format. Data plots are presented on the same scale, where possible, to facilitate comparisons of performance.

4.2   Rainfall

Figure 4.2 shows the monthly rainfall data from June 2010 through December 2010 as measured at the weather station next to the test track. Rainfall was measured during all four Phase 3a HVS tests. There were no significant 24 hour rainfall events.
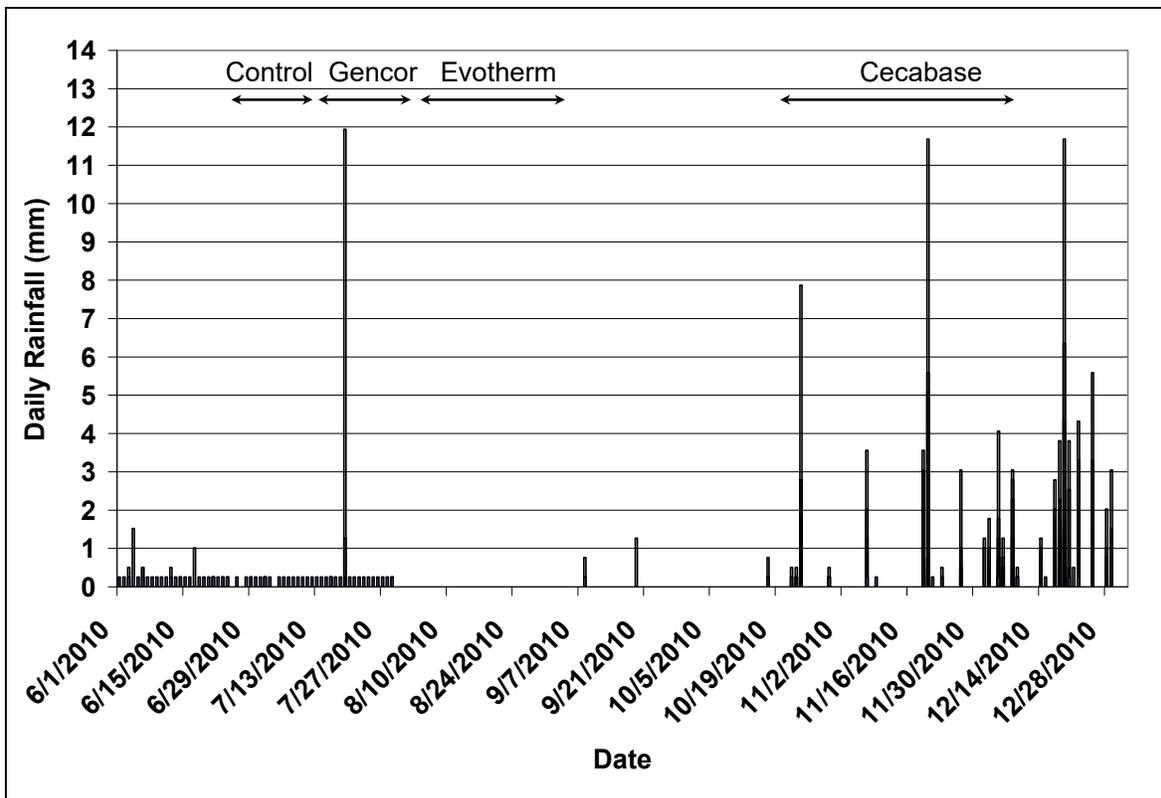

Figure 4.2: Measured rainfall during Phase 3a HVS testing.

4.3   Section 620HA: Control

4.3.1   Test Summary

Loading commenced on June 25, 2010, and ended on July 13, 2010. A total of 74,000 load repetitions were applied and 18 datasets were collected. Testing was interrupted for five days (July 2, 2010, through July 7, 2010) due to a test carriage computer malfunction. The HVS loading history for Section 620HA is shown in Figure 4.3.
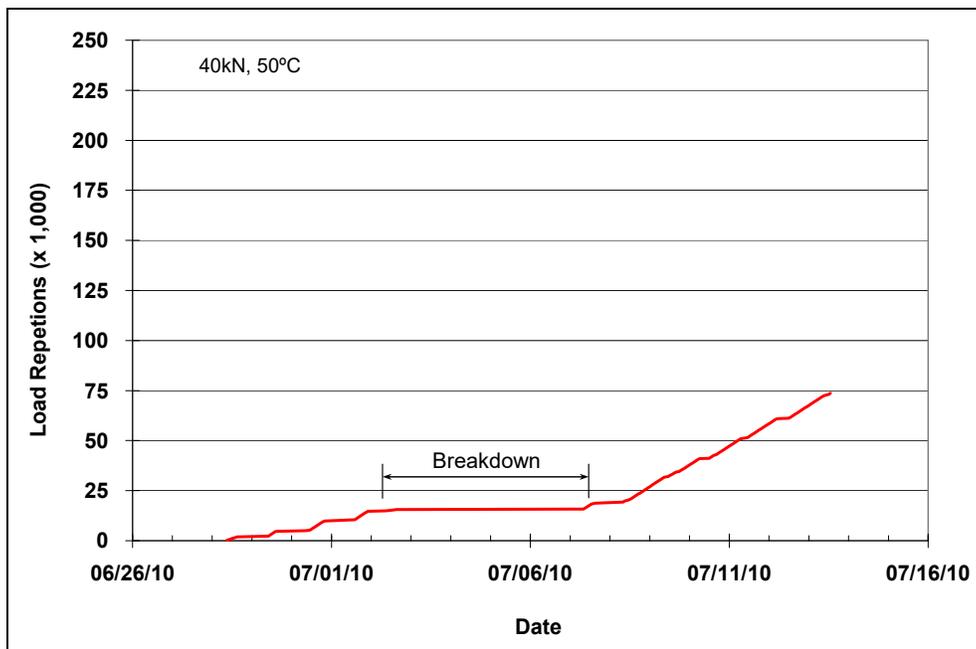
Figure 4.3: 620HA: Load history.

4.3.2   Outside Air Temperatures

Daily average outside air temperatures are summarized in Figure 4.4. Vertical error bars on each point on the graph show the daily temperature range. Temperatures ranged from 14°C to 40°C (58°F to 104°F) during the course of HVS testing, with a daily average of 28°C (82°F), an average minimum of 18°C (64°F), and an average maximum of 34°C (94°F).

4.3.3   Air Temperatures in the Temperature Control Unit

During the test, air temperatures inside the temperature control chamber ranged from 23°C to 50°C (75°F to 122°F) with an average of 42°C (108°F) and standard deviation of 2.9°C (5.2°F). Air temperature was adjusted to maintain a pavement temperature of 50°C±4°C (122°F±7°F), which is expected to promote rutting damage. The recorded pavement temperatures discussed in Section 4.3.4 indicate that the inside air temperatures were adjusted appropriately to maintain the required pavement temperature. The daily

average air temperatures recorded in the temperature control unit, calculated from the hourly temperatures recorded during HVS operation, are shown in Figure 4.5. Vertical error bars on each point on the graph show the daily temperature range.

4.3.4 Temperatures in the Asphalt Concrete Layers

Daily averages of the surface and in-depth temperatures of the asphalt concrete layers are listed in Table 4.1 and shown in Figure 4.6. Pavement temperatures decreased slightly with increasing depth in the pavement, which was expected as there is usually a thermal gradient between the top and bottom of the asphalt concrete pavement layers.

Table 4.1: 620HA: Temperature Summary for Air and Pavement

Temperature	Average (°C)	Std. Dev. (°C)	Average (°F)	Std. Dev. (°F)
Outside air	28	–	82	–
Inside air	42	2.9	107	5.2
Pavement surface	51	1.6	123	2.9
- 25 mm below surface	51	1.1	123	2.0
- 50 mm below surface	50	0.7	122	1.3
- 90 mm below surface	49	0.7	120	1.3
- 120 mm below surface	48	0.9	118	1.6
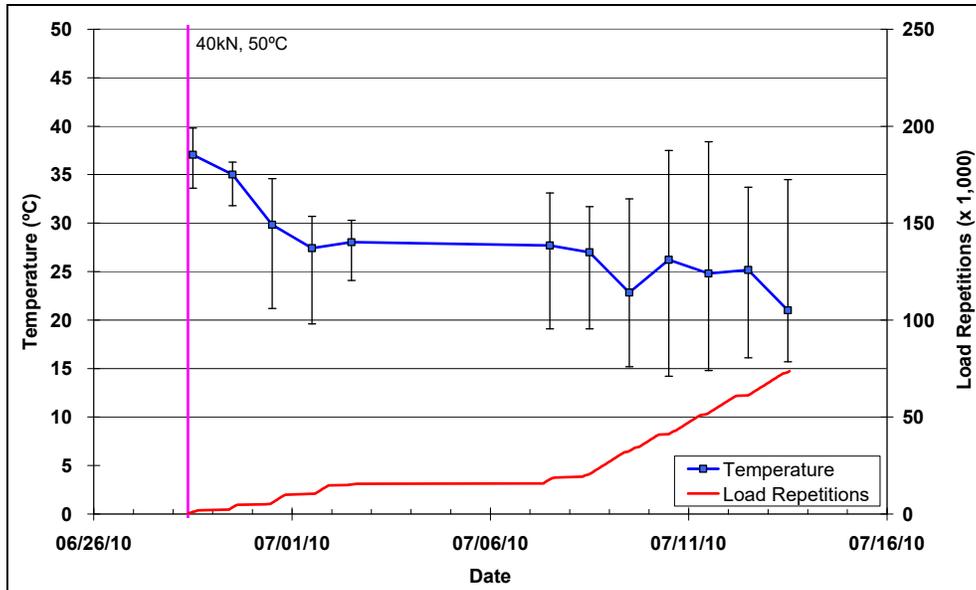
Figure 4.4: 620HA: Daily average outside air temperatures.

Figure 4.5: 620HA: Daily average inside air temperatures.
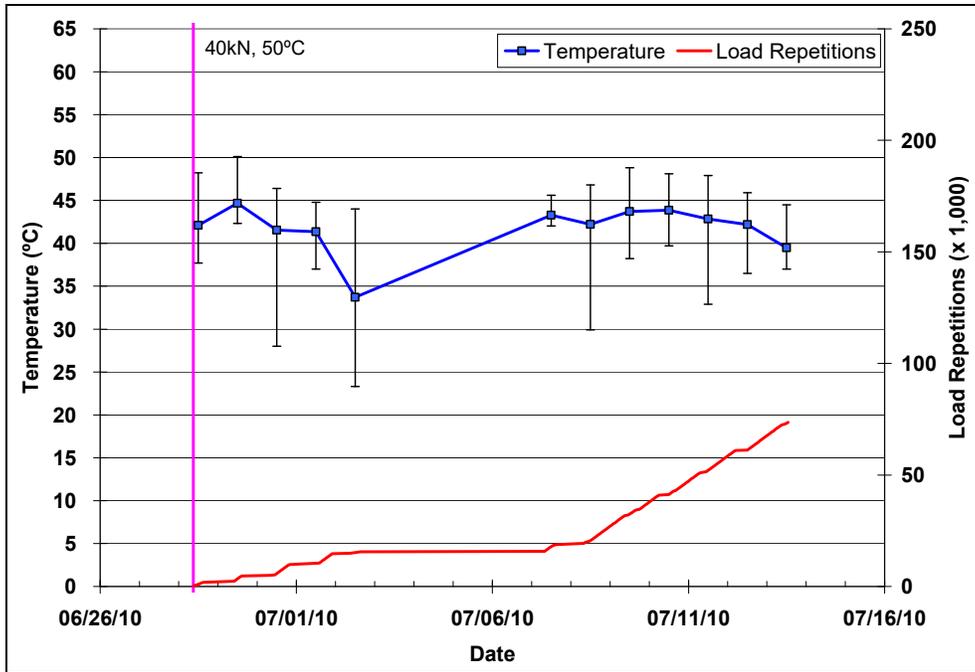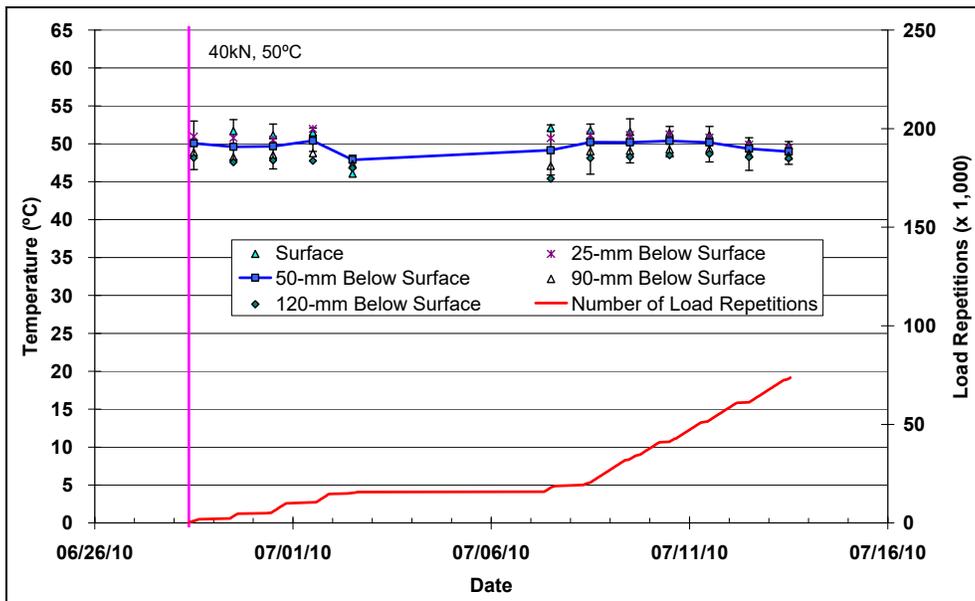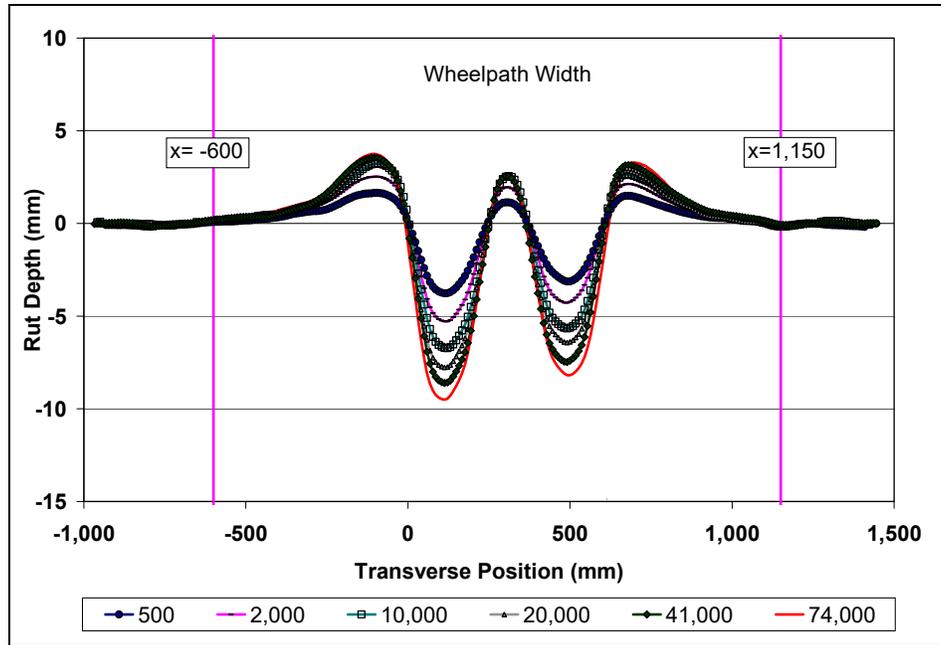

Figure 4.6: 620HA: Daily average temperatures at pavement surface and at various depths.

4.3.5   Permanent Surface Deformation (Rutting)

Figure 4.7 shows the average transverse cross section measured with the laser profilometer at various stages of the test. This plot clearly shows the increase in rutting and deformation over the duration of the test.

Figure 4.7: 620HA: Profilometer cross section at various load repetitions.

During HVS testing, rutting usually occurs at a high rate initially, and then it typically diminishes as trafficking progresses until reaching a steady state. This initial phase is referred to as the "embedment" phase. Figure 4.8 and Figure 4.9 show the development of permanent deformation (average maximum rut and average deformation, respectively) with load repetitions as measured with the laser profilometer for the test section. The embedment phase, although relatively short in terms of the number of load repetitions (i.e., ± 5,000), ended with a fairly significant rut of about 8.0 mm (0.32 in.). It was not clear why this occurred given that the air-void content of the layer was within an acceptable range. The combination of asphalt age (approximately six weeks after placement), high pavement temperatures, and relatively high loading probably influenced performance. Error bars on the average readings indicate that there was very little variation along the length of the section.

Figure 4.10 shows contour plots of the pavement surface at the start and end of the test (74,000 repetitions) that also indicate minimal variation along the section. A slightly deeper rut was recorded in one of the wheel tracks, which was attributed to the positioning of the HVS on the crossfall of the section. Terminal rut depth (12.5 mm [0.5 in.]) was reached after 46,000 repetitions. Testing was continued for an additional 28,000 repetitions to further assess rutting trends.

After completion of trafficking, the average maximum rut depth and the average deformation were 13.5 mm (0.53 in.) and 6.4 mm (0.25 in.), respectively. The maximum rut depth measured on the section was 15.6 mm (0.61 in.), recorded at Station 5.
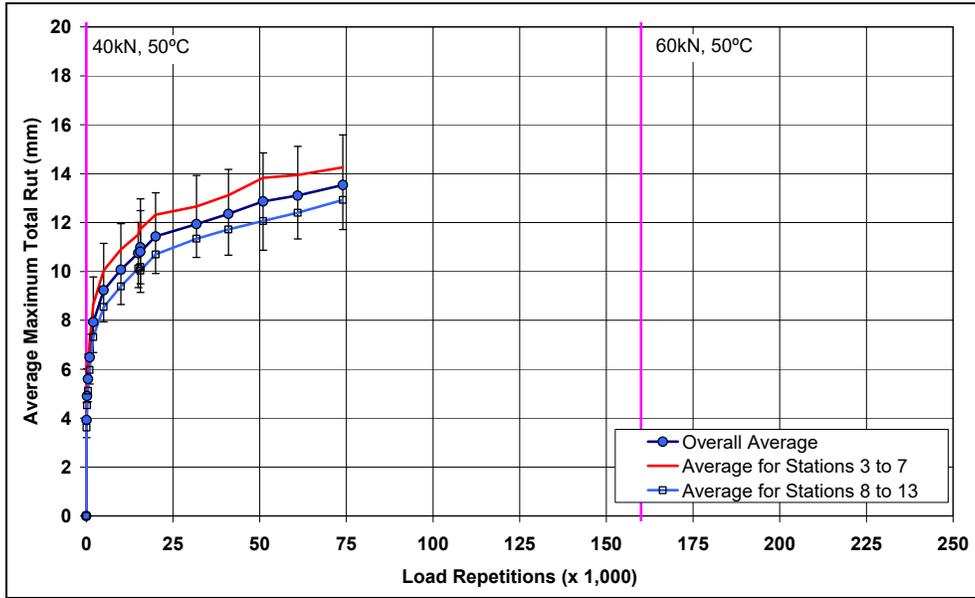
Figure 4.8: 620HA: Average maximum rut.
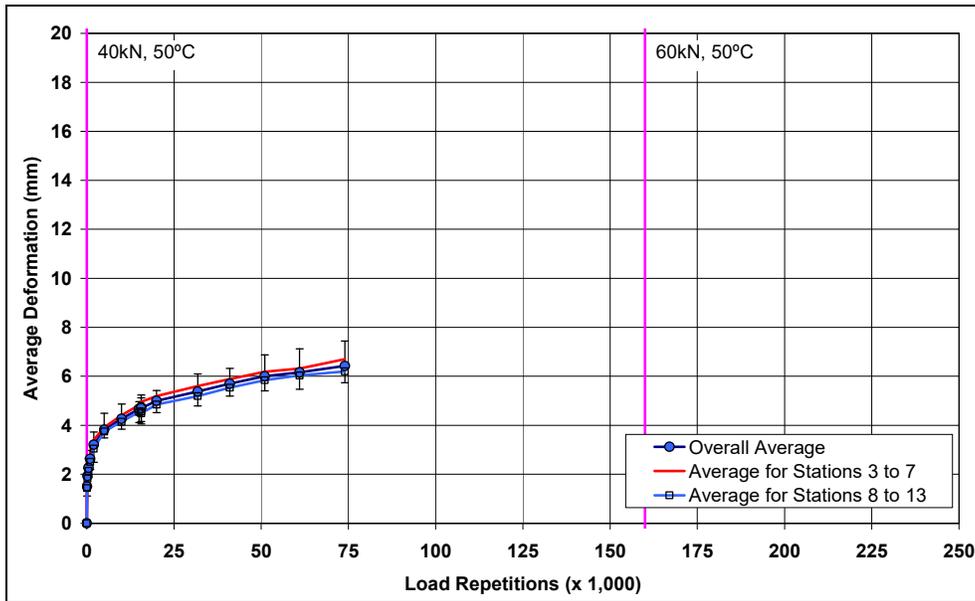
Figure 4.9: 620HA: Average deformation.
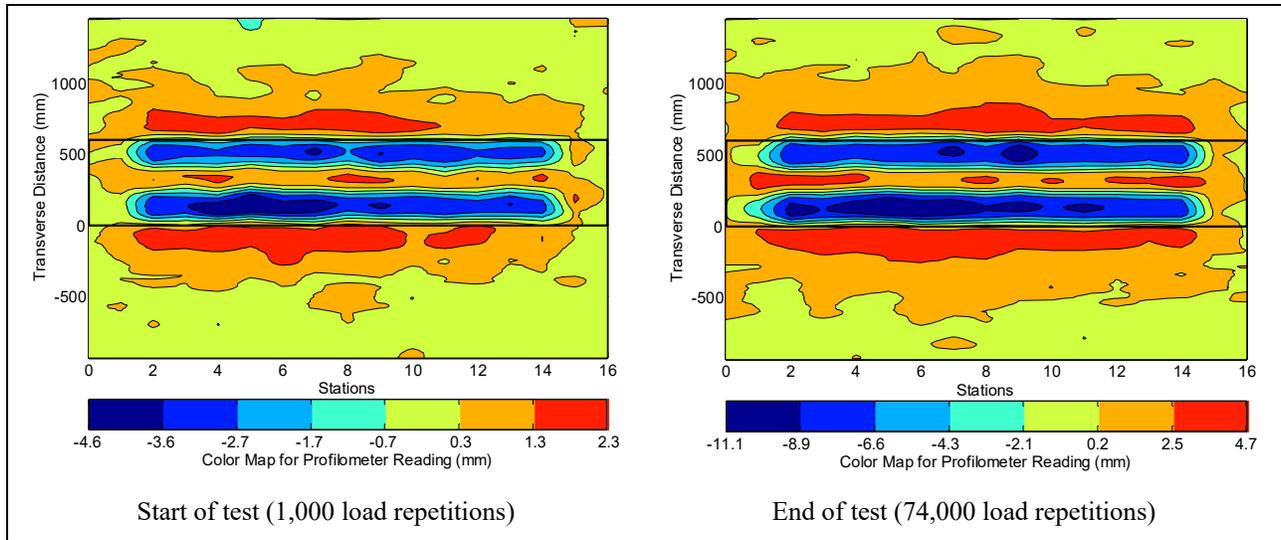
Figure 4.10: 620HA: Contour plots of permanent surface deformation.
(Note that key scales are different.)

4.3.6 Visual Inspection

Apart from rutting, no other distress was recorded on the section. Figure 4.11 is a photograph taken of the surface at the end of the test.
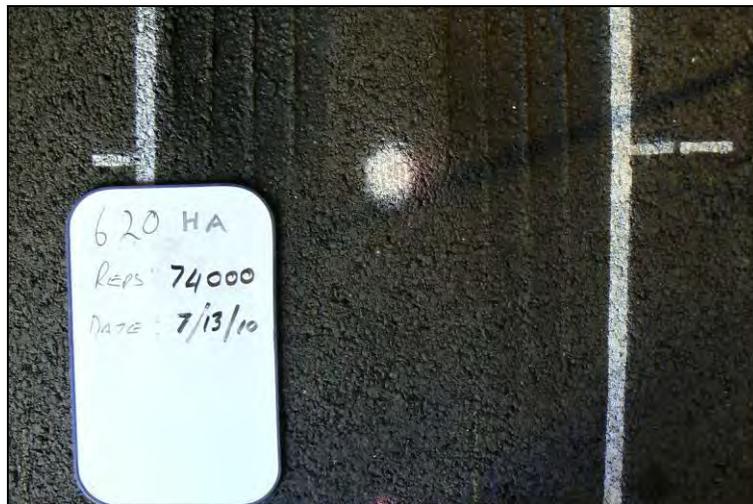
Figure 4.11: 620HA: Section photograph at test completion.

4.4 Section 621HA: Gencor

4.4.1 Test Summary

Loading commenced on July 16, 2010, and ended on August 03, 2010. A total of 159,000 load repetitions were applied and 23 datasets were collected. The HVS loading history for Section 621HA is shown in Figure 4.12. No breakdowns occurred during this test.
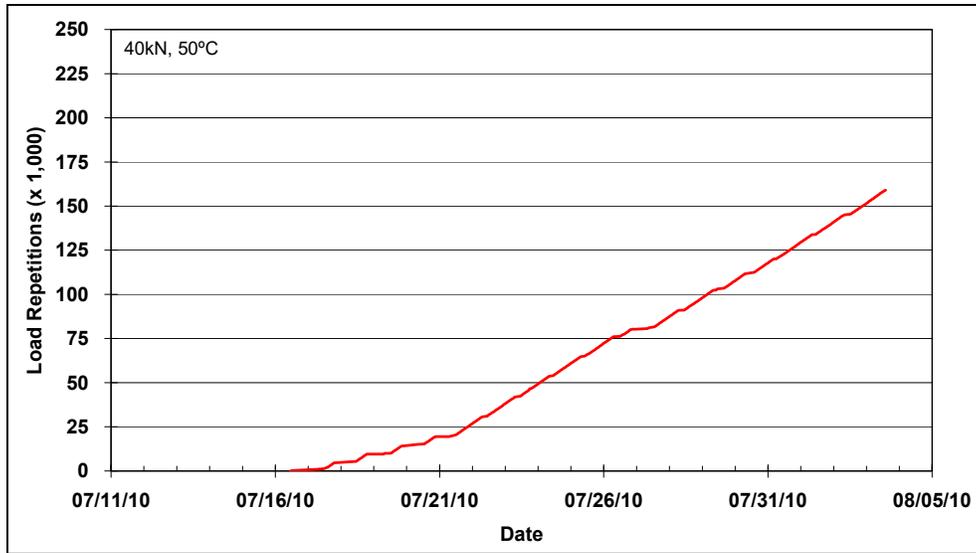
Figure 4.12: 621HA: Load history.

4.4.2 Outside Air Temperatures

Daily average outside air temperatures are summarized in Figure 4.13. Vertical error bars on each point on the graph show the daily temperature range. Temperatures ranged from 10°C to 45°C (50°F to 113°F) during the course of HVS testing, with a daily average of 25°C (77°F), an average minimum of 14°C (57°F), and an average maximum of 34°C (93°F). Outside air temperatures were in a similar range to those recorded during testing of the Control.
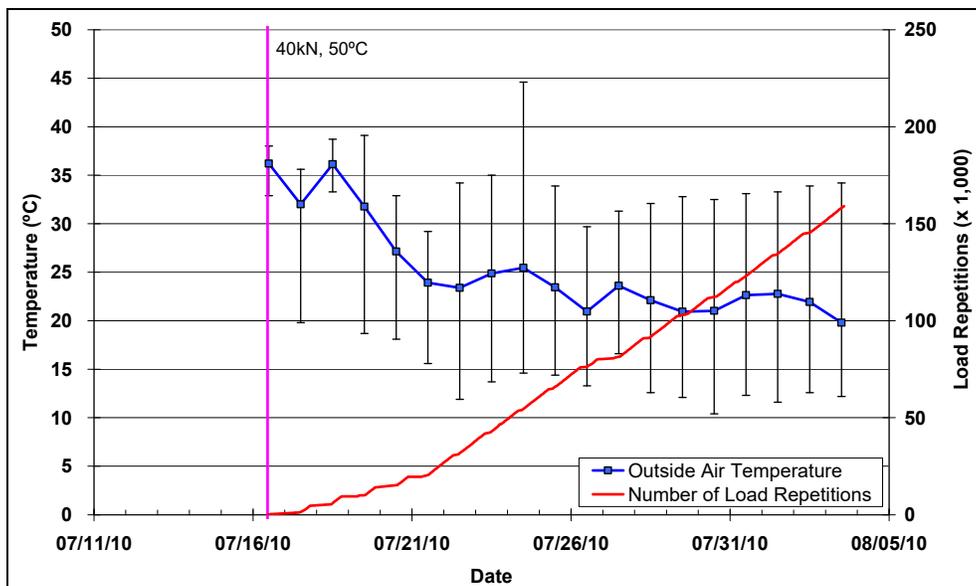
Figure 4.13: 621HA: Daily average outside air temperatures.

4.4.3   Air Temperatures in the Temperature Control Unit

During the test, the measured air temperatures inside the temperature control chamber ranged from 33°C to 53°C (91°F to 127°F) with an average of 42°C (108°F) and standard deviation of 3.7°C (6.7°F). The air temperature was adjusted to maintain a pavement temperature of 50°C±4°C (122°F±7°F). The daily average air temperatures recorded in the temperature control unit, calculated from the hourly temperatures recorded during HVS operation, are shown in Figure 4.14. Vertical error bars on each point on the graph show the daily temperature range.
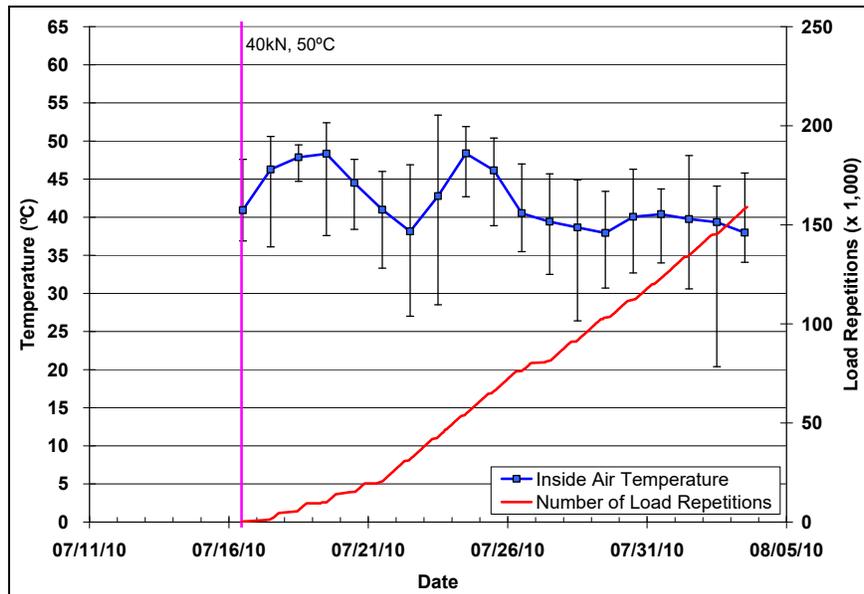
Figure 4.14: 621HA: Daily average inside air temperatures.

4.4.4   Temperatures in the Asphalt Concrete Layers

Daily averages of the surface and in-depth temperatures of the asphalt concrete layers are listed in Table 4.2 and shown in Figure 4.15. Data for the Control section are included for comparison. Temperatures were very similar to those recorded on the Control section. Pavement temperatures decreased slightly with increasing depth in the pavement, as expected. Average pavement temperatures at all depths of Section 621HA were similar to those recorded on the Control.

Table 4.2: 621HA: Temperature Summary for Air and Pavement

Temperature	621HA				620HA
	Average (°C)	Std. Dev. (°C)	Average (°F)	Std. Dev. (°F)	Average (°C)
Outside air	25	-	77	-	28
Inside air	42	3.7	108	6.7	42
Pavement surface	49	1.3	120	2.3	51
- 25 mm below surface	50	0.9	122	1.6	51
- 50 mm below surface	50	0.7	122	1.3	50
- 90 mm below surface	49	0.8	120	1.4	49
- 120 mm below surface	48	0.9	118	1.6	48
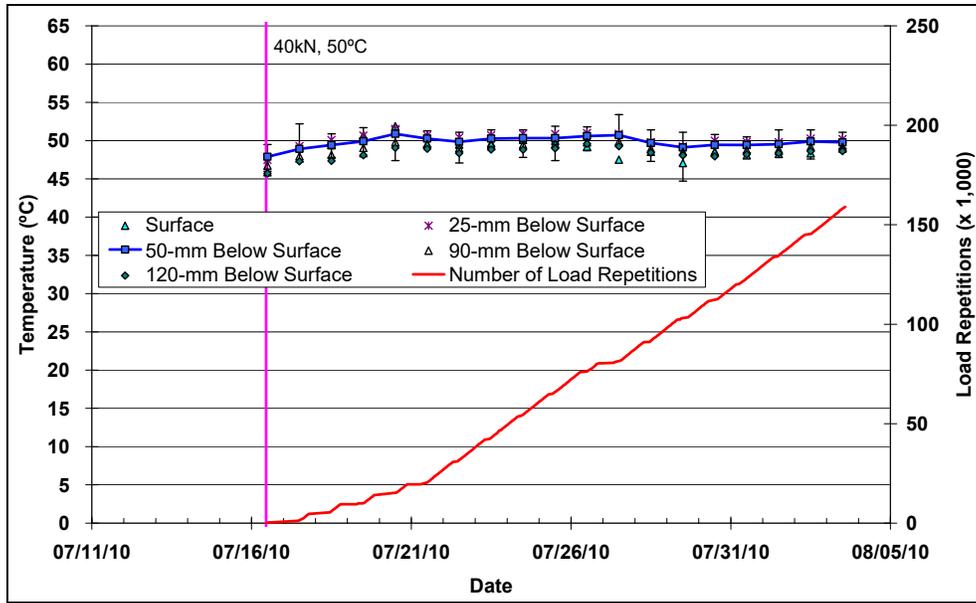
Figure 4.15: 621HA: Daily average temperatures at pavement surface and at various depths.

4.4.5 Permanent Surface Deformation (Rutting)

Figure 4.16 shows the average transverse cross section measured with the laser profilometer at various stages of the test and shows the increase in rutting and deformation over time.

Figure 4.16: 621HA: Profilometer cross section at various load repetitions.

Figure 4.17 and Figure 4.18 show the development of permanent deformation (average maximum rut and average deformation, respectively) with load repetitions as measured with the laser profilometer for the test section. Results for the Control section (Section 620HA) are also shown for comparative purposes. Although the embedment phase was of similar 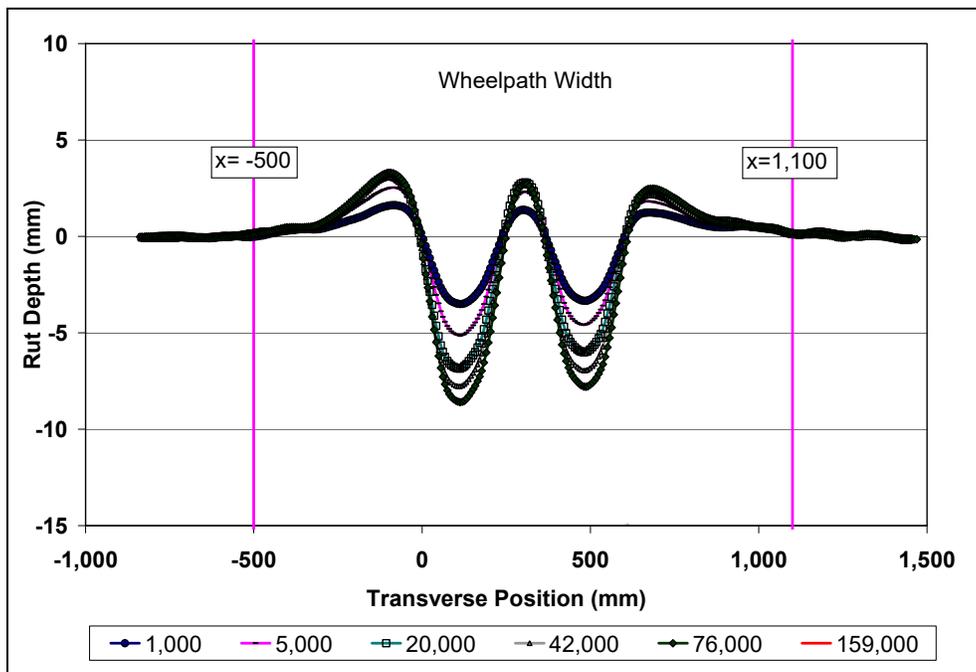duration for both sections, a slightly shallower average maximum rut was recorded on Section 621HA at the end of the embedment phase (6.5 mm [0.26 in.]) compared to the control (7.9 mm [0.31 in.]), despite this section having a slightly higher air-void content than the Control section (6.3 percent compared to 4.9 percent) and having thinner asphalt layers than the Control (see Section 5.7 for forensic investigation measurements). This behavior differs from earlier testing on dense-graded mixes with conventional binders, which have typically shown warm mixes to have deeper rutting than the control at the end of the embedment phases. The better rutting performance on this mix could be related to the additional "curing" time between construction and the start of HVS testing. These parameters are being investigated in another phase of the Caltrans warm-mix asphalt study and will be discussed in a separate report. After the embedment phase, the Gencor section continued to deform at a slightly slower rate than the control, equating to considerably more load repetitions being applied before the terminal rut depth of 12.5 mm (0.5 in.) was reached (112,000 repetitions compared to 46,000 repetitions on the control). Average deformation (down rut) on the Gencor section was slightly higher than that recorded on the Control (6.7 mm [0.26 in.] compared to 6.4 mm [0.25 in.]). Error bars on the average reading indicate that there was very little variation along the length of the section.
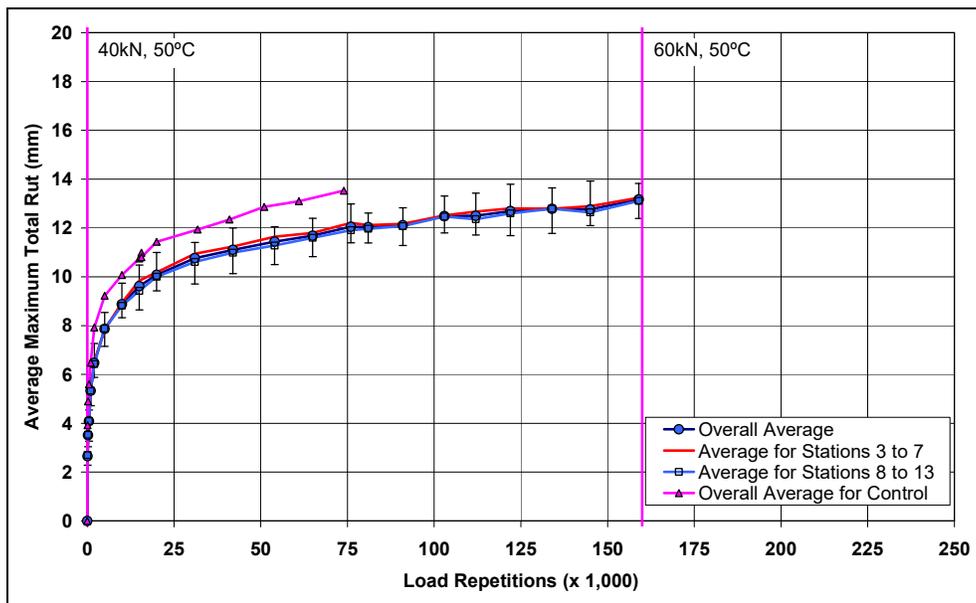
Figure 4.17: 621HA: Average maximum rut.
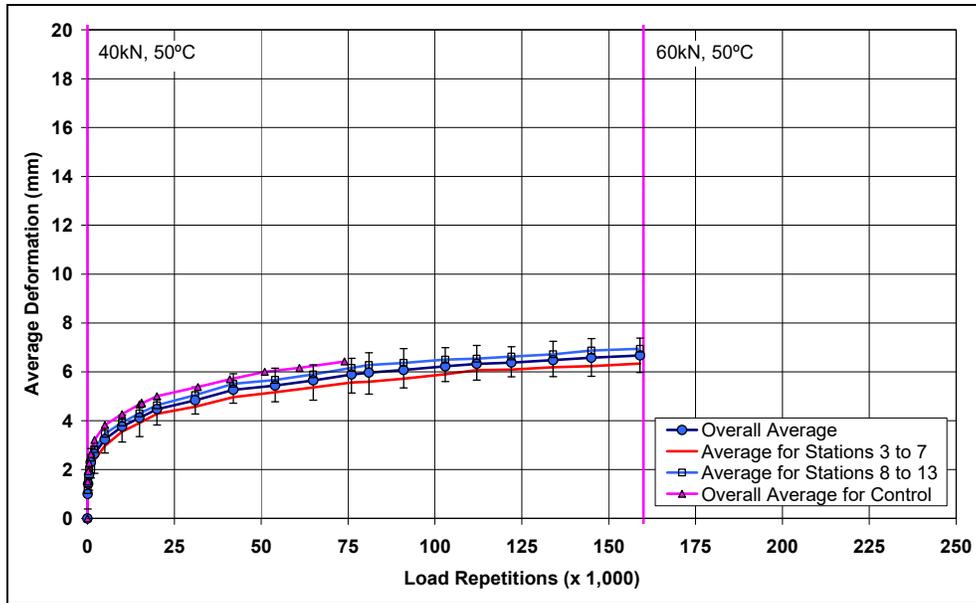
Figure 4.18: 621HA: Average deformation.

Figure 4.19 shows contour plots of the pavement surface at the start and end of the test (159,000 repetitions), also indicating minimal variation along the section.

After completion of trafficking, the average maximum rut depth and the average deformation were 13.2 mm (0.52 in.) and 6.7 mm (0.26 in.), respectively. The maximum rut depth measured on the section was 13.8 mm (0.54 in.) recorded at Station 11.

Start of test (1,000 load repetitions) End of test (159,000 load repetitions)
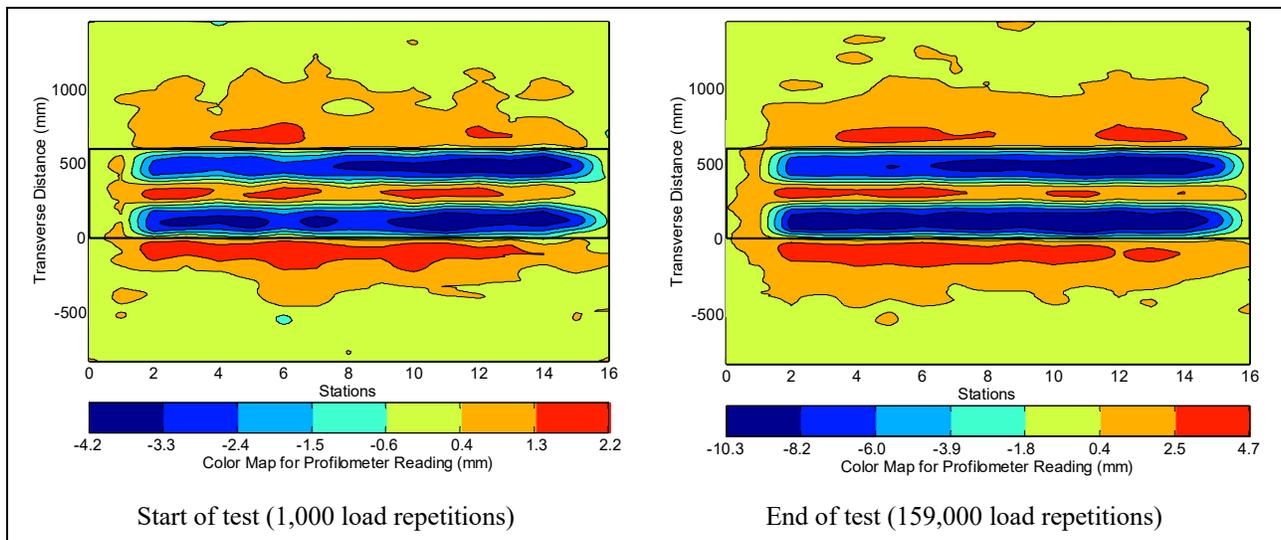
Figure 4.19: 621HA: Contour plots of permanent surface deformation.
(Note that key scales are different.)

4.4.6 Visual Inspection

Apart from rutting, no other distress was recorded on the section, which was similar in appearance to the Control (Figure 4.11) at the end of testing. Figure 4.20 shows a photograph taken of the surface at the end of the test.

Figure 4.20: 621HA: Section photograph at test completion.

4.5 Section 622HA: Evotherm

4.5.1 Test Summary

Loading commenced on August 9, 2010, and ended on September 3, 2010. A total of 200,000 load repetitions were applied and 29 datasets were collected. Terminal rut (i.e., 12.5 mm [0.5 in.]) was reached after 42,000 repetitions, which was very similar to the Control section (46,000). However, testing was continued for the additional 158,000 repetitions to gather rutting performance data for a separate mechanistic-empirical modeling study. Load was increased to 60 kN (13,500 lb) after 160,000 repetitions as part of this additional study. Results from this additional testing are not discussed in this report. The HVS loading history for Section 622HA is shown in Figure 4.21. A short carriage computer breakdown occurred in the latter part of the test.
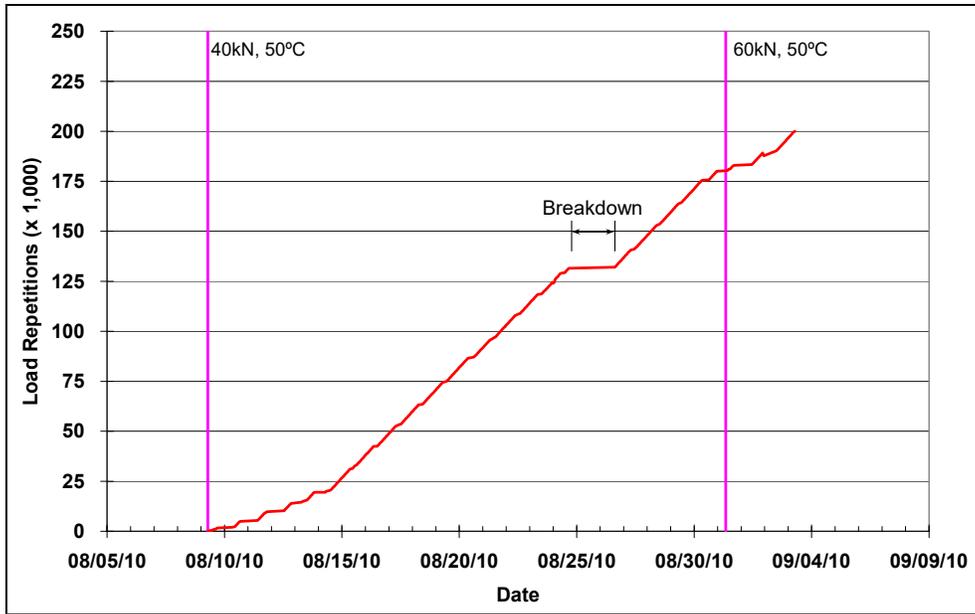
Figure 4.21: 622HA: Load history.

4.5.2 Outside Air Temperatures

Daily average outside air temperatures are summarized in Figure 4.22. Vertical error bars on each point on the graph show the daily temperature range. Temperatures ranged from 11°C to 40°C (52°F to 104°F) during the course of HVS testing, with a daily average of 24°C (75°F), an average minimum of 16°C (61°F), and an average maximum of 31°C (88°F). Outside air temperatures were slightly cooler during testing on Section 622HA compared to those during testing of the Control.
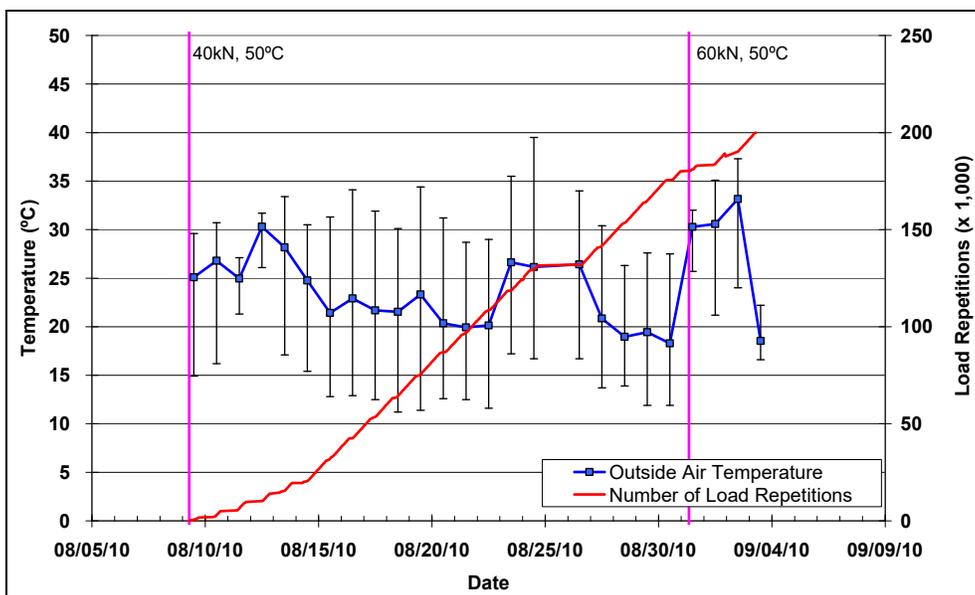
Figure 4.22: 622HA: Daily average outside air temperatures.

4.5.3 Air Temperatures in the Temperature Control Unit

During the test, air temperatures inside the temperature control chamber ranged from 25°C to 55°C (77°F to 131°F) with an average of 42°C (108°F) and standard deviation of 2.6°C (4.7°F). The air temperature was adjusted to maintain a pavement temperature of 50°C±4°C (122°F±7°F). The daily average air temperatures recorded in the temperature control unit, calculated from the hourly temperatures recorded during HVS operation, are shown in Figure 4.23. Vertical errors bars on each point on the graph show the daily temperature range.
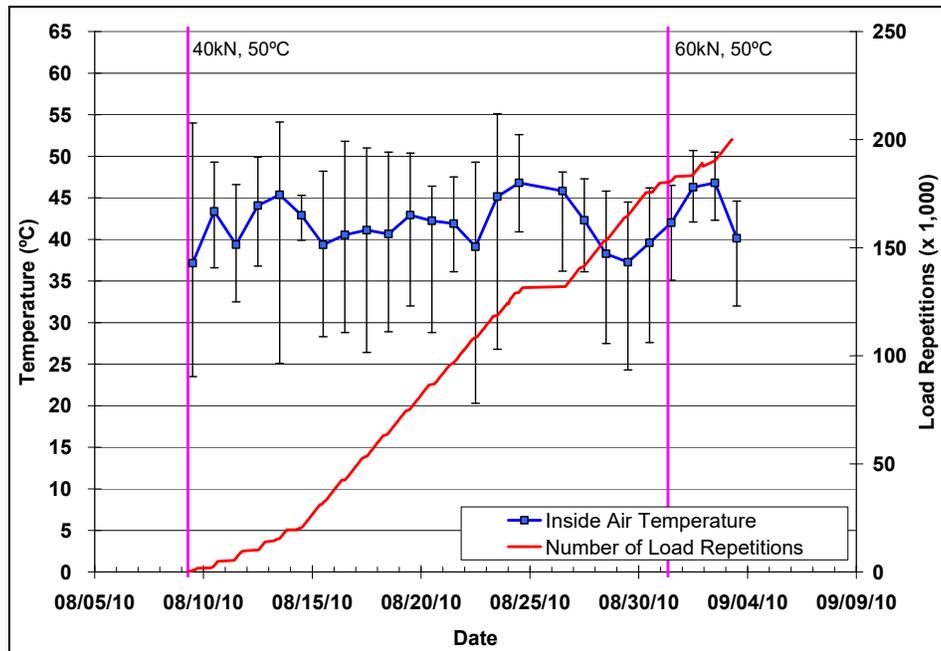
Figure 4.23: 622HA: Daily average inside air temperatures.

4.5.4 Temperatures in the Asphalt Concrete Layers

Daily averages of the surface and in-depth temperatures of the asphalt concrete layers are listed in Table 4.3 and shown in Figure 4.24. Pavement temperatures decreased slightly with increasing depth in the pavement, as expected. Average pavement temperatures at all depths of Section 622HA were similar to those recorded on the Control, despite slightly lower outside temperatures.

Table 4.3: 622HA: Temperature Summary for Air and Pavement

Temperature	622HA				620HA
	Average (°C)	Std. Dev. (°C)	Average (°F)	Std. Dev. (°F)	Average (°C)
Outside air	24	-	75	-	28
Inside air	42	3.7	108	6.7	42
Pavement surface	51	1.3	124	2.3	51
- 25 mm below surface	50	1.2	122	2.2	51
- 50 mm below surface	50	1.1	122	2.0	50
- 90 mm below surface	49	1.0	120	1.8	49
- 120 mm below surface	48	1.0	118	1.8	48
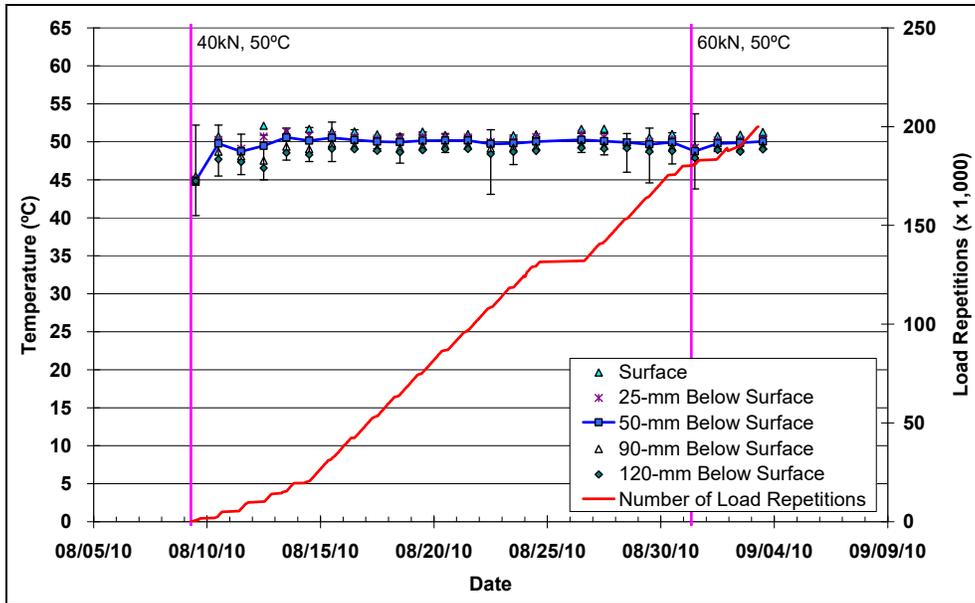
Figure 4.24: 622HA: Daily average temperatures at pavement surface and at various depths.

4.5.5   Permanent Surface Deformation (Rutting)

Figure 4.25 shows the average transverse cross section measured with the laser profilometer at various stages of the test, and shows the increase in rutting and deformation over time.
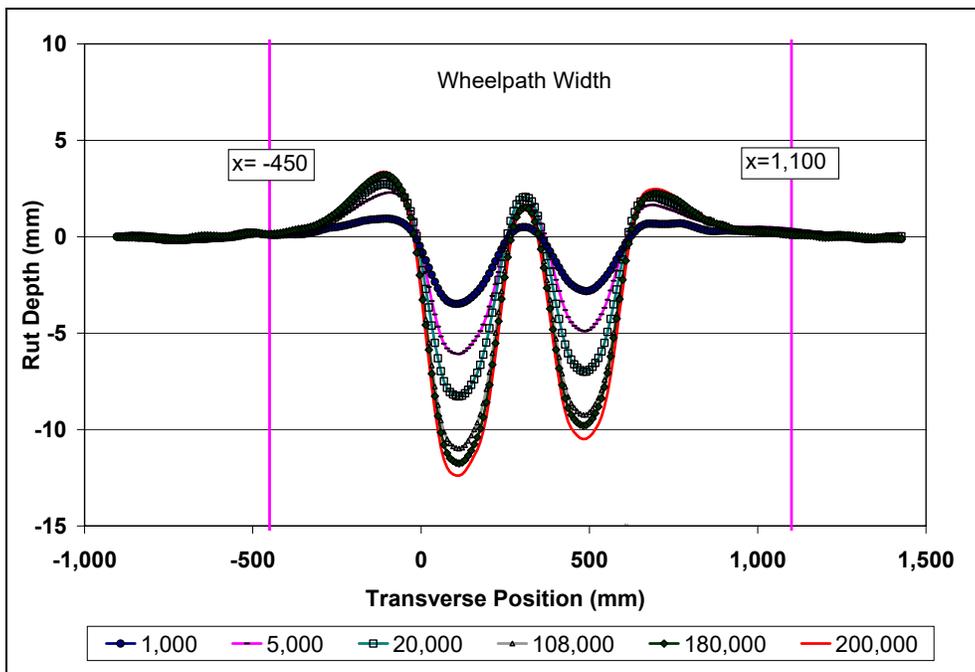
Figure 4.25: 622HA: Profilometer cross section at various load repetitions.

Figure 4.26 and Figure 4.27 show the development of permanent deformation (average maximum rut and average deformation, respectively) with load repetitions as measured with the laser profilometer for the test section. Results for the Control section (Section 620HA) are also shown for comparative purposes. The embedment phases for the Evotherm and Control sections were almost identical, both in terms of duration and rut depth, despite this section having a slightly higher air-void content than the Control section (6.2 percent compared to 4.9 percent) and thinner asphalt layers (see Section 5.7 for forensic investigation discussion). Rutting performance after the embedment phase was similar for both sections with a similar number of load repetitions being applied before the terminal rut depth of 12.5 mm (0.5 in.) was reached (42,000 repetitions compared to 46,000 on the control). This was despite the thinner asphalt layers and very low production and paving temperatures of the Evotherm mix, which would typically result in a mix with lower stiffness than a mix produced at higher temperatures, and consequently poorer rutting performance. Average deformation (down rut) on the Evotherm section was slightly higher than that recorded on the Control (7.2 mm [0.28 in.] compared to 6.4 mm [0.25 in.]) when the terminal rut was reached. Error bars on the average reading indicate that there was some variation along the length of the section, with a slightly deeper rut between Stations 8 and 13 compared to Stations 2 and 7.
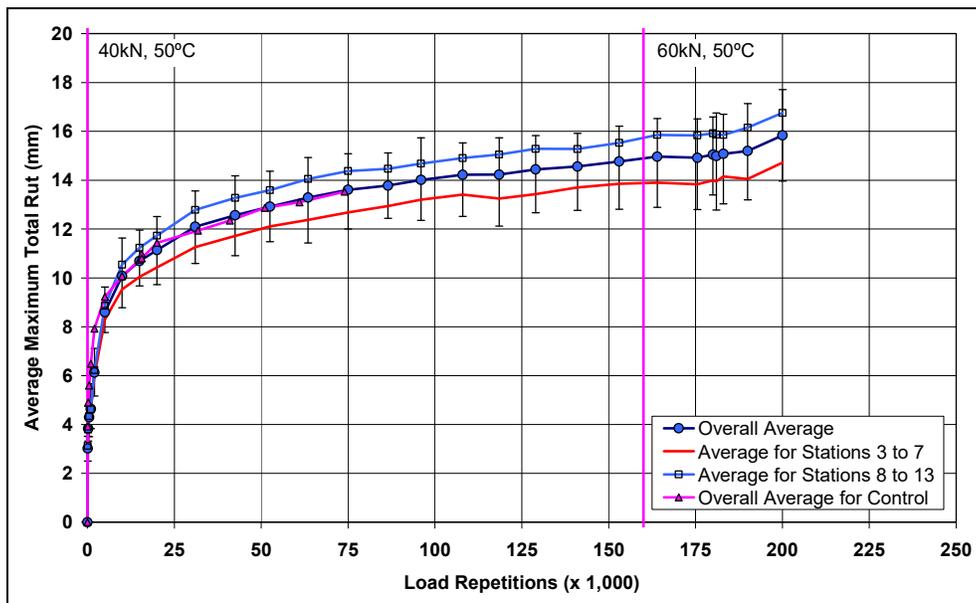
Figure 4.26: 622HA: Average maximum rut.
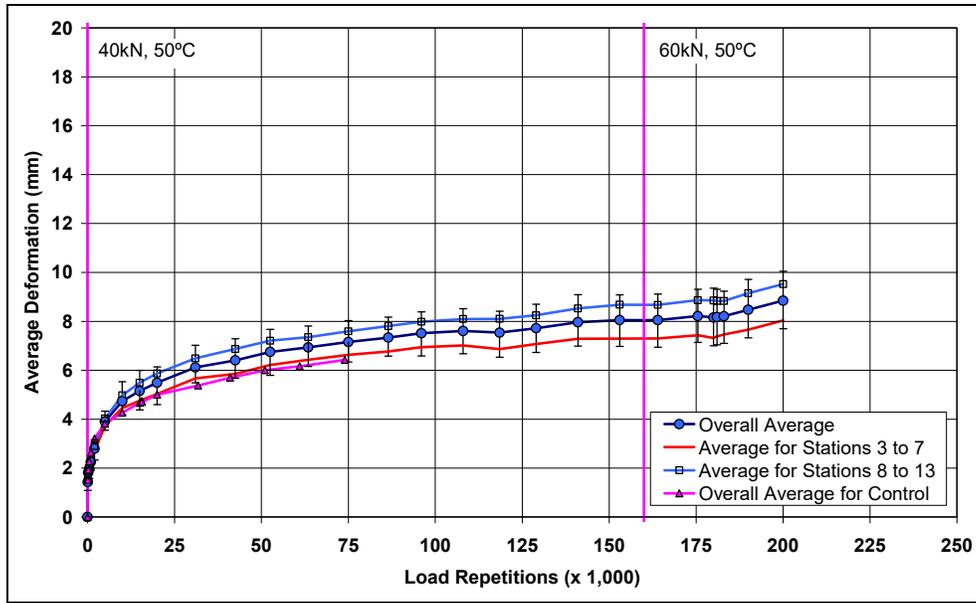
Figure 4.27: 622HA: Average deformation.

Figure 4.28 shows contour plots of the pavement surface at the start and end of the test (200,000 repetitions), also indicating a slightly deeper average maximum rut on one half of the section.

The mix showed some load sensitivity after the load change to 60 kN, as expected. After completion of all trafficking, the average maximum rut depth and the average deformation were 15.8 mm (0.62 in.) and 8.8 mm (0.35 in.), respectively. The maximum rut depth measured on the section was 17.7 mm (0.70 in.) recorded at Station 11.

Start of test (1,000 load repetitions)   End of test (200,000 load repetitions)
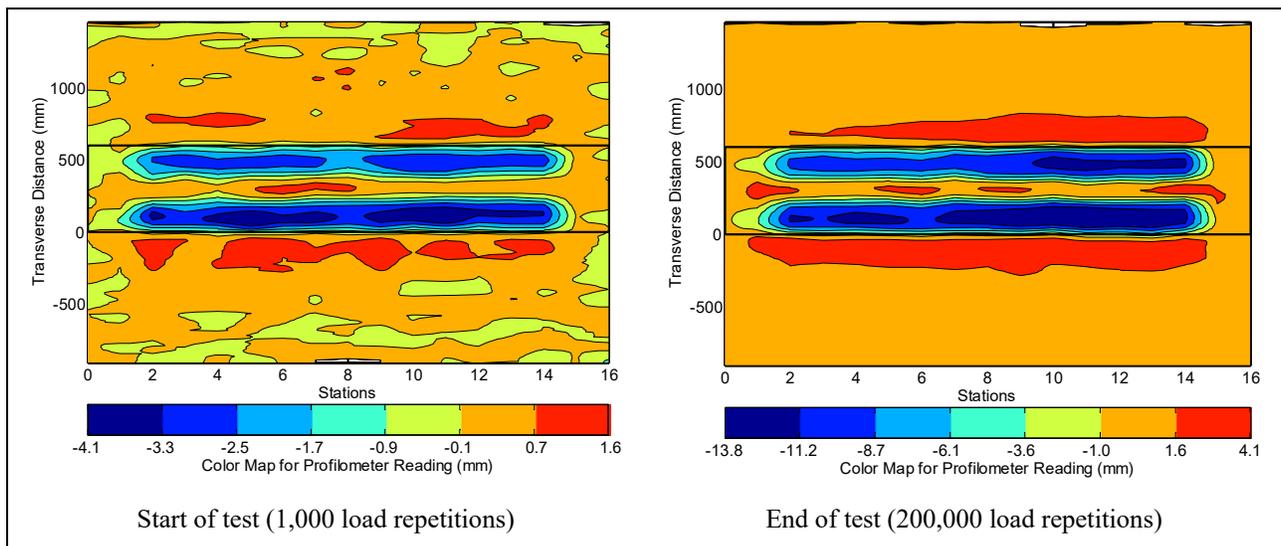
Figure 4.28: 622HA: Contour plots of permanent surface deformation.
(Note that key scales are different.)

4.5.6   Visual Inspection

Apart from rutting, no other distress was recorded on the section. Figure 4.29 shows a photograph taken of the surface at the end of the test.

Figure 4.29: 622HA: Section photograph at test completion.

4.6   Section 623HA: Cecabase

4.6.1   Test Summary

Loading commenced on October 25, 2010, and ended on December 8, 2010. A total of 224,000 load repetitions were applied and 30 datasets were collected. Load was increased to 60 kN (13,500 lb) after 160,000 load repetitions in line with the test plan. The HVS loading history for Section 623HA is shown in Figure 4.30. Two carriage computer breakdowns occurred in the latter part of the test.

4.6.2   Outside Air Temperatures

Daily average outside air temperatures are summarized in Figure 4.31. Vertical error bars on each point on the graph show the daily temperature range. Temperatures ranged from 0°C to 28°C (32°F to 82°F) during the course of HVS testing, with a daily average of 13°C (55°F), an average minimum of 9°C (48°F), and an average maximum of 18°C (64°F). Average outside air temperatures were considerably cooler during testing on Section 623HA compared to those during testing on the Control (daily average of 15°C [27°F] cooler).
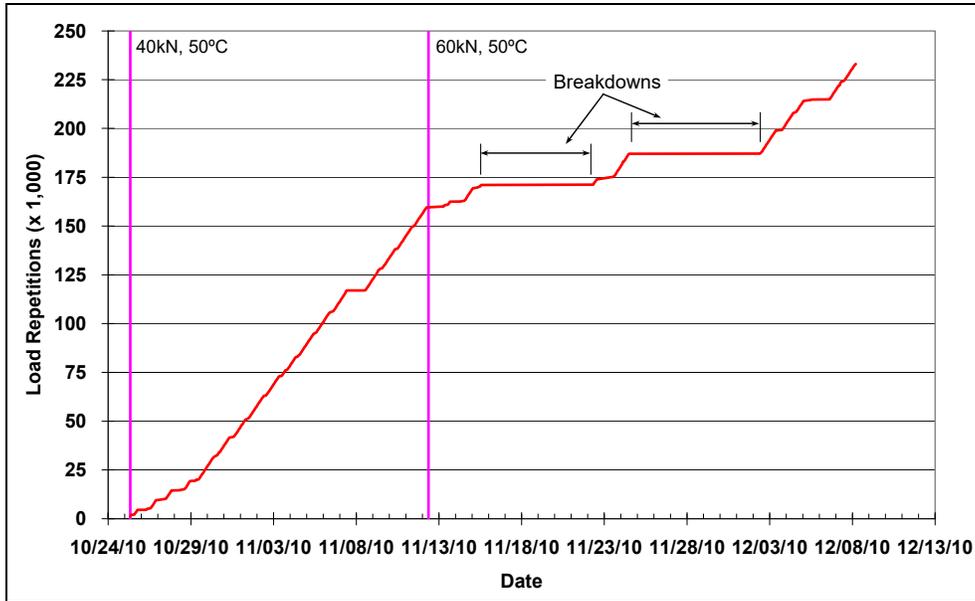
Figure 4.30: 623HA: Load history.
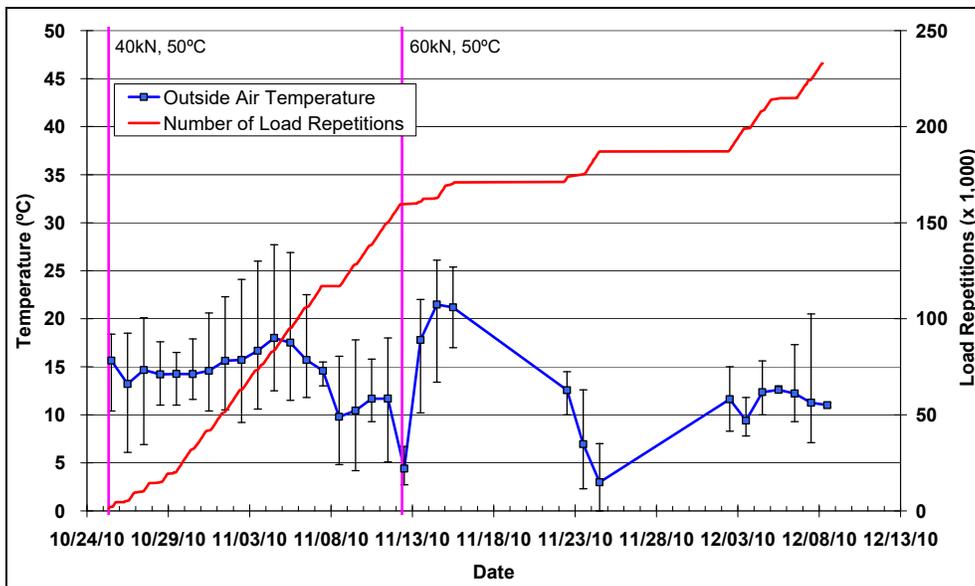
Figure 4.31: 623HA: Daily average outside air temperatures.

4.6.3   Air Temperatures in the Temperature Control Unit

During the test, air temperatures inside the temperature control chamber ranged from 35°C to 46°C (95°F to 115°F) with an average of 41°C (106°F) and standard deviation of 3°C (5°F). The air temperature was

adjusted to maintain a pavement temperature of 50°C±4°C (122°F±7°F). The daily average air temperatures recorded in the temperature control unit, calculated from the hourly temperatures recorded during HVS operation, are shown in Figure 4.32. Vertical error bars on each point on the graph show the daily temperature range.
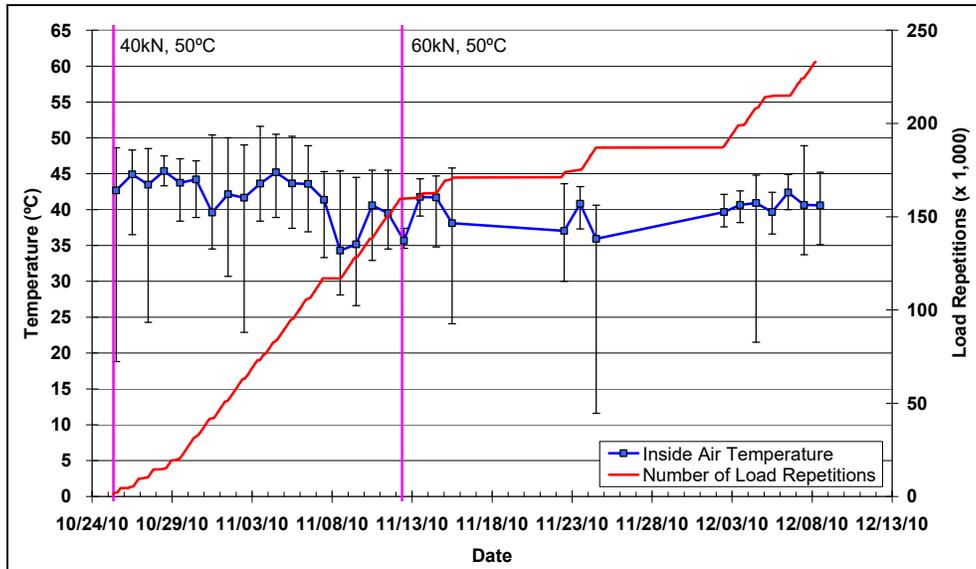
Figure 4.32: 623HA: Daily average inside air temperatures.

4.6.4   Temperatures in the Asphalt Concrete Layers

Daily averages of the surface and in-depth temperatures of the asphalt concrete layers are listed in Table 4.4 and shown in Figure 4.33. Pavement temperatures decreased slightly with increasing depth in the pavement, as expected. Average pavement temperatures at all depths on Section 623HA were similar to those recorded on the Control, despite lower outside temperatures.

Table 4.4: 623HA: Temperature Summary for Air and Pavement

Temperature	623HA				620HA
	Average (°C)	Std. Dev. (°C)	Average (°F)	Std. Dev. (°F)	Average (°C)
Outside air	13	-	55	-	28
Inside air	41	3.0	106	5.4	42
Pavement surface	49	1.9	120	3.4	51
- 25 mm below surface	50	1.4	122	2.5	51
- 50 mm below surface	50	1.3	122	2.3	50
- 90 mm below surface	49	1.3	120	2.3	49
- 120 mm below surface	49	1.3	120	2.3	48
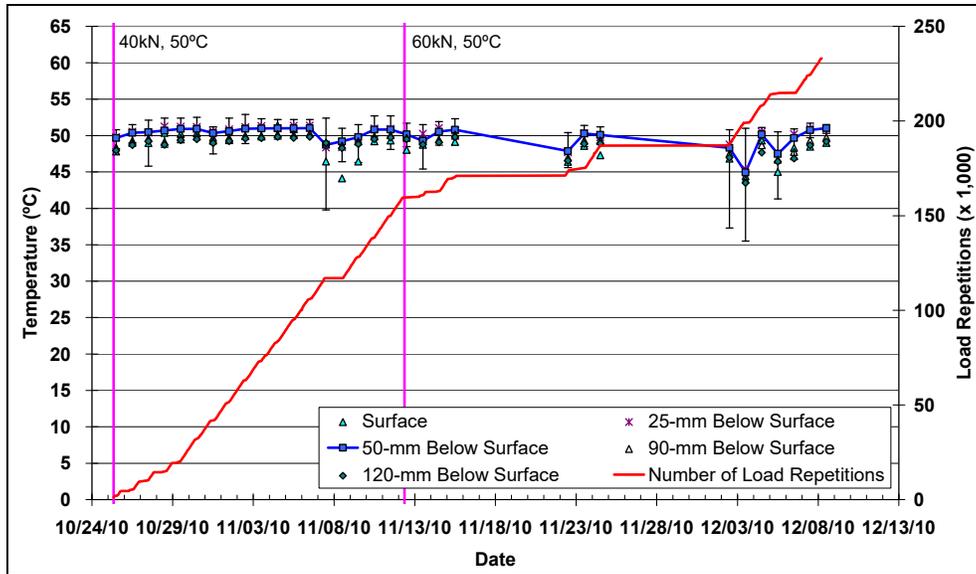
Figure 4.33: 623HA: Daily average temperatures at pavement surface and at various depths.

4.6.5   Permanent Surface Deformation (Rutting)

Figure 4.34 shows the average transverse cross section measured with the laser profilometer at various stages of the test and shows the increase in rutting and deformation over time.
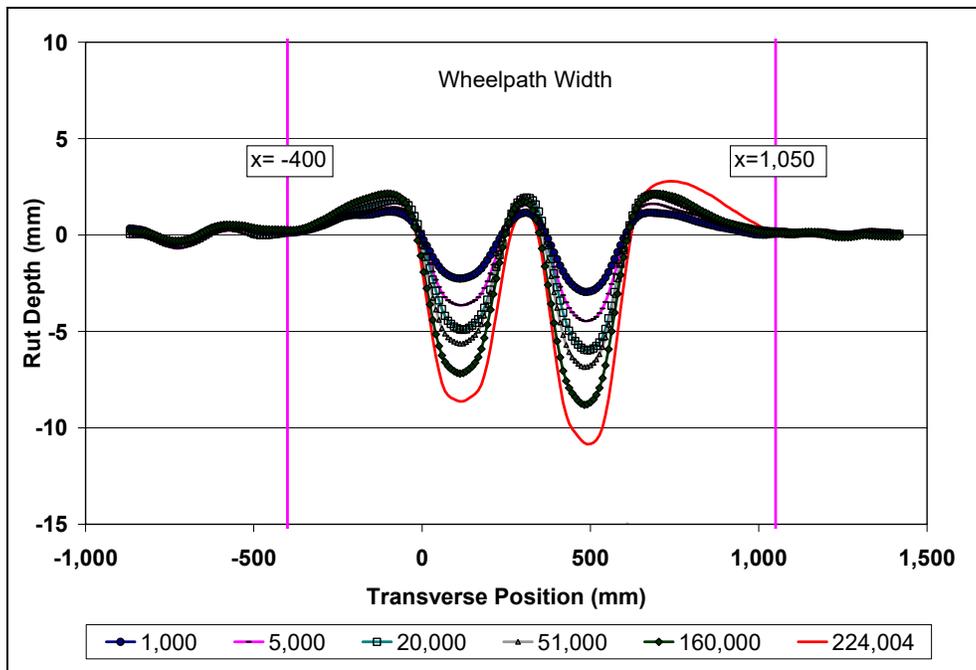
Figure 4.34: 623HA: Profilometer cross section at various load repetitions.

Figure 4.35 and Figure 4.36 show the development of permanent deformation (average maximum rut and average deformation, respectively) with load repetitions as measured with the laser profilometer for the test section. Results for the Control section (Section 620HA) are also shown for comparative purposes. Although the embedment phase was of similar duration for both sections, a shallower average maximum rut was recorded on Section 623HA at the end of the embedment phase (5.5 mm [0.22 in.]) compared to the control (7.9 mm [0.31 in.]) despite this section having a slightly higher air-void content than the Control section (6.4 percent compared to 4.9 percent) and slightly thinner asphalt layers (see Section 5.7). This behavior again differs from earlier testing on dense-graded mixes with conventional binders, which typically showed warm mixes to have deeper rutting than the control at the end of the embedment phase. Rutting performance on this mix was again attributed to the additional "curing" time between construction and the start of HVS testing (testing on this section started four months after the start of the Control). After the embedment phase, the Cecabase section deformed at a considerably slower rate than the Control, equating to considerably more load repetitions being applied before the terminal rut depth of 12.5 mm (0.5 in.) was reached (200,000 repetitions compared to 46,000 on the control). The rate of deformation increased after the load change to 60 kN, as expected. Average deformation (down rut) on the Cecabase section was slightly higher than that recorded on the Control (7.5 mm [0.30 in.] compared to 6.4 mm [0.25 in.]). This was attributed to the higher number of load repetitions. Error bars on the average reading indicate that there was very little variation along the length of the section.
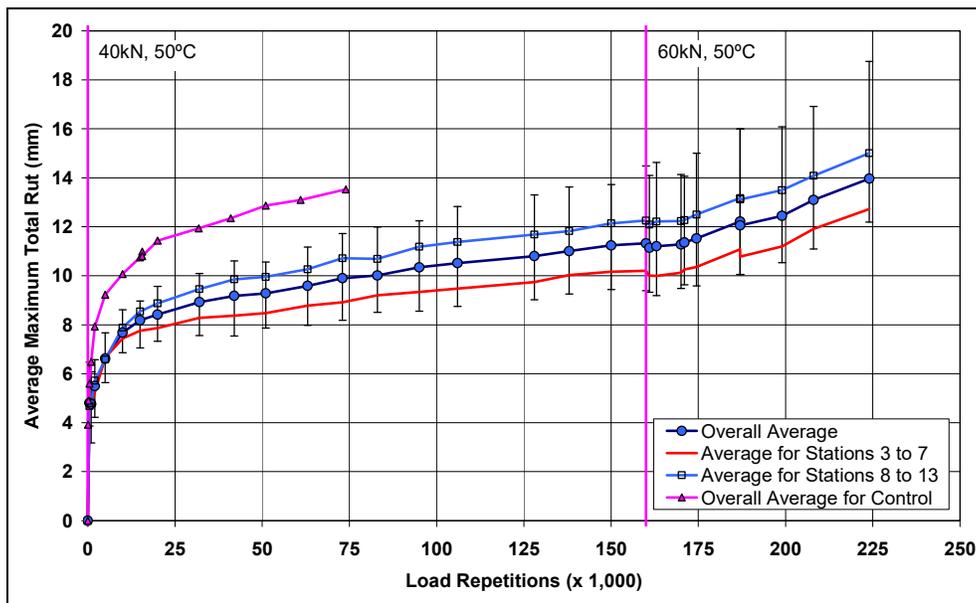
Figure 4.35: 623HA: Average maximum rut.
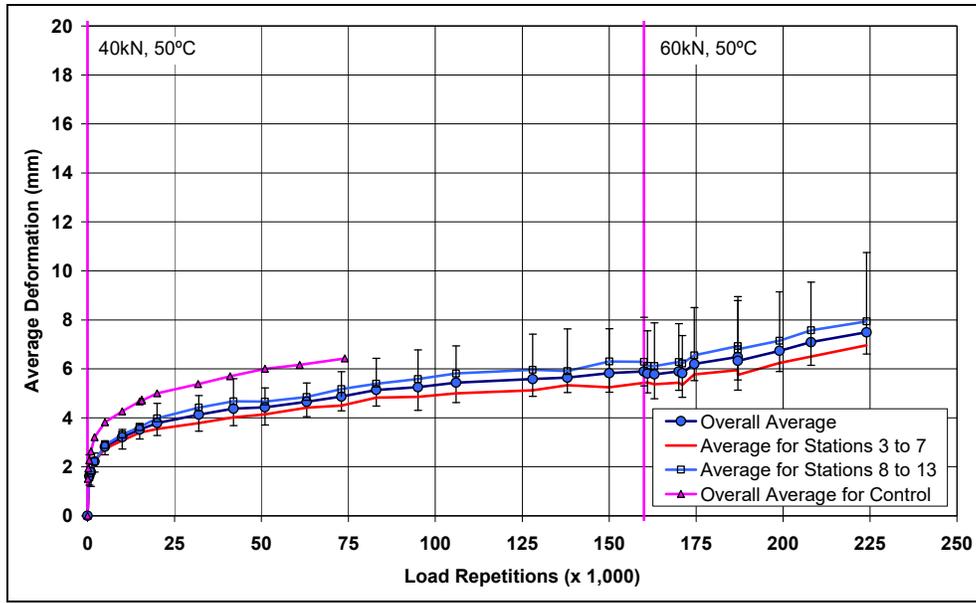
Figure 4.36: 623HA: Average deformation.

Figure 4.37 shows contour plots of the pavement surface at the start and end of the test (224,000 repetitions), also indicating minimal variation along the section.

After completion of trafficking, the average maximum rut depth and the average deformation were 14.0 mm (0.55 in.) and 7.5 mm (0.30 in.), respectively. The maximum rut depth measured on the section was 18.8 mm (0.74 in.) recorded at Station 8.

Start of test (1,000 load repetitions)   End of test (224,000 load repetitions)
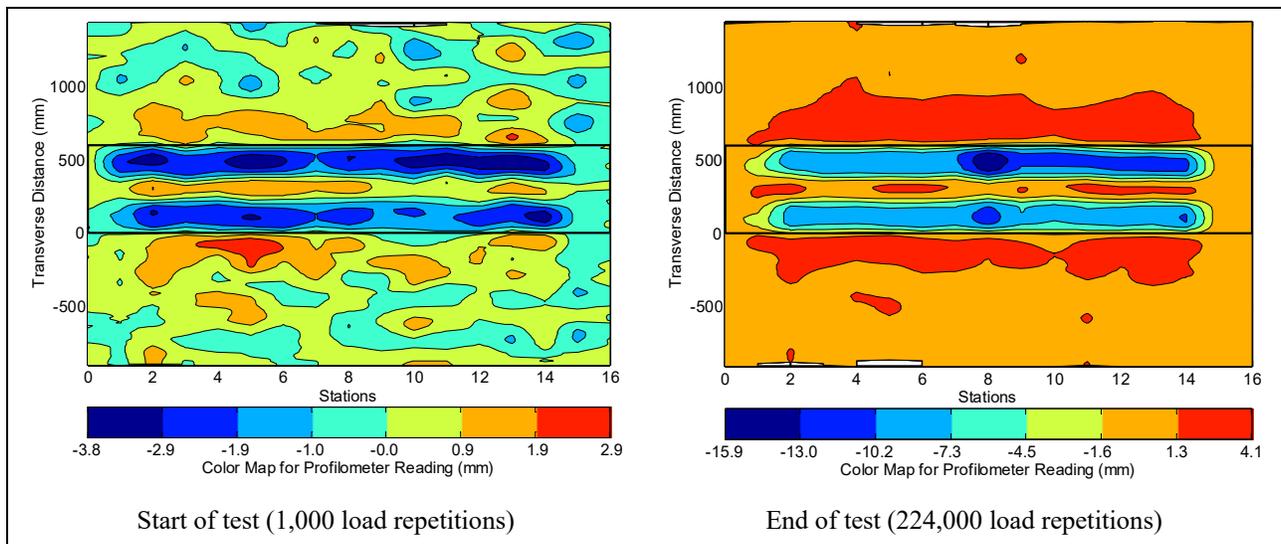
Figure 4.37: 623HA: Contour plots of permanent surface deformation.
(Note that key scales are different.)

4.6.6 Visual Inspection

Apart from rutting, no other distress was recorded on the section. Appearance was similar to that of the other sections. Figure 4.38 shows a photograph taken of the surface at the end of the test. The hairline cracks and water seepage from them observed after construction and discussed in Section 2.9 did not appear to have influenced performance of this section in any way.
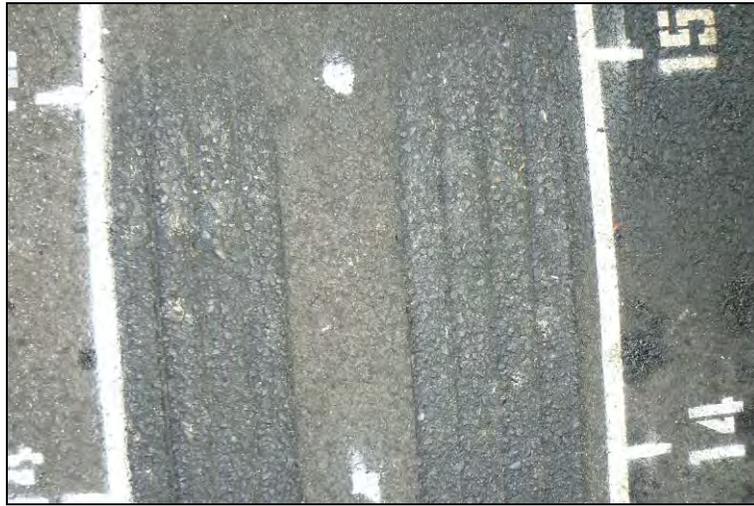
Figure 4.38: 623HA: Section photograph at test completion.

4.7   Test Summary

Testing on the four sections was started in the summer of 2010 and ended in the fall of the same year. A range of daily average temperatures was therefore experienced; however, pavement temperatures remained constant throughout HVS trafficking. The duration of the tests to terminal rut (12.5 mm [0.5 in.]) on the four sections varied from 42,000 load repetitions (Section 622HA, Evotherm) to 200,000 load repetitions (Section 623HA, Cecabase) (Table 4.5).

Table 4.5: Summary of Embedment Phase and Test Duration

Section		Embedment	Repetitions to	Load change to
Number	Technology	(mm [in.])	12.5 mm rut	60 kN
620HA	Control	7.9 (0.31)	46,000	No
621HA	Gencor	6.5 (0.26)	112,000	No
622HA	Evotherm	7.9 (0.31)	42,000	No
623HA	Cecabase	5.5 (0.22)	200,000	Yes

Rutting behavior for the four sections is compared in Figure 4.39 (average maximum rut) and Figure 4.40 (average deformation). The duration of the embedment phases on all sections were similar; however, the depth of the ruts at the end of the embedment phases differed slightly between sections, with the Gencor (6.5 mm [0.26 in.]) and Cecabase (5.5 mm [0.22 in.]) having less embedment than the Control and

Evotherm sections, which had similar embedment (7.9 mm [0.31 in.]). This is opposite to the early rutting performance in the Phase 1 study *(2)* and is being investigated in a separate study. Rut rate (rutting per load repetition) after the embedment phase on the Control and Evotherm sections was almost identical. On the Gencor and Cecabase sections, rut rate was considerably slower than the Control after the embedment phase. The difference in performance between the three warm-mix sections is attributed in part to the lower production and paving temperatures of the Evotherm mix (125°C [248°F] and 120°C [237°F], respectively) compared to the Gencor (140°C [284°F] and 128°C [262°F) and Cecabase (130°C [266°F] and 128°C [262°F]) mixes, as well as to the thickness of the asphalt layers (the Evotherm section had thinner asphalt layers than the Control and Cecabase sections). Lower production and paving temperatures typically result in less oxidation of the binder, which can influence early rutting performance. Preliminary findings from research into binder aging in warm asphalt mixes indicates that there is fairly rapid oxidation (and consequent stiffening) of the binder after construction, which may explain the slower rut rate on the Cecabase section. Binder aging in warm-mix asphalt is being investigated in another phase of the Caltrans warm-mix asphalt study and will be discussed in a separate report.
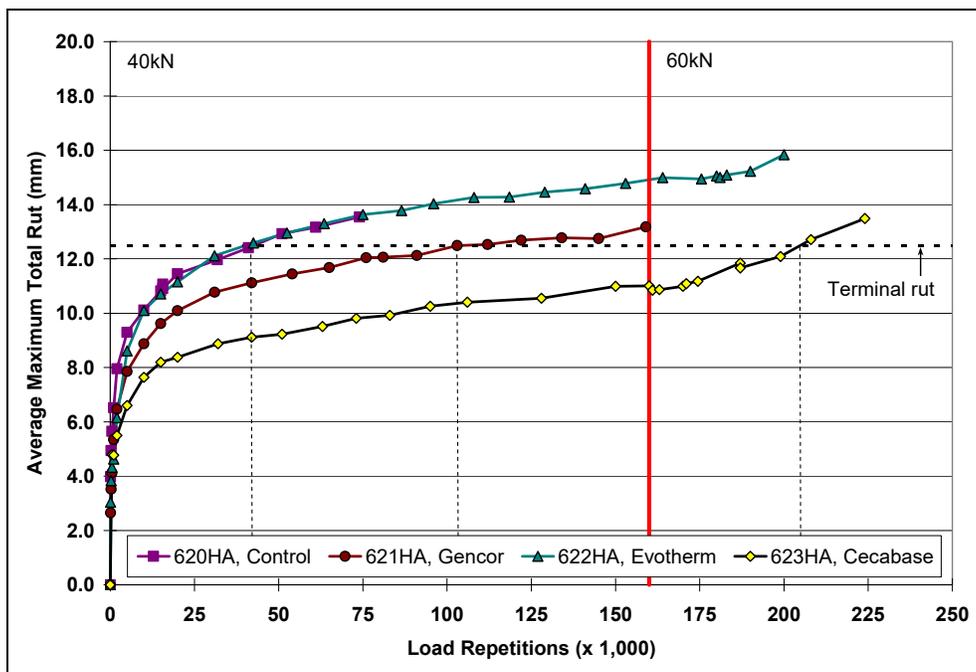
Figure 4.39: Comparison of average maximum rut.
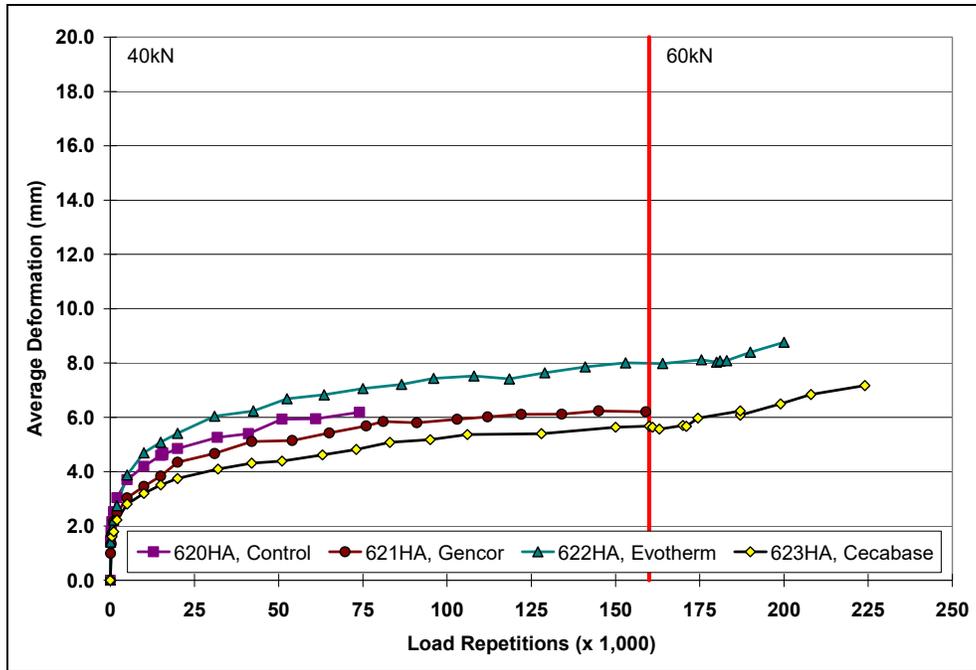
Figure 4.40: Comparison of average deformation.

Based on the results from this phase of accelerated pavement testing on gap-graded, rubberized mixes, it can be concluded that the use of any of the three warm-mix asphalt technologies assessed and subsequent compaction of the mixes at lower temperatures will not significantly influence rutting performance of the mix. Performance of the warm-mix sections exceeded that of the Control, despite all the warm-mix sections having thinner total asphalt concrete layer thicknesses than the Control.

5.   FORENSIC INVESTIGATION

5.1   Introduction

A forensic investigation was carried out after completion of all HVS testing to compare the condition of the asphalt concrete and underlying layers within and outside the HVS trafficked area, and to remove samples for laboratory testing.

5.2   Forensic Investigation Procedure

The forensic investigation included the following tasks:

1.   Demarcate test pit locations;
2.   Saw the asphalt concrete;
3.   Remove the slab and inspect surfacing/base bond;
4.   Determine the wet density of the base (nuclear density gauge);
5.   Determine the in situ strength of the base and subgrade (dynamic cone penetrometer);
6.   Remove the base and subgrade material;
7.   Sample material from the base and subgrade for moisture content determination;
8.   Measure layer thicknesses;
9.   Describe the profile;
10. Photograph the profile;
11. Sample additional material from the profile if required; and
12. Reinstate the pit.

The following additional information is relevant to the investigation:

- The procedures for HVS test section forensic investigations, detailed in the document entitled *Quality Management System for Site Establishment, Daily Operations, Instrumentation, Data Collection and Data Storage for APT Experiments (8)* were followed.
- The saw cuts were made at least 50 mm into the base to ensure that the slab could be removed from the pit without breaking.
- Nuclear density measurements were taken between the test section centerline and the inside (caravan side) edge of the test section. Two readings were taken: the first with the gauge aligned with the direction of trafficking and the second at 90° to the first measurement (Figure 5.1).
- DCP measurements were taken between the test section centerline and inside (caravan side) edge of the test section, and between the outside edge of the test section and the edge of the test pit on the traffic side (Figure 5.1). A third DCP measurement was taken between these two points if inconsistent readings were obtained.
- Layer thicknesses were measured from a leveled reference straightedge above the pit. This allowed the crossfall of the section to be included in the profile. Measurements were taken across the pit at 50-mm (2.0-in.) intervals.
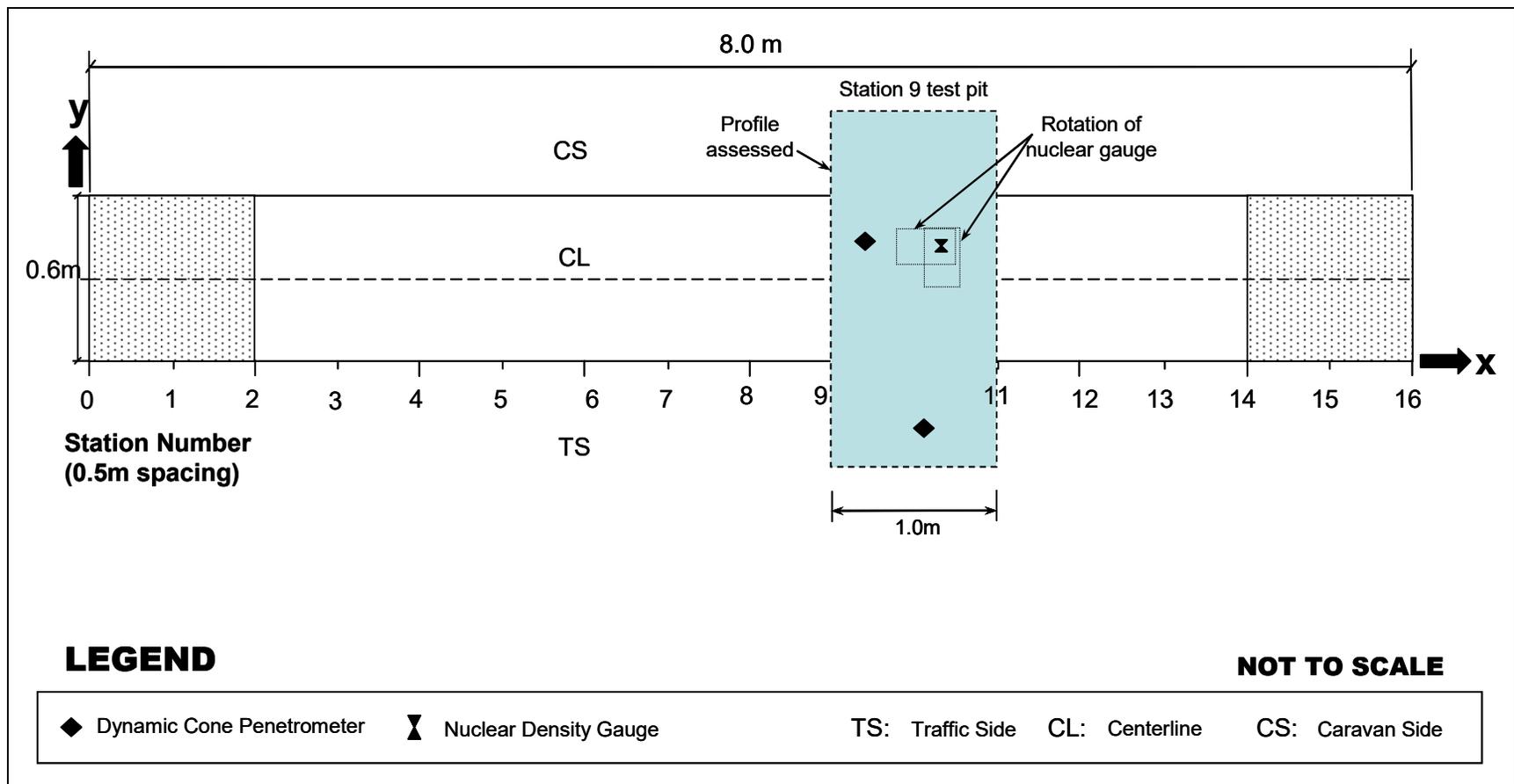
Figure 5.1: Test pit layout.

5.3 Test Pit Excavation

One test pit was excavated on each HVS test section (between Stations 9 and 11 [see Figure 5.1]). The Station 9 test pit face was evaluated. Test pits were excavated to a depth approximately 200 mm (8 in.) into the subgrade.

5.4 Base-Course Density and Moisture Content

Table 5.1 summarizes the base-course density and moisture content measurements on each section. The table includes the wet and dry density and moisture content of the base in the HVS wheelpath and in the adjacent untrafficked area (see Figure 5.1). Measurements were taken with a nuclear gauge. Laboratory-determined gravimetric moisture contents of the base material (average of two samples from the top and bottom of the excavated base) and subgrade material, as well as recalculated dry densities of the base (using the average gauge-determined wet density and laboratory-determined gravimetric moisture content), are also provided. Each gauge measurement is an average of two readings taken at each location in the pit (gauge perpendicular to wheelpath and parallel to wheelpath as shown in Figure 5.1). Subgrade densities were not measured. The following observations were made:

- Densities increased with increasing depth, following a similar pattern to the densities measured after construction of the test track.
- Densities were consistent throughout the test track and there was very little difference between the densities measured in the trafficked and untrafficked areas. Average nuclear gauge–determined dry densities of the base-course for the six depths measured ranged between 2,155 kg/m^3 (134.5 lb/ft^3) in the untrafficked area on Section 623HA and 2,255 kg/m^3 (140.8 lb/ft^3) on the untrafficked area of Section 620HA for the four test pits. The average dry density and standard deviation for the four test pits were 2,188 kg/m^3 (136.6 lb/ft^3) and 29 kg/m^3 (1.8 lb/ft^3), respectively, which corresponds with the average dry density of 2,200 kg/m^3 (137.3 lb/ft^3) recorded after construction, indicating that the base density did not increase under trafficking. The laboratory-determined maximum dry density was 2,252 kg/m^3 (140.6 lb/ft^3). The average nuclear gauge–determined wet density was 2,347 kg/m^3 (146.1 lb/ft^3) with a standard deviation of 28 kg/m^3 (2.4 lb/ft^3).
- Nuclear gauge–determined moisture contents of the four test pits, measured at six intervals in the top 300 mm of the base, ranged between 6.5 percent and 7.8 percent with an average of 7.2 percent (standard deviation of 0.6 percent), very similar to the measurements recorded after construction (7.3 percent). Moisture contents at the top of the base were generally slightly higher compared to those in the lower regions of the base. The laboratory-determined optimum moisture content of the base material was 6.0 percent.

Table 5.1: Summary of Base-Course Density and Moisture Content Measurements

Section	Depth	Nuclear Gauge										Laboratory			
		Wheelpath					Untrafficked								
		Base Wet Density		MC[1]	Base Dry Density		Base Wet Density		MC	Base Dry Density		Base MC	Recalculated Dry Density*		SG[2] MC
		(kg/m³)	(lb/ft³)	(%)	(kg/m³)	(lb/ft³)	(kg/m³)	(lb/ft³)	(%)	(kg/m³)	(lb/ft³)	(%)	(kg/m³)	(lb/ft³)	(%)
620HA (Control)	50	2,290	143.0	6.6	2,151	134.3	2,358	147.2	6.8	2,206	137.7		2,225	138.9	
	100	2,293	143.1	6.2	2,156	134.6	2,393	149.4	6.5	2,247	140.3		2,241	139.9	
	150	2,319	144.8	6.3	2,179	136.0	2,413	150.6	6.6	2,263	141.3	4.5	2,265	141.4	16.5
	200	2,322	144.9	6.6	2,181	136.1	2,415	150.8	6.5	2,264	141.3		2,266	141.4	
	250	2,358	147.2	6.9	2,207	137.8	2,416	150.8	6.7	2,266	141.4		2,284	142.6	
	300	2,372	148.1	6.3	2,231	139.3	2,438	152.2	6.7	2,284	142.6		2,302	143.7	
	Avg[3]	2,326	145.2	6.5	2,184	136.3	2,406	150.2	6.6	2,255	140.8	-	2,264	141.3	-
	SD[4]	34	2.1	0.2	30	1.9	27	1.7	0.1	27	1.7		28	1.7	
621HA (Gencor)	50	2,199	137.3	7.1	2,054	128.2	2,241	139.9	7.1	2,092	130.6		2,133	133.1	
	100	2,285	142.7	7.0	2,136	133.4	2,313	144.4	6.9	2,164	135.1		2,209	137.9	
	150	2,330	145.4	7.2	2,174	135.7	2,340	146.1	6.9	2,190	136.7	4.1	2,243	140.0	16.2
	200	2,371	148.0	6.8	2,221	138.6	2,368	147.9	6.7	2,220	138.6		2,277	142.2	
	250	2,387	149.0	6.8	2,235	139.5	2,370	147.9	6.7	2,221	138.7		2,284	142.6	
	300	2,404	150.1	6.7	2,253	140.6	2,384	148.8	6.9	2,230	139.2		2,300	143.6	
	Avg	2,330	145.4	6.9	2,179	136.0	2,336	145.8	6.9	2,186	136.5	-	2,241	139.9	-
	SD	77	4.8	0.2	75	4.7	53	3.3	0.2	52	3.3		62	3.9	
622HA (Evotherm)	50	2,264	141.4	7.4	2,108	131.6	2,288	142.8	8.2	2,115	132.0		2,166	135.2	
	100	2,329	145.4	8.0	2,158	134.7	2,347	146.5	7.6	2,181	136.1		2,225	138.9	
	150	2,349	146.6	8.0	2,174	135.7	2,353	146.9	7.9	2,181	136.2	5.1	2,237	139.6	16.2
	200	2,356	147.1	8.2	2,177	135.9	2,380	148.6	7.5	2,213	138.2		2,253	140.7	
	250	2,382	148.7	7.7	2,212	138.1	2,385	148.9	7.7	2,215	138.3		2,268	141.6	
	300	2,395	149.5	7.5	2,229	139.2	2,414	150.7	8.0	2,235	139.5		2,288	142.8	
	Avg	2,346	146.4	7.8	2,176	135.9	2,361	147.4	7.8	2,190	136.7	-	2,239	139.8	-
	SD	46	2.9	0.3	43	2.7	43	2.7	0.3	43	2.7		42	2.6	
623HA (Cecabase)	50	2,260	141.1	8.1	2,092	130.6	2,257	140.9	7.7	2,096	130.8		2,155	134.5	
	100	2,330	145.4	7.7	2,163	135.1	2,296	143.4	7.8	2,130	133.0		2,207	137.8	
	150	2,346	146.4	8.4	2,164	135.1	2,312	144.3	8.0	2,140	133.6	4.8	2,222	138.7	17.5
	200	2,379	148.5	7.8	2,207	137.8	2,326	145.2	7.5	2,164	135.1		2,245	140.2	
	250	2,399	149.8	7.2	2,238	139.7	2,355	147.0	7.0	2,199	137.3		2,268	141.6	
	300	2,417	150.9	7.5	2,248	140.3	2,364	147.6	7.5	2,200	137.4		2,281	142.4	
	Avg	2,355	147.0	7.8	2,185	136.4	2,319	141.7	7.6	2,155	134.5	-	2,230	139.2	-
	SD	57	35	0.4	58	3.6	40	2.5	0.3	41	2.6		46	2.9	

* Recalculated dry density using nuclear gauge wet density and laboratory gravimetric moisture content.
[1] MC – Moisture content   [2] SG = Subgrade   [3] Avg = Average   [4] SD = Standard Deviation

- Laboratory-determined gravimetric moisture contents varied between 4.1 percent (Section 621HA, Gencor) and 5.1 percent (Section 622HA, Evotherm), with an average of 4.6 percent and standard deviation of 0.4 percent. These moisture contents were on average 2.6 percent lower than those recorded by the nuclear gauge, and appeared more consistent with visual evaluations of the test pit face and more representative of typical dry back conditions in base materials. The higher moisture contents determined with the nuclear gauge could be associated with the presence of some excess moisture from the saw cutting operation during pit excavation. Recalculated dry densities, determined using the gauge wet density and gravimetric moisture content, were therefore slightly higher than the gauge-determined dry densities.

5.5 Subgrade Moisture Content

Laboratory-determined gravimetric moisture contents for the subgrade materials ranged between 16.2 percent and 17.5 percent for the four test pits, indicating a significant difference in moisture contents between the base and subgrade materials. Visual observations in the test pits confirmed this difference.

5.6 Dynamic Cone Penetrometer

Dynamic cone penetrometer (DCP) measurements were recorded in each test pit, both in the wheelpath and in untrafficked areas. Measurements and plots are provided in Appendix B. A summary of the measurements is provided in Table 5.2. The results show some variation; however, this is attributed more to stones in the material and not to any significant differences in strength/stiffness. Variation in the subgrade strengths was attributed to remnants of lime treatments during construction of the UCPRC facility. The strength of the material was considered relatively low for base-course standard, but appropriate for accelerated pavement tests.

Table 5.2: Summary of Dynamic Cone Penetrometer Measurements

Section	Blows to 800 mm		Layer	mm/Blow		Estimated Modulus (MPa [ksi])	
	Wheelpath	Untrafficked		Wheelpath	Untrafficked	Wheelpath	Untrafficked
620HA	121	122	Base	5	5	213 (31)	243 (35)
621HA	224	148		4	4	297 (43)	259 (38)
622HA	133	130		5	5	227 (33)	222 (32)
623HA	121	106		6	4	306 (44)	245 (39)
620HA			Subgrade	14	20	71 (10)	48 (7)
621HA				7	16	151 (22)	60 (9)
622HA				14	15	66 (10)	63 (9)
623HA				21	16	45 (7)	60 (9)

5.7 Test Pit Profiles and Observations

Test pit profile illustrations are provided in Appendix B. Average measurements for each profile at Station 9 are listed in Table 5.3. The average layer thicknesses include the wheelpath depression and

adjacent material displacement (bulge). As expected, minimum thickness measurements were always recorded in one of the wheelpaths, while maximum thickness measurements were always recorded in one of the adjacent areas of displacement. Design thicknesses for the top and bottom lifts of asphalt and the base were 60 mm, 60 mm, and 400 mm, respectively (0.2 ft., 0.2 ft., and 1.3 ft.).

Table 5.3: Average Layer Thicknesses from Test Pit Profiles (Station 9)

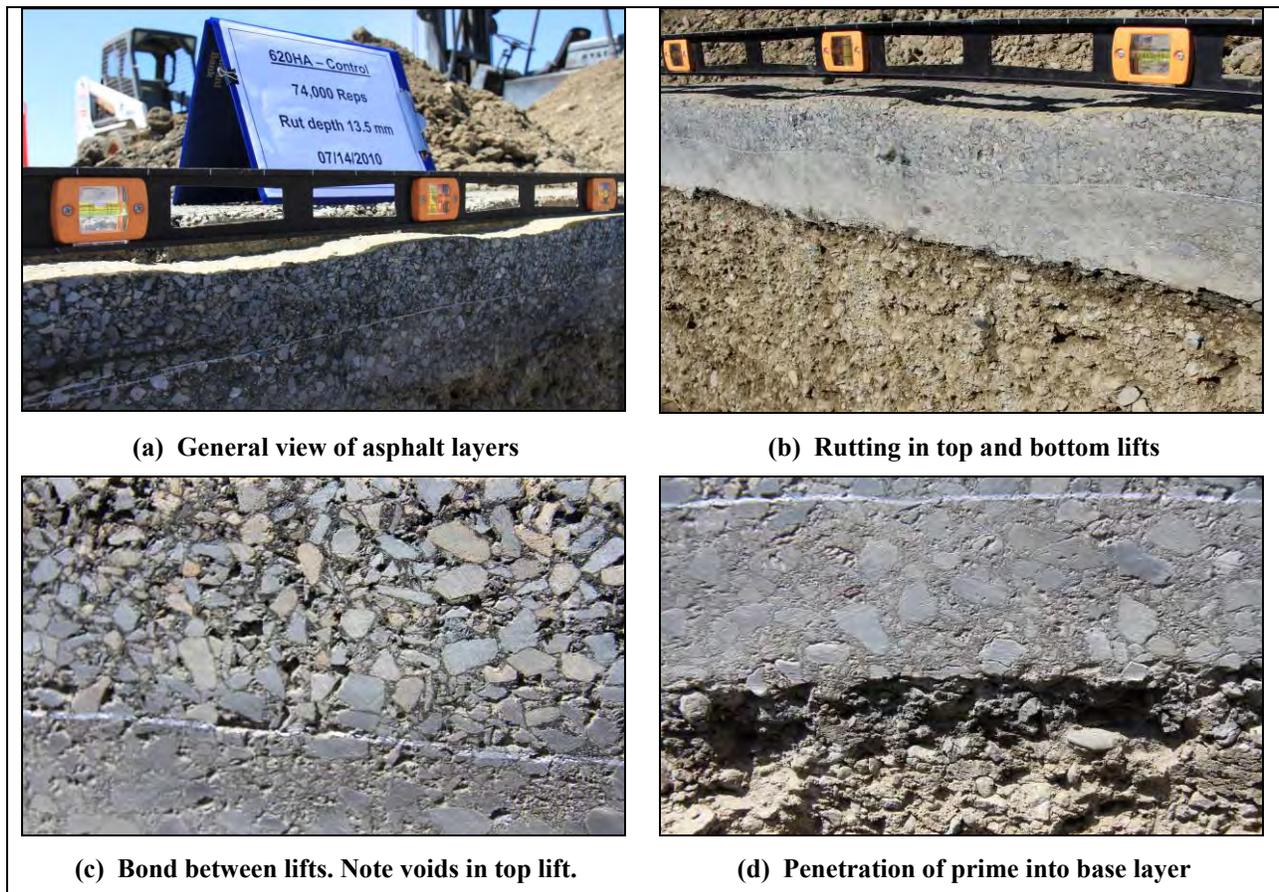| Section	Layer	Average		Std. Deviation		Minimum		Maximum	
		(mm)	(ft.)	(mm)	(ft.)	(mm)	(ft.)	(mm)	(ft.)
620HA	AC – top	69	0.23	2	0.01	64	0.21	74	0.24
	AC – bottom	80	0.26	5	0.02	66	0.22	89	0.29
	AC – total	149	0.49	-	-	137	0.43	160	0.53
	Base	439	1.44	6	0.02	427	1.40	451	1.48
621HA	AC – top	65	0.22	3	0.01	57	0.18	70	0.23
	AC – bottom	65	0.22	3	0.01	58	0.19	70	0.23
	AC – total	130	0.43	-	-	124	0.41	136	0.45
	Base	459	1.51	6	0.02	448	1.47	472	1.55
622HA	AC – top	66	0.22	3	0.01	61	0.20	76	0.25
	AC – bottom	71	0.23	5	0.02	62	0.20	78	0.26
	AC – total	138	0.45	-	-	128	0.42	146	0.48
	Base	485	1.59	7	0.03	470	1.54	495	1.63
623HA	AC – top	64	0.21	4	0.02	55	0.18	78	0.26
	AC – bottom	79	0.26	5	0.02	62	0.20	89	0.29
	AC – total	143	0.47	-	-	135	0.44	153	0.50
	Base	437	1.43	4	0.02	429	1.41	445	1.46

The measurements from each test pit show that layer thickness consistency on each test section was fairly good based on the low standard deviations recorded. The average base thickness varied between 437 mm (1.43 ft.) on Section 623HA and 485 mm (1.6 ft.) on Section 622HA (slightly higher than the design), while the combined asphalt concrete thickness varied between 130 mm (0.43 ft.) on Section 621HA and 149 mm (0.49 ft.) on Section 620HA (also thicker than the design). Average asphalt concrete thicknesses measured in the test pits were consistent with the measurements from cores discussed in Section 2.7.10. A discussion of the observations from each test pit is provided in the following sections.

5.7.1 Section 620HA: Control

Observations from the Section 620HA test pit (Figure 5.2) include:

- The average thickness of the bottom lift of asphalt concrete was considerably thicker (80 mm [0.26 ft.]) than the design thickness (60 mm [0.2 ft.]), while the average top lift thickness, which includes rut and bulge measurements, was slightly thicker (69 mm [0.23 ft.]) than the design. The average combined thickness was considerably thicker (149 mm [0.49 ft.]) than the design (120 mm [0.4 ft.]).
- Rutting was mostly restricted to the upper region of the top lift of asphalt, although some evidence of rutting was noted in the bottom lift (about 3 mm [0.12 in.]) and at the top of the base (Figure 5.2b). No rutting was measured/observed in the subgrade. Some displacement was recorded on either side of the trafficked area in both lifts of asphalt and at the top of the base.

- The two asphalt concrete layers were well bonded to each other (Figure 5.2c) and well bonded to the aggregate base. The precise location of the bond between the two asphalt lifts was clear. The prime coat appeared to have penetrated between 10 mm and 15 mm (0.4 in. and 0.6 in.) into the base (Figure 5.2d).

- Apart from rutting, no other distresses were noted in the asphalt layers other than some signs of segregation and some visible voids, attributed to the cold placement temperatures.

- Base thickness showed very little variation across the profile. The material was well graded and aggregates were mostly rounded (little evidence of crushing) with some flakiness. No oversize material was observed, and the properties appeared to be consistent (Figure 5.2e). Material consistency was rated as very hard throughout the layer. No organic matter was observed.

- Moisture content in the base was rated as moist, with moisture content appearing to increase near the subgrade. There was no indication of higher moisture content at the interface between the base and asphalt concrete layers.

- The layer definition between the base and subgrade was clear. Some punching of the base into the subgrade was noted.

- The subgrade was moist, silty-clay material. Consistency was rated as soft and some shrinkage and slickenslides were observed. Some evidence (hydrochloric acid reaction) of the lime treatment during the original site preparation for construction of the UCPRC facility in 2008 was noted (Figure 5.2f). No organic matter was observed.

(a) General view of asphalt layers

(b) Rutting in top and bottom lifts

(c) Bond between lifts. Note voids in top lift.

(d) Penetration of prime into base layer

Figure 5.2: 620HA: Test pit photographs.

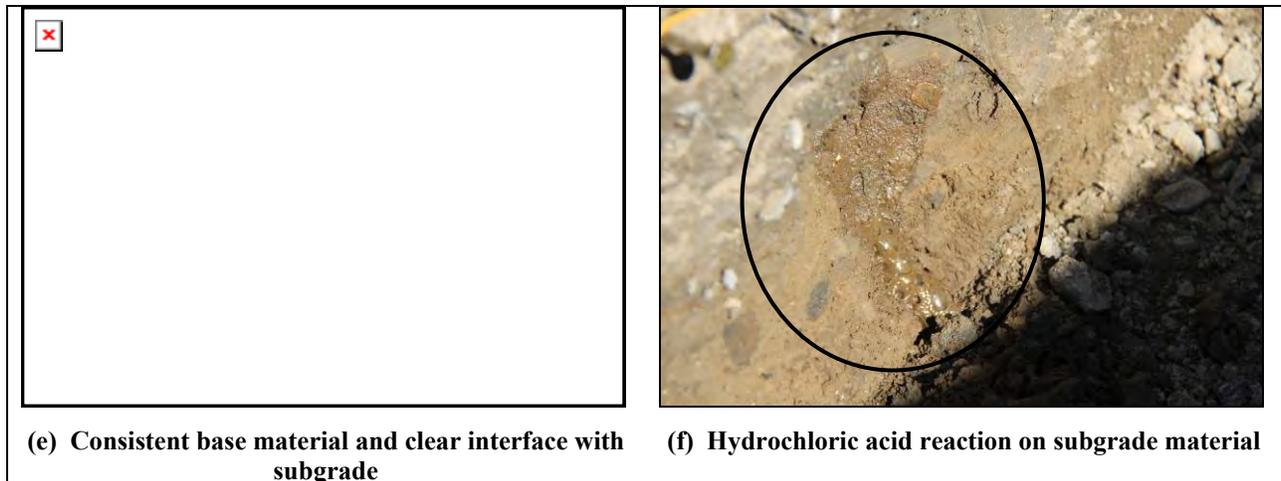| (e) Consistent base material and clear interface with subgrade | (f) Hydrochloric acid reaction on subgrade material |

Figure 5.2: 620HA: Test pit photographs *(continued).*

5.7.2 Section 621HA: Gencor

Observations from the Section 621HA test pit (Figure 5.3) include:

- The average thicknesses of both lifts of asphalt concrete were thicker (65 mm [0.22 ft.]) than the design thickness. The average combined thickness was also marginally thicker (130 mm [0.43 ft.]) than the design, but almost 20 mm (0.01 ft.) thinner than the Control.
- Rutting was mostly restricted to the upper region of the top lift of asphalt, although some evidence of rutting was noted in the bottom lift (about 3 mm to 5 mm [0.12 to 0.2 in.]), top of the base, and top of the subgrade. Some displacement was recorded on either side of the trafficked area in both lifts of asphalt and at the top of the base.
- The two asphalt concrete layers were well bonded to each other and well bonded to the aggregate base. The precise location of the bond between the two asphalt lifts was clear. The prime coat appeared to have penetrated in a similar way to that observed on the Control.
- Apart from rutting, no other distresses were noted in the asphalt layers, other than some bleeding in the wheelpaths and some visible voids.

Figure 5.3: 621HA: Test pit photograph.

- Base thickness showed very little variation across the profile. The material was consistent with the observations on the Control.
- Moisture content in the base was rated as moist, with moisture content appearing to increase near the subgrade. There was no indication of higher moisture content at the interface between the base and asphalt concrete layers.
- The layer definition between the base and subgrade was clear. Some punching of the base into the subgrade was noted.
- Observations of the subgrade were consistent with those of the Control, but the material appeared to have a slightly higher plasticity.

5.7.3 Section 622HA: Evotherm

Observations from the Section 622HA test pit (Figure 5.4) include:

- The average thicknesses of both lifts of asphalt concrete were thicker (66 mm [0.22 ft.] and 71 mm [0.23 ft.], respectively) than the design thickness. The average combined thickness was also marginally thicker (138 mm [0.45 ft.]) than the design, but about 11 mm thinner than the Control.
- Rutting was mostly restricted to the upper region of the top lift of asphalt, although some evidence of rutting was noted in the bottom lift (about 3 mm to 5 mm [0.12 to 0.2 in.]). No rutting was evident in the base or subgrade layers (Figure 5.4a). Some displacement was recorded on either side of the trafficked area in both lifts of asphalt.
- The two asphalt concrete layers were well bonded to each other and well bonded to the aggregate base. The precise location of the bond between the two asphalt lifts was clear. The prime coat appeared to have penetrated in a similar way to that observed on the Control.
- Apart from rutting, no other distresses were noted in the asphalt layers.
- Base thickness showed very little variation across the profile. The material was consistent with the observations on the Control.
- Moisture content in the base was rated as moist, with moisture content appearing to increase near the subgrade. There was no indication of higher moisture content at the interface between the base and asphalt concrete layers.
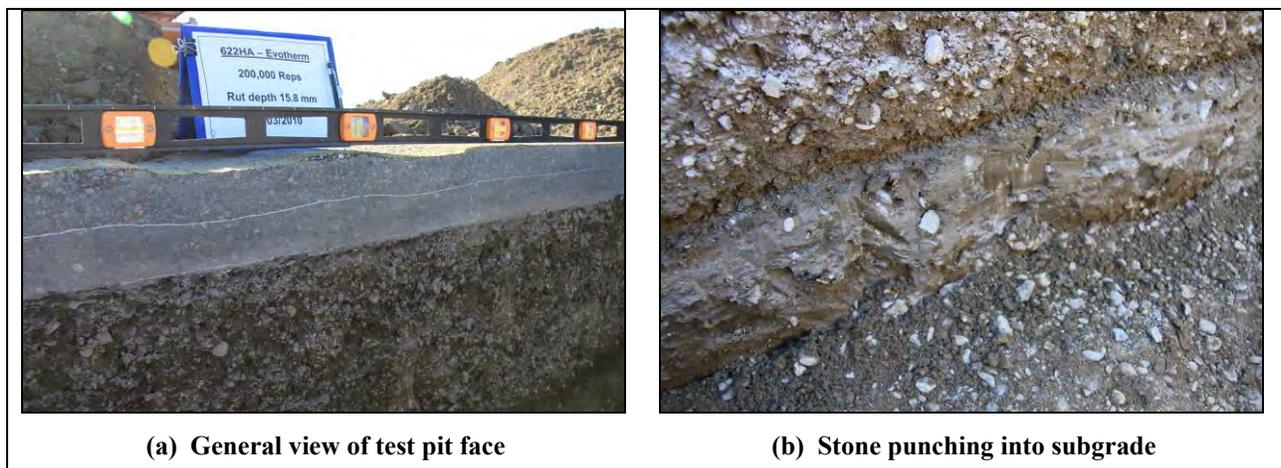

| (a) General view of test pit face | (b) Stone punching into subgrade |

Figure 5.4: 622HA: Test pit photographs.

- The layer definition between the base and subgrade was clear. Some punching of the base into the subgrade was noted (Figure 5.4b).
- Observations of the subgrade were consistent with those of the Control.

5.7.4   Section 623HA: Cecabase

Observations from the Section 623HA test pit (Figure 5.5) include:

- The average thicknesses of both lifts of asphalt concrete were thicker (64 mm [0.21 ft.] and 79 mm [0.26 ft.], respectively) than the design thickness. The average combined thickness was considerably thicker (143 mm [0.47 ft.]) than the design but still less than the thickness of the asphalt layers on the Control (149 mm [0.49 ft.]).
- Rutting was mostly restricted to the upper region of the top lift of asphalt, although some evidence of rutting was noted in the bottom lift (about 3 mm [0.12 in.]), top of the base, and top of the subgrade (Figure 5.5a). Some displacement was recorded on either side of the trafficked area in both lifts of asphalt and at the top of the base.
- The two asphalt concrete layers were well bonded to each other, and to the aggregate base. The precise location of the bond between the two asphalt lifts was clear, but some evidence of moisture in the bond was observed (Figure 5.5b). The prime coat appeared to have penetrated in a similar way to that observed on the Control.
- Apart from rutting, no other distresses were noted in the asphalt layers.
- Base thickness showed very little variation across the profile. The material was consistent with the observations on the Control.
- Moisture content in the base was rated as moist, with moisture content appearing to increase near the subgrade. There was some indication of higher moisture content at the interface between the base and asphalt concrete layers (Figure 5.5a).
- The layer definition between the base and subgrade was clear. Some punching of the base into the subgrade was noted.
- Observations of the subgrade were consistent with those of the Control.
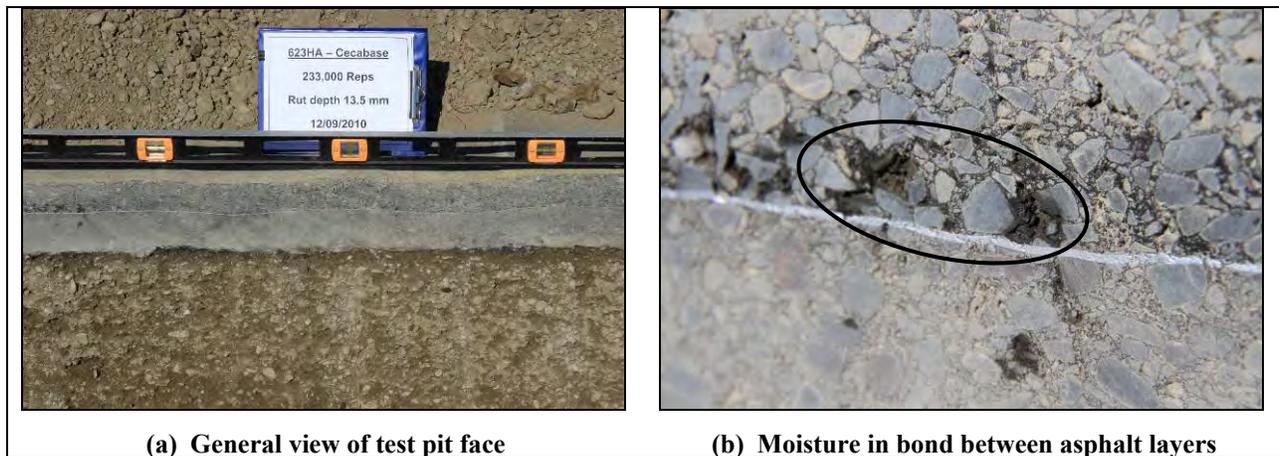

(a) General view of test pit face   (b) Moisture in bond between asphalt layers

Figure 5.5: 623HA: Test pit photographs.

5.8   Forensic Investigation Summary

A forensic investigation of all test sections indicated that rutting was mostly confined to the upper lift of the asphalt concrete, with limited rutting in the bottom lift, base, and top of the subgrade. There was some variation in asphalt layer lift thicknesses between the four sections. Materials were consistent throughout the four sections. No evidence of moisture damage was noted. There was no visible difference between the Control and warm-mix asphalt sections.

6.   PHASE 3a LABORATORY TEST DATA SUMMARY

6.1   Experiment Design

Phase 3a laboratory testing included rutting performance (shear), fatigue cracking, and moisture sensitivity tests. Tests on these mix properties were carried out on beams and cores cut from the test track after construction (see Section 2.8). Typical experimental designs used in previous studies were adopted for this warm-mix asphalt study to facilitate comparison of results.

6.1.1   Shear Testing for Rutting Performance

<u>Test Method</u>

The AASHTO T 320 Permanent Shear Strain and Stiffness Test was used for shear testing in this study. In the standard test methodology, cylindrical test specimens 150 mm (6.0 in.) in diameter and 50 mm (2.0 in.) thick are subjected to repeated loading in shear using a 0.1-second haversine waveform followed by a 0.6-second rest period. Three different shear stresses are applied while the permanent (unrecoverable) and recoverable shear strains are measured. The permanent shear strain versus applied repetitions is normally recorded up to a value of five percent although 5,000 repetitions are called for in the AASHTO procedure. A constant temperature is maintained during the test (termed the *critical temperature)*, representative of the high temperature causing rutting in the local environment. In this study, specimens were cored from the test track and then trimmed to size.

<u>Number of Tests</u>

A total of 18 shear tests were carried out on each mix (total of 72 tests for the four mixes) as follows:

- Two temperatures (45°C and 55°C [113°F and 131°F])
- Three stresses (70 kPa, 100 kPa, and 130 kPa [10.2, 14.5, and 18.9 psi])
- Three replicates

6.1.2   Flexural Beam Testing for Fatigue Performance

<u>Test Method</u>

The AASHTO T-321 Flexural Controlled-Deformation Fatigue Test method was followed. In this test, three replicate beam test specimens, 50 mm (2.0 in.) thick by 63 mm (2.5 in.) wide by 380 mm (15 in.) long, which were sawn from the test track, were subjected to four-point bending using a haversine waveform at a loading frequency of 10 Hz. Testing was performed in both dry and wet condition at two different strain levels at one temperature. Flexural Controlled-Deformation Frequency Sweep Tests were used to establish the relationship between complex modulus and load frequency. The same sinusoidal waveform was used in a controlled deformation mode and at frequencies of 15, 10, 5, 2, 1, 0.5, 0.2, 0.1,

0.05, 0.02, and 0.01 Hz. The upper limit of 15 Hz is a constraint imposed by the capabilities of the test machine. To ensure that the specimen was tested in a nondestructive manner, the frequency sweep test was conducted at a small strain amplitude level, proceeding from the highest frequency to the lowest in the sequence noted above.

The wet specimens used in the fatigue and frequency sweep tests were conditioned following the beam-soaking procedure described in Appendix C. The beam was first vacuum-saturated to ensure a saturation level greater than 70 percent, and then placed in a water bath at 60°C (140°F) for 24 hours, followed by a second water bath at 20°C (68°F) for two hours. The beams were then wrapped with Parafilm™ and tested within 24 hours after soaking.

<u>Number of Tests</u>

A total of 12 beam fatigue tests and 12 flexural fatigue frequency sweep tests were carried out on each mix (total of 96 tests for the four mixes) as follows:

- Flexural fatigue test:
  + Two conditions (wet and dry)
  + One temperature (20°C [68°F])
  + Two strains (200 microstrain and 400 microstrain)
  + Three replicates
- Frequency sweep test:
  + Two conditions (wet and dry)
  + Three temperatures (10°C, 20°C, and 30°C [50°F, 68°F, and 86°F])
  + One strain (100 microstrain)
  + Two replicates

6.1.3 Moisture Sensitivity Testing

<u>Test Methods</u>

Two additional moisture sensitivity tests were conducted, namely the Hamburg Wheel-Track test and the Tensile Strength Retained (TSR) test.

- The AASHTO T-324 test method was followed for Hamburg Wheel-Track testing on 152 mm (6.0 in.) cores removed from the test track. All testing was carried out at 50°C (122°F).
- The Caltrans CT 371 test method was followed for the Tensile Strength Retained Test on 100 mm cores removed from the test track and trimmed to a thickness of 63 mm (2.5 in.). This test method is similar to the AASHTO T-283 test, however, it has some modifications specific for California conditions.

<u>Number of Tests</u>

Four replicates of the Hamburg Wheel-Track test and four replicates of the Tensile Strength Retained test were carried out for each mix (16 tests per method).

## 6.2 Test Results

6.2.1 Rutting Performance Tests

Air-Void Content

Shear specimens were cored from the test track and trimmed to size. Air-void contents were measured using the CoreLok method and results are listed in Table D.1 through Table D.4 in Appendix D. Table 6.1 summarizes the air-void distribution categorized by mix type, test temperature, and test shear stress level. Figure 6.1 presents the summary boxplots of air-void content of all the specimens tested according to additive type. The differences in air-void content distributions between the mixes with various additives are clearly apparent. The mean difference for the highest mean air-void content (Evotherm) and the smallest mean air-void content (Control) could be as high as 2.0 percent. The Gencor specimens had the largest range in air-void content.

Table 6.1: Summary of Air-Void Contents of Shear Test Specimens

Temperature		Stress Level	Air-Void Content (%)							
			Control		Gencor		Evotherm		Cecabase	
°C	°F	(kPa)	Mean[1]	SD[2]	Mean	SD	Mean	SD	Mean	SD
45	113	70	4.9	0.5	6.1	1.9	6.0	0.5	5.7	0.5
		100	4.8	0.6	6.4	1.5	6.1	0.3	5.8	0.2
		130	4.6	0.3	8.6	0.9	6.1	0.3	5.5	0.7
55	131	70	4.7	0.7	5.0	0.8	5.8	0.4	5.2	0.7
		100	5.2	0.3	6.2	2.4	5.7	0.2	5.9	0.9
		130	4.8	0.4	4.9	0.2	5.7	0.2	5.2	0.6
		Overall	4.8	0.4	6.2	1.8	5.9	0.3	5.5	0.6
[1] Mean of three replicates			[2] SD: Standard deviation							
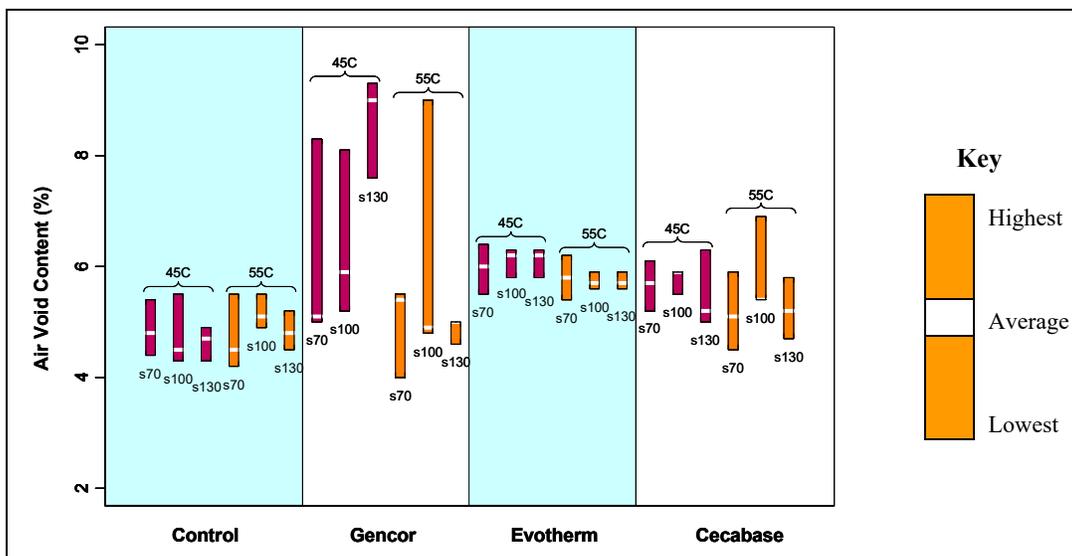
Figure 6.1: Air-void contents of shear specimens.

Resilient Shear Modulus (G*)

The resilient shear modulus results for the four mixes are summarized in Figure 6.2 and Figure 6.3. The following observations were made:

- The resilient shear modulus was influenced by temperature, with the modulus increasing with decreasing temperature. Resilient shear modulus was not influenced by stress.
- The variation of resilient shear moduli at 45°C was higher than at 55°C except for the Evotherm mix, which showed considerable variability in the results for stress levels of 70 kPa and 100 kPa. A check of the test data for the individual specimens indicated suspect data for one specimen (probably due to aggregate size), and if this is removed from the dataset, the results are consistent with the other mixes.
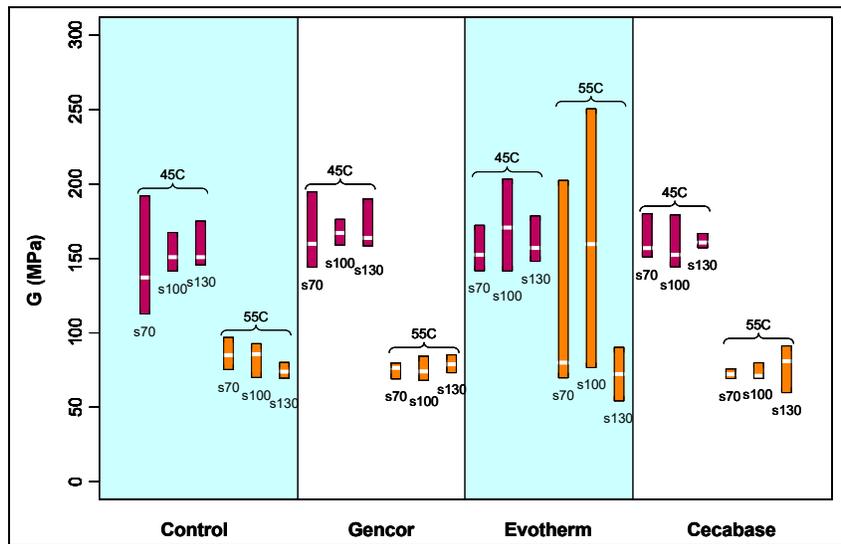
Figure 6.2: Summary boxplots of resilient shear modulus.
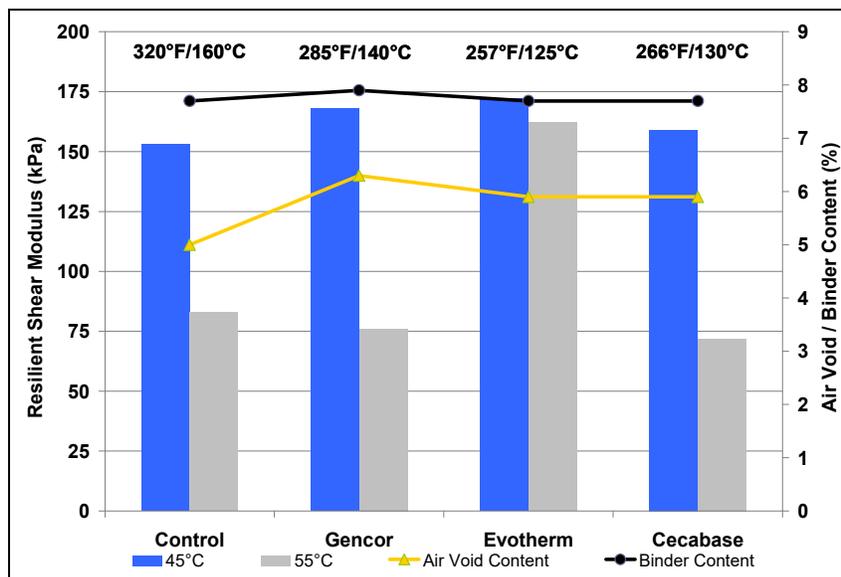
Figure 6.3: Average resilient shear modulus at 45°C and 55°C at 100 kPa stress level.
(Average mix production temperature, binder content, and air-void content shown.)

- Statistical analyses (t-test and Kolmogorov-Smirnov test) indicated that there was no statistically significant difference (confidence level of 0.1) in performance between the Control and the three warm mixes after variation in mix production temperature, binder content, specimen air-void content, actual test stress level, and actual test temperature were taken into consideration. This indicates that the use of the warm-mix technologies and lower production and compaction temperatures did not significantly influence the performance of the mixes in this test.
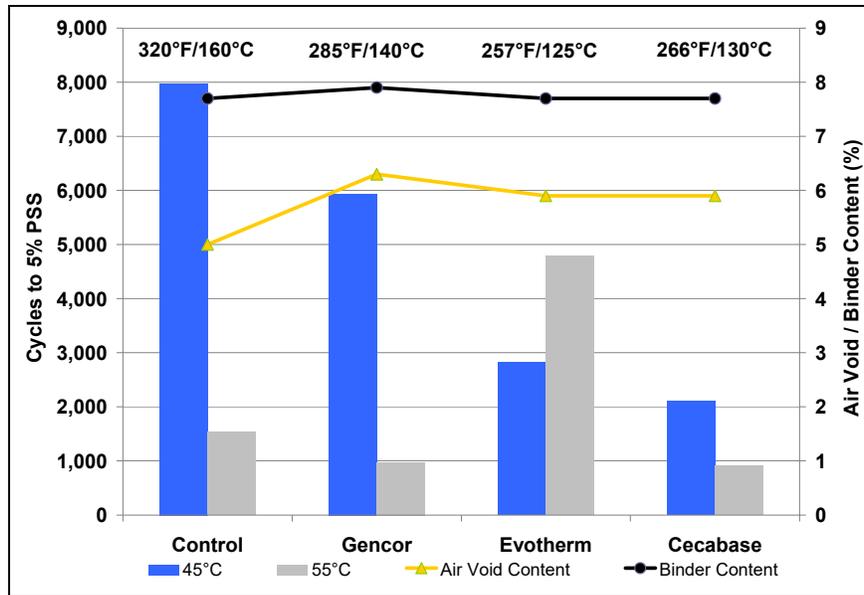
Cycles to Five Percent Permanent Shear Strain

The number of cycles to five percent permanent shear strain provides an indication of the rut-resistance of an asphalt mix, with higher numbers of cycles implying better rut-resistance. Figure 6.4 and Figure 6.5 summarize the shear test results in terms of the natural logarithm of this parameter. The following observations were made:

- Variation between results was in line with typical result ranges for this test.
- As expected, the rut-resistance capacity decreased with increasing temperature and stress level.
- Statistical analyses (t-test and Kolmogorov-Smirnov test) indicated that there was no statistically significant difference (confidence level of 0.1) in performance in this test between the Control and the three warm-mixes after variation in mix production temperature, binder content, specimen air-void content, actual test stress level, and actual test temperature were taken into consideration. This indicates that the use of the warm-mix technologies and lower production and compaction temperatures did not significantly influence the performance of the mixes in this test.
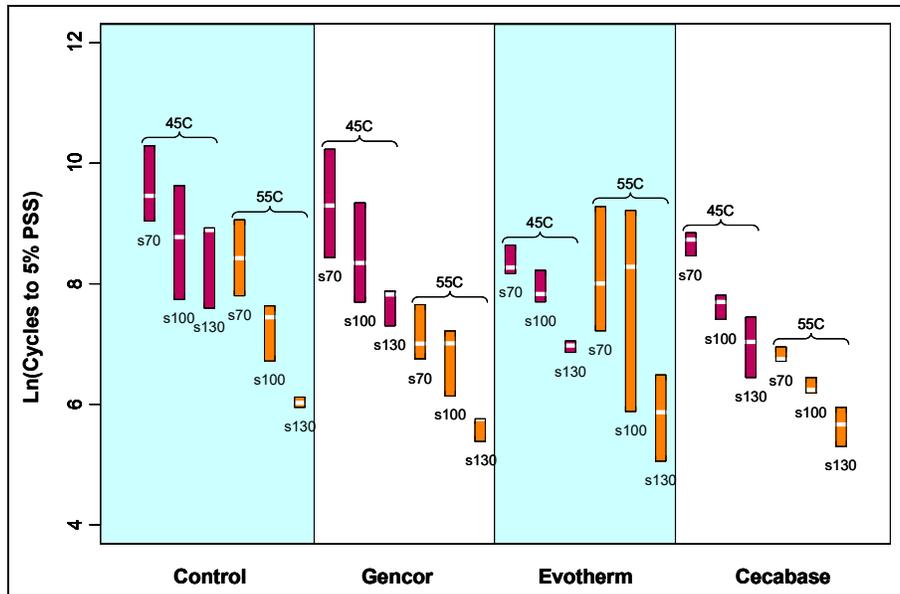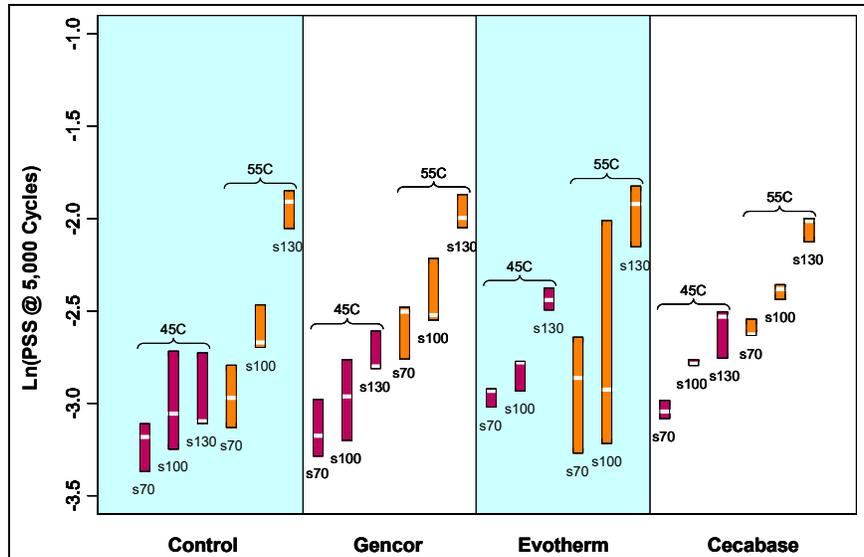

Figure 6.4: Summary boxplots of cycles to five percent permanent shear strain.

Figure 6.5: Average cycles to 5% permanent shear strain at 45°C and 55°C at 100 kPa stress level.
(Average mix production temperature, binder content, and air-void content shown.)

Permanent Shear Strain at 5,000 Cycles

The measurement of permanent shear strain (PSS) accumulated after 5,000 cycles provides an alternative indication of the rut-resistance capacity of an asphalt mix. The smaller the permanent shear strain the better the mixture's rut-resistance capacity. Figure 6.6 and Figure 6.7 summarize the rutting performance of the four mixes in terms of the natural logarithm of this parameter (i.e., increasingly negative values represent smaller cumulative permanent shear strain). The following observations were made:

- Variation between results was in line with typical result ranges for this test.
- As expected, the effect of shear stress level was more significant at higher temperatures, and the higher the temperature and stress level the larger the cumulative permanent shear strain.
- Statistical analyses (t-test and Kolmogorov-Smirnov test) indicated that there was no statistically significant difference (confidence level of 0.1) in performance between the Control and the three warm mixes after variation in mix production temperature, binder content, specimen air-void content, actual test stress level, and actual test temperature were taken into consideration. This indicates that the use of the warm-mix technologies and lower production and compaction temperatures did not significantly influence the performance of the mixes in this test.

Figure 6.6: Summary boxplots of cumulative permanent shear strain at 5,000 cycles.
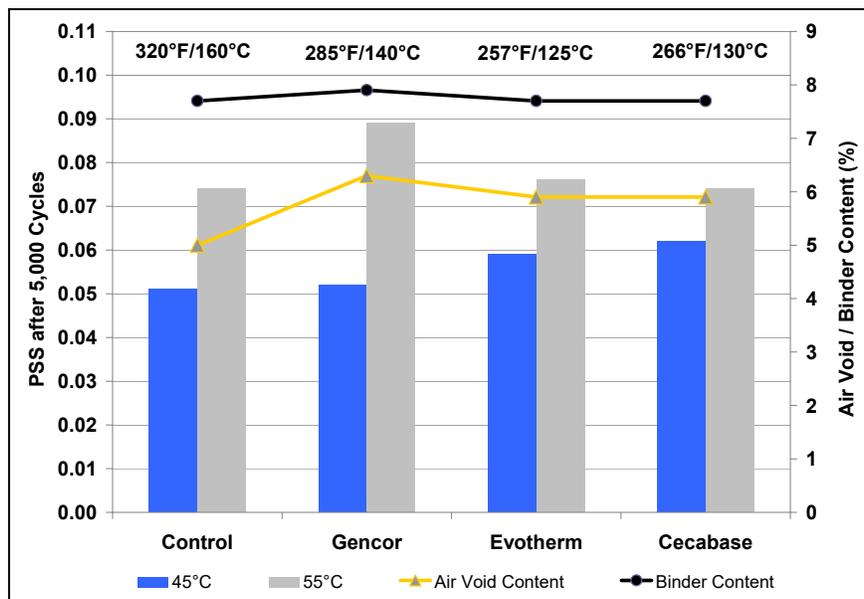

Figure 6.7: Average PSS after 5,000 cycles at 45°C and 55°C at 100 kPa stress level.
(Average mix production temperature, binder content, and air-void content shown.)

6.2.2   Beam Fatigue Tests

Air-Void Content

Fatigue beams were saw-cut from the top lift of the slabs sampled from the test track. Air-void contents were measured using the CoreLok method and results are listed in Table D.5 in Appendix D. Table 6.2 and Table 6.3 summarize the air-void distribution categorized by mix type and test tensile strain level for the beam fatigue and frequency sweep specimens, respectively. Figure 6.8 shows summary boxplots of air-void content for the wet and dry beam fatigue specimens.

Table 6.2: Summary of Air-Void Contents of Beam Fatigue Specimens

Condition	Strain	Temp.		Air-Void Content (%)							
				Control		Gencor		Evotherm		Cecabase	
	(µstrain)	°C	°F	Mean[1]	SD[2]	Mean	SD	Mean	SD	Mean	SD
Dry	200	20	68	4.5	0.7	6.7	0.2	6.1	0.2	7.1	0.7
	400			4.6	1.0	7.0	0.5	6.0	0.3	7.1	0.8
		Overall		4.6	0.8	6.9	0.4	6.1	0.3	7.1	0.7
Wet	200	20	68	4.3	0.8	6.6	0.6	6.2	0.8	6.5	0.4
	400			4.6	0.5	6.9	0.6	6.5	0.5	6.6	0.5
		Overall		4.4	0.7	6.7	0.6	6.3	0.7	6.6	0.5

[1] Mean of two replicates   [2] SD: Standard deviation

Table 6.3: Summary of Air-Void Contents of Flexural Frequency Sweep Specimens

Condition	Temp.		Air-Void Content (%)							
			Control		Gencor		Evotherm		Cecabase	
	°C	°F	Mean[1]	SD[2]	Mean	SD	Mean	SD	Mean	SD
Dry	10	50	4.4	0.9	6.3	1.1	6.2	0.6	7.3	0.1
	20	68	4.1	0.4	6.8	0.1	6.1	0.0	6.9	0.4
	30	86	4.0	0.5	6.3	1.5	6.4	0.4	6.9	0.1
	Overall		4.1	0.6	6.4	0.9	6.2	0.3	7.0	0.2
Wet	10	50	4.7	1.2	6.8	1.3	5.8	0.3	6.7	0.3
	20	68	3.0	1.3	7.4	0.1	6.2	0.1	6.2	0.2
	30	86	4.3	0.8	7.1	0.1	6.0	0.1	6.9	0.6
	Overall		4.0	1.1	7.1	0.5	6.0	0.2	6.6	0.4

[1] Mean of three replicates   [2] SD: Standard deviation
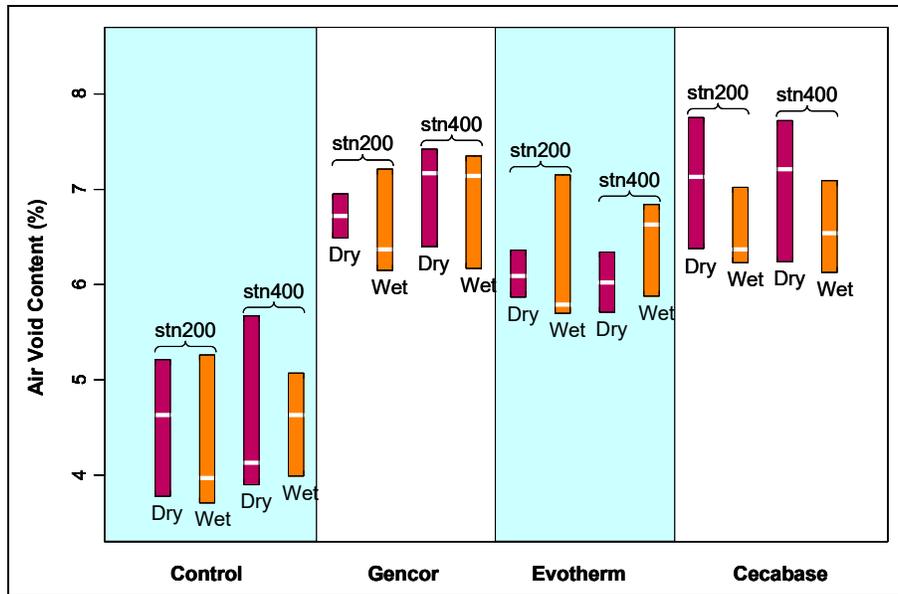
Figure 6.8: Air-void contents of beam fatigue specimens (dry and wet).

For the beam fatigue specimens, there was no significant difference in air-void content between the specimens used for testing at the different strain levels and moisture condition within each mix, apart from the 0.5 percent difference between the specimens for the Cecabase dry and wet testing. There was, however, a notable difference in air-void contents between the Control and the warm mixes as a group,

and between the different warm-mixes, with the Evotherm specimens having a lower average air-void content than the Gencor and Cecabase specimens. For the frequency sweep specimens, where only two specimens for each variable were tested, the air-void contents show a little more variability, but show similar trends to the beam fatigue specimens. Suggested reasons for the difference in air-void content are discussed in Section 0. The differences in air-void content were factored into the test result analyses, discussed below.

Initial Stiffness

Figure 6.9 illustrates the initial stiffness comparison at various strain levels, temperatures, and conditioning for the different mix types. Figure 6.10 shows the average results in relation to production temperature, binder content, and average air-void content. The following observations were made:

- Variation between results was in line with typical result ranges for this test.
- Initial stiffness was generally strain-independent for both the dry and wet tests.
- In the dry tests, there was no significant difference between the four mixes, indicating that the use of the warm-mix technologies and lower production and compaction temperatures did not significantly influence the performance of the mixes in this test.
- A reduction of initial stiffness due to soaking was apparent for each mix type, indicating a potential loss of structural capacity due to moisture damage. The reduction in initial stiffness after soaking was most prominent for the Gencor mix.
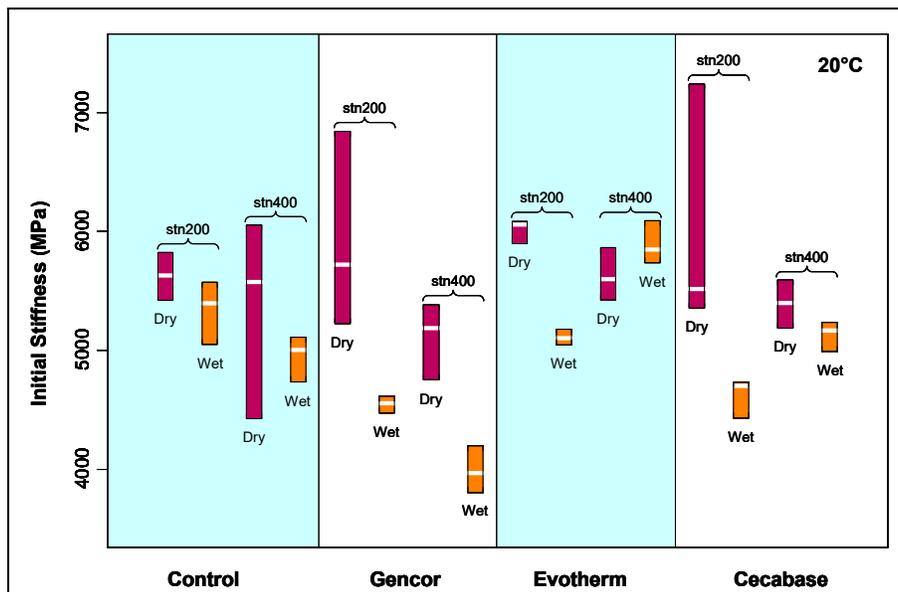
Figure 6.9: Summary boxplots of initial stiffness.
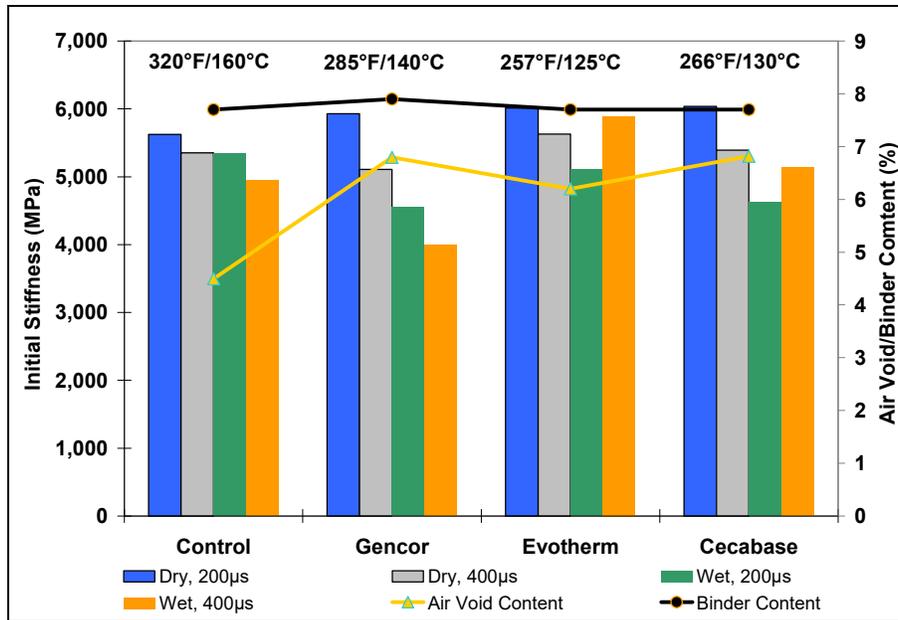
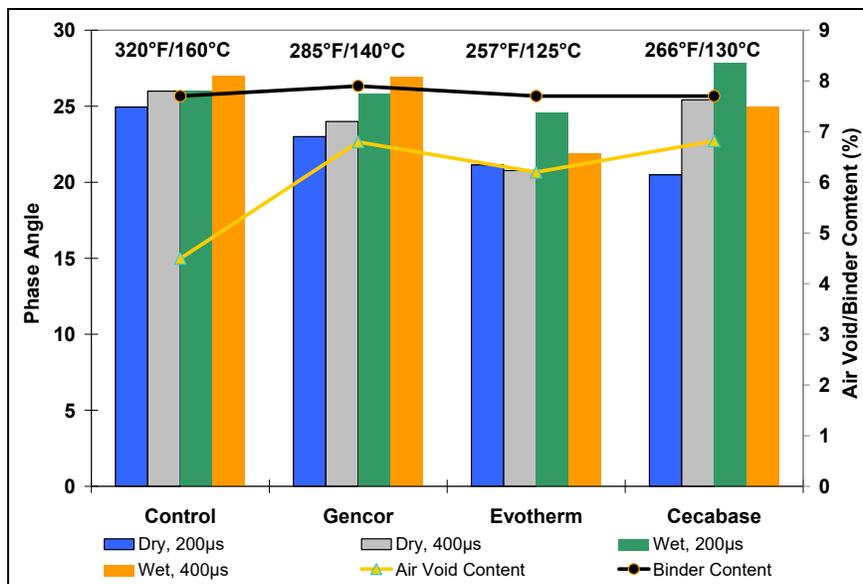**Figure 6.10: Plot of average initial stiffness.**
(Average mix production temperature, binder content, and air-void content shown.)

Initial Phase Angle

The initial phase angle can be used as an index of mix viscosity properties, with higher phase angles corresponding to more viscous and less elastic properties. Figure 6.11 illustrates the side-by-side phase angle comparison of dry and wet tests for the four mixes. Figure 6.12 shows the average results in relation to production temperature, binder content, and average air-void content. The following observations were made:

- The initial phase angle appeared to be strain-independent.
- There was less variation in results of the soaked tests between the three replicates in each mix compared to the dry tests. Soaking appeared to increase the phase angle slightly.
- The initial phase angle was highly negative-correlated with the initial stiffness.
- Statistical analyses (t-test and Kolmogorov-Smirnov test) indicated that there was no statistically significant difference (confidence level of 0.1) in performance between the Control and the three warm mixes after variation in mix production temperature, binder content, specimen air-void content, actual test strain level, and actual test temperature were taken into consideration. This indicates that the use of the warm-mix technologies and lower production and compaction temperatures did not significantly influence the performance of the mixes in this test.
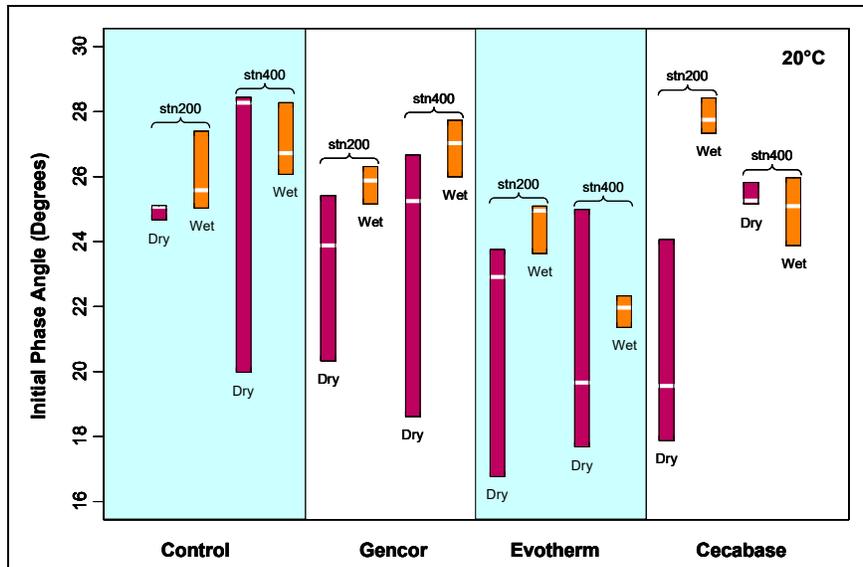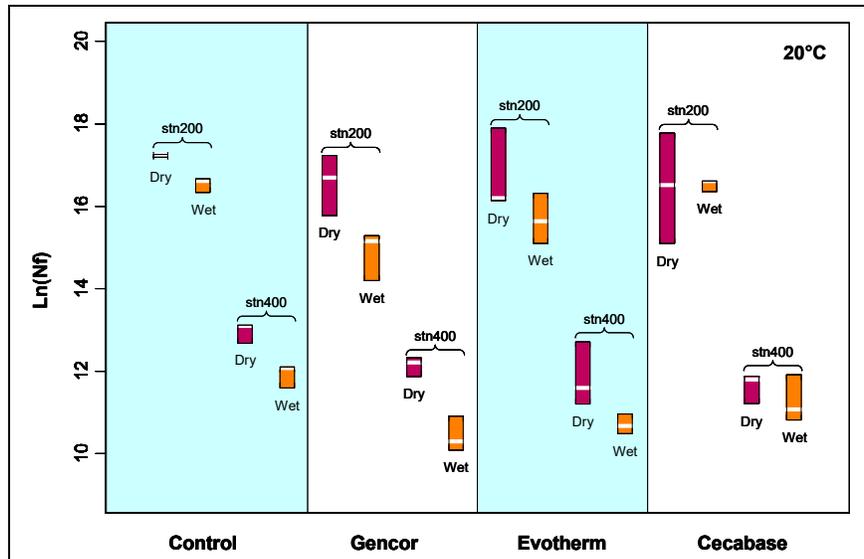
Figure 6.11: Summary boxplots of initial phase angle.

Figure 6.12: Plot of average initial phase angle.
(Average mix production temperature, binder content, and air-void content shown.)

Fatigue Life at 50 Percent Stiffness Reduction

Mix stiffness decreases with increasing test-load repetitions. Conventional fatigue life is defined as the number of load repetitions when 50 percent stiffness reduction has been reached. A high fatigue life implies a slow fatigue damage rate and consequently higher fatigue-resistance. The side-by-side fatigue life comparison of dry and wet tests is plotted in terms of the natural logarithm of this parameter in Figure 6.13. Figure 6.14 shows the average results in relation to production temperature, binder content, and average air-void content. The following observations were made:

- Fatigue life was strain-dependent as expected, with lower strains resulting in higher fatigue life.

- Soaking generally resulted in a lower fatigue life compared to the unsoaked specimens.
- Statistical analyses (t-test and Kolmogorov-Smirnov test) indicated that there was no statistically significant difference (confidence level of 0.1) in terms of fatigue life at 50 percent stiffness reduction performance between the Control and the three warm mixes after variation in mix production temperature, binder content, specimen air-void content, actual test strain level, and actual test temperature were taken into consideration. This indicates that the use of the warm-mix technologies and lower production and compaction temperatures did not significantly influence the performance of the mixes in this test.

Figure 6.13: Summary boxplots of fatigue life.
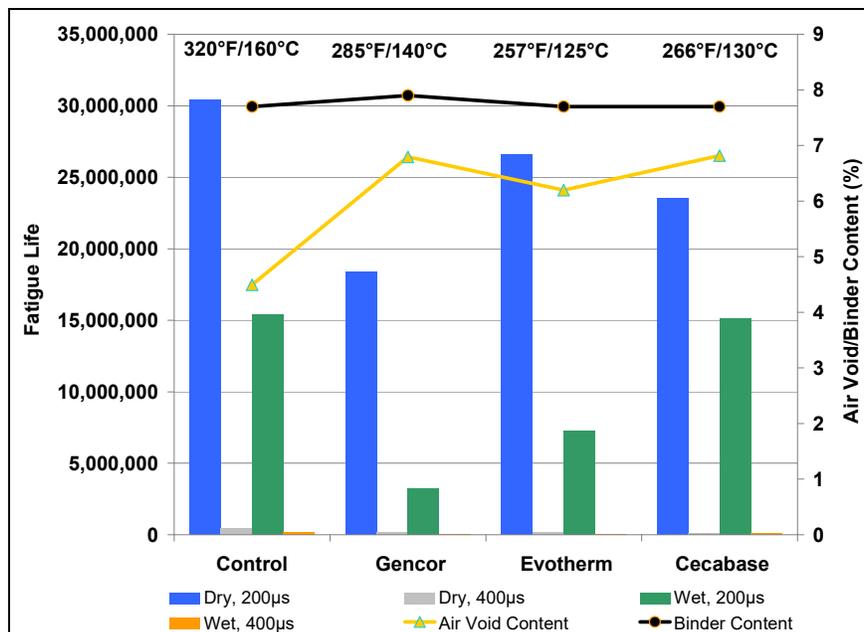
Figure 6.14: Plot of average fatigue life.

(Average mix production temperature, binder content, and air-void content shown.)

<u>Flexural Frequency Sweep</u>

The average stiffness values of the two replicates tested at the three temperatures were used to develop the flexural complex modulus ($E*$) master curve. This is considered a useful tool for characterizing the effects of loading frequency (or vehicle speed) and temperature on the initial stiffness of an asphalt mix (i.e., before any fatigue damage has occurred). The shifted master curve with minimized residual-sum-of-squares derived using a generic algorithm approach can be appropriately fitted with the following modified Gamma function (Equation 6.1):

$$E* = D + A\left(1 - \exp\left(-\frac{(x-C)}{B}\right) \cdot \sum_{m}^{n-1} \frac{(x-C)^m}{B^m m!}\right) \qquad \textbf{(6.1)}$$

where: $E* =$ flexural complex modulus (MPa);
        $x = \ln freq + \ln aT =$ is the loading frequency in Hz and $\ln aT$ can be obtained from the temperature-shifting relationship (Equation 6.2);
        A, B, C, D, and n are the experimentally-determined parameters.

$$\ln aT = A\left(1 - \exp\left(-\frac{T - Tref}{B}\right)\right) \qquad \textbf{(6.2)}$$

where: $lnaT =$ is a horizontal shift to correct the temperature effect with the same unit as $\ln freq$,
        $T =$ is the temperature in °C,
        $Tref =$ is the reference temperature, in this case, $Tref = 20$°C
        A and B are the experimentally determined parameters.

The experimentally determined parameters of the modified Gamma function for each mix type are listed in Table 6.4, together with the parameters in the temperature-shifting relationship.

Figure 6.15 and Figure 6.16 show the shifted master curves with Gamma-fitted lines and the temperature-shifting relationships, respectively, for the dry frequency sweep tests. The temperature-shifting relationships were obtained during the construction of the complex modulus master curve and can be used to correct the temperature effect on initial stiffness. Note that a positive temperature shift ($\ln aT$) value needs to be applied when the temperature is lower than the reference temperature, while a negative temperature shift value needs to be used when the temperature is higher than the reference temperature. The following observations were made from the dry frequency sweep test results:

- There was no apparent difference between the complex modulus master curves of the Control and Evotherm mixes. The curves for the Gencor and Cecabase mixes were below that of the Control. This was attributed to the higher air-void contents of the tested beams from these mixes.
- The temperature-shifting relationships indicate that there was very little difference in temperature sensitivity among the four mixes. Higher temperature-sensitivity implies that a per unit change of temperature will cause a larger change of stiffness (i.e., larger change of $\ln aT$).

Table 6.4: Summary of Master Curves and Time-Temperature Relationships

Mix	Conditioning	Master Curve					Time-Temperature Relationship	
		Number	A	B	C	D	A	B
Control	Dry	3	28929.32	6.26361	-7.48909	186.1060	28.6493	- 93.239
Gencor		3	18036.35	4.81871	-6.82995	273.4475	88.3407	-302.942
Evotherm		3	23419.05	5.47160	-7.27919	237.0034	-156.8730	522.782
Cecabase		3	12045.32	3.36214	-5.85569	442.2764	-18.7266	63.296
Control	Wet	3	25412.95	6.07384	-7.70255	190.4917	5.8064	-19.5429
Gencor		3	26716.69	7.13615	-7.71639	175.0177	22.0331	-67.0559
Evotherm		3	78224.31	12.77743	-9.25152	97.1018	29.2673	-84.6037
Cecabase		3	42008.68	8.51963	-7.63484	187.8012	-18.7079	54.9038

Notes:

1. The reference temperature is 20°C.
2. The wet test specimens were soaked at 60°C.
3. Master curve Gamma-fitted equations:

If $n = 3$, $E^* = D + A\left(1 - \exp\left(-\dfrac{(x-C)}{B}\right) \cdot \left(1 + \dfrac{x-C}{B} + \dfrac{(x-C)^2}{2B^2}\right)\right)$,

   where $x = \ln freq + \ln aT$

4. Time-temperature relationship:

$\ln aT = A\left(1 - \exp\left(-\dfrac{T - Tref}{B}\right)\right)$
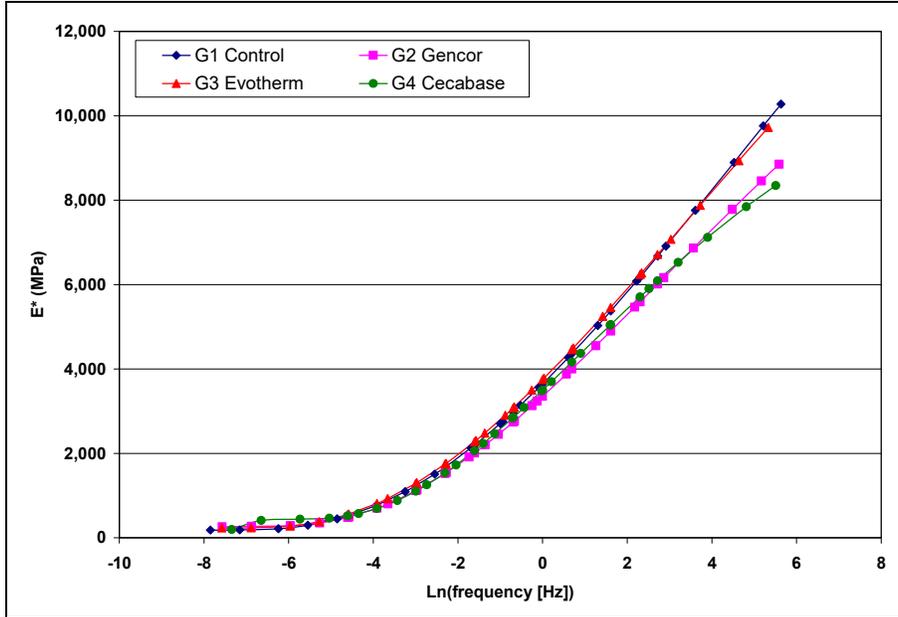
Figure 6.15: Complex modulus (*E**) master curves (dry).
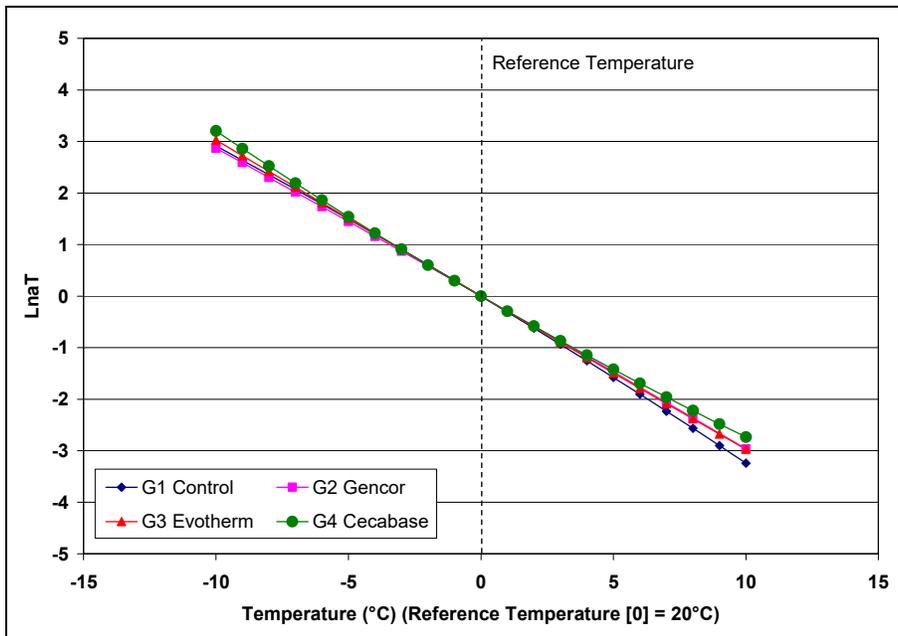
Figure 6.16: Temperature-shifting relationship (dry).

Figure 6.17 and Figure 6.18 respectively show the shifted master curves with Gamma-fitted lines and the temperature-shifting relationships for the wet frequency sweep tests. The comparison of dry and wet complex modulus master curves is shown in Figure 6.19 for each mix type. The following observations were made with regard to the wet frequency sweep test results:

- The complex modulus curve of the Control was higher than those of the warm mixes. The Evotherm and Cecabase mixes had similar performance, while the Gencor mix had a lower complex

modulus. This was attributed to the higher air-void contents of the tested beams from the warm mixes.

- There were no significant temperature-sensitivity differences between the four mixes at higher temperatures (i.e., higher than 20°C). At lower temperatures (i.e., lower than 20°C), there was a small difference in temperature-sensitivity between the Control and the warm mixes.
- Some loss of stiffness attributed to moisture damage was apparent in all four mixes.
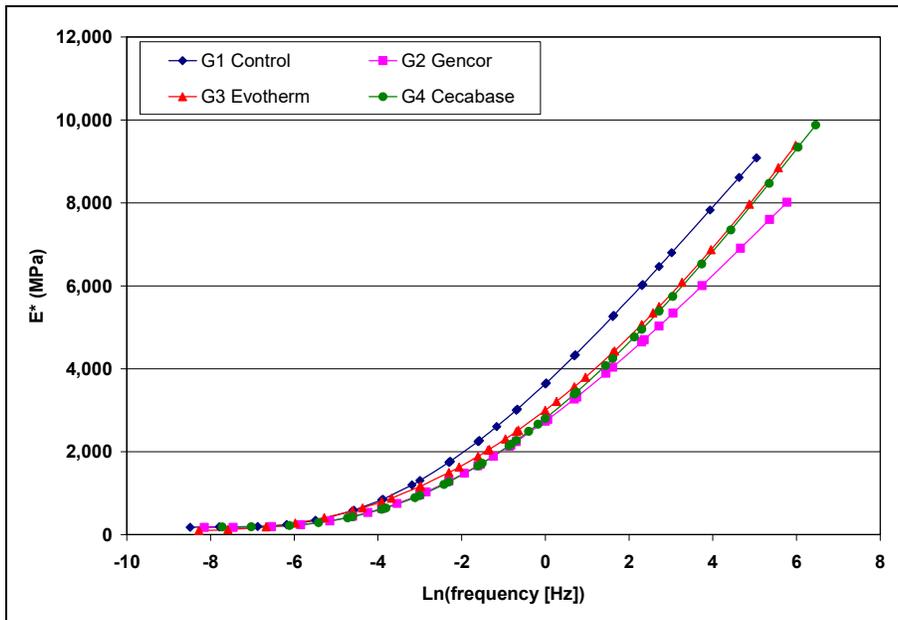
Figure 6.17: Complex modulus (*E**) master curves (wet).
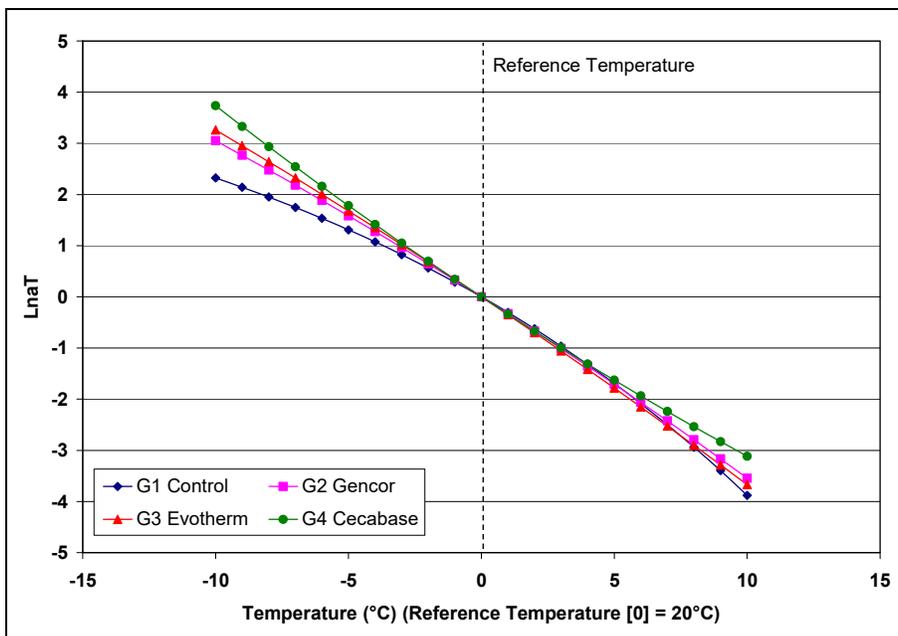
Figure 6.18: Temperature-shifting relationship (wet).
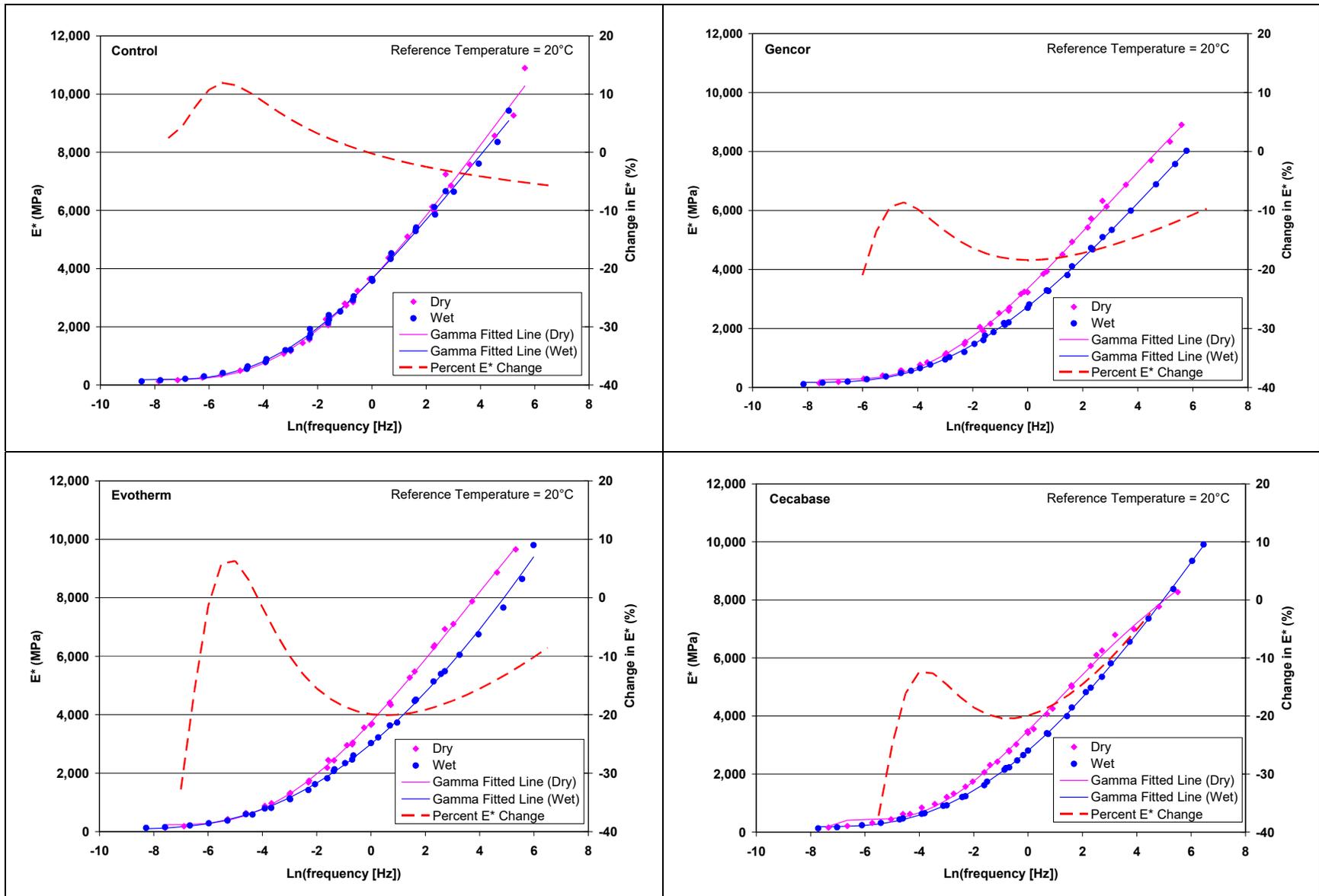
Figure 6.19: Comparison of dry and wet complex modulus master curves.
(Includes percent reduction in stiffness at each frequency from dry to wet master curve.)

6.2.3 Moisture Sensitivity: Hamburg Wheel-Track Test

Air-Void Content

The air-void content of each core was determined using the CoreLok method. The air-void contents ranged between 4.8 and 7.9 percent, with the Control mix specimens having slightly lower air-void contents than those of the other three mixes (Table 6.5).

Table 6.5: Summary of Air-Void Contents of Hamburg Test Specimens

Air-Void Content (%)							
Control		Gencor		Evotherm		Cecabase	
Mean[1]	Std Dev[2]	Mean	Std Dev	Mean	Std Dev	Mean	Std Dev
6.3	0.3	6.5	0.7	7.0	0.4	6.9	0.6

[1] Mean of four replicates   [2] Std Dev: Standard deviation

Testing

The testing sequence of the specimens was randomized to avoid any potential block effect. Rut depth was recorded at 11 equally spaced points along the wheelpath on each specimen. The average of the middle seven points was then used in the analysis. This method ensures that localized distresses are smoothed and variance in the data is minimized. It should be noted that some state departments of transportation only measure the point of maximum final rut depth, which usually results in a larger variance in the test results.

Average maximum rut depths after 10,000 and 20,000 passes and the creep and stripping slopes are summarized in Table 6.6. There was no apparent stripping inflection point.

Table 6.6: Summary of Results of Hamburg Wheel-Track Tests

Test Set	Rut depth (mm)							
	Control		Gencor		Evotherm		Cecabase	
	Mean[1]	SD[2]	Mean	SD	Mean	SD	Mean	SD
10,000 passes								
1	7.3	0.1	8.7	1.9	7.9	0.6	6.3	1.1
2	7.0	0.7	13.5	1.8	7.5	0.9	8.8	1.5
Overall	7.1	0.4	11.1	1.8	7.7	0.8	7.6	1.3
20,000 passes								
1	10.4	0.7	11.9	2.4	10.9	0.2	9.5	2.3
2	9.5	2.0	16.7	2.0	9.7	0.6	11.2	1.8
Overall	10.0	1.3	14.3	2.2	10.3	0.4	10.4	2.1
Creep Slope (mm/pass)								
1	-0.0004		-0.0004		-0.0003		-0.0003	
2	-0.0004		-0.0004		-0.0004		-0.0004	
Overall	-0.0004		-0.0004		-0.0004		-0.0004	
Stripping Slope (mm/pass)								
1	-0.0003		-0.0003		-0.0003		-0.0003	
2	-0.0003		-0.0003		-0.0003		-0.0003	
Overall	-0.0003		-0.0003		-0.0003		-0.0003	

[1] Mean of four replicates   [2] SD: Standard deviation

Figure 6.20 shows the average rut progression curves of all tests, and Figure 6.21 and Figure 6.22 show the average rut progression curves and average maximum rut for each mix, respectively. No clear stripping inflection points were noted in any tests, indicating that no stripping occurred in any of the mixes.
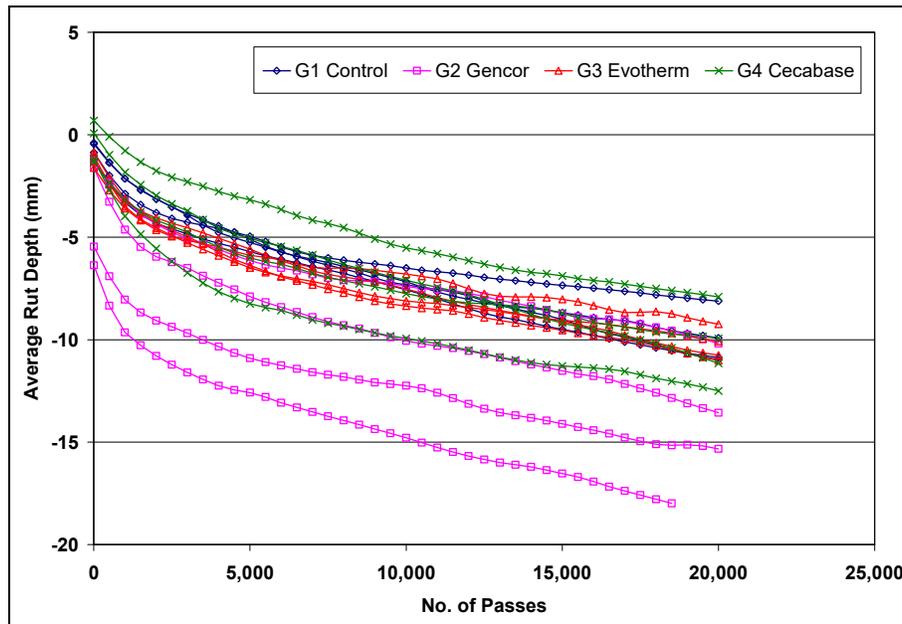

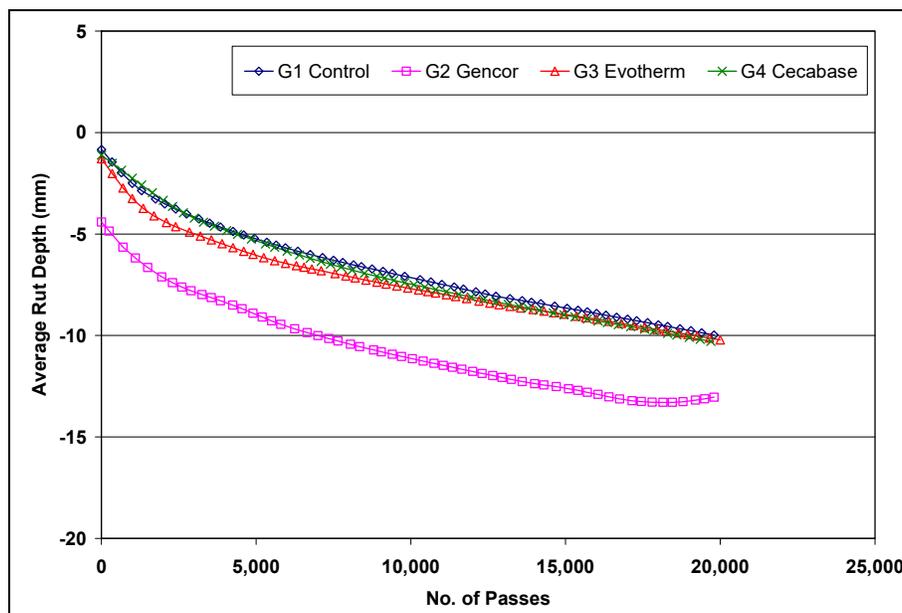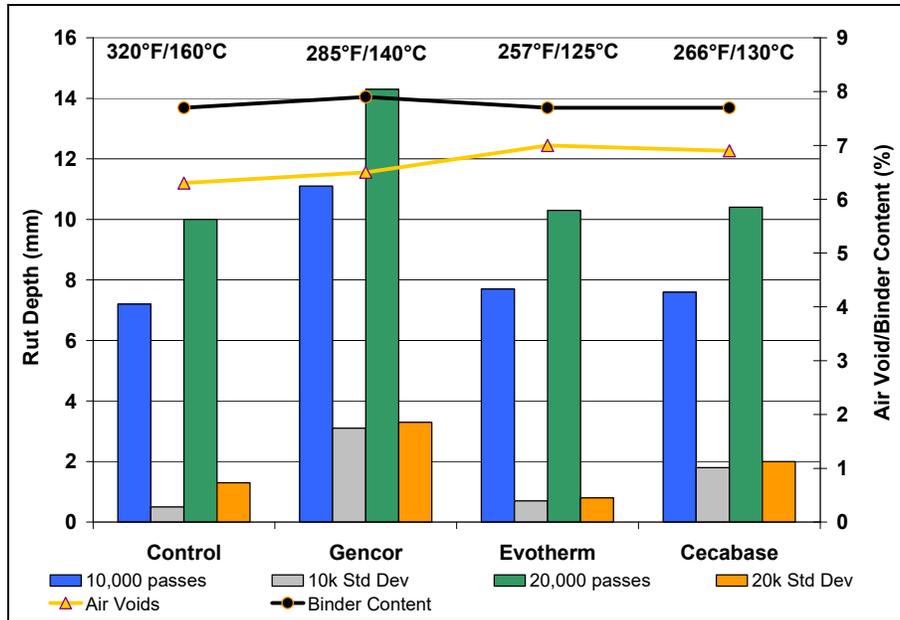**Figure 6.20: Hamburg Wheel-Track rut progression curves for all tests.**

Figure 6.21: Average Hamburg Wheel-Track rut progression curves for each mix.

Figure 6.22: Average Hamburg Wheel-Track rut depth for each mix.
(Average mix production temperature, binder content, and air-void content shown.)

The mixes all show similar trends, with very little difference in performance between the Control, Evotherm and Cecabase mixes. The average maximum rut measured after 10,000 and 20,000 repetitions on the Gencor mix specimens was notably higher than the other mixes. Air-void content did not appear to have a significant impact on performance.

6.2.4 Moisture Sensitivity: Tensile Strength Retained (TSR) Test

Air-Void Content

The air-void content of each core was determined using the CoreLok method. The air-void contents ranged between 4.5 and 7.0 percent, with the Control mix specimens having slightly lower air-void contents than the other three mixes (Table 6.7). It should be noted that laboratory TSR tests that are carried out as part of a mix design require a specimen air-void content of seven percent.

Table 6.7: Summary of Air-Void Contents of Tensile Strength Retained Test Specimens

Condition	Air-Void Content (%)							
	Control		Gencor		Evotherm		Cecabase	
	Mean[1]	Std Dev[2]	Mean	Std Dev	Mean	Std Dev	Mean	Std Dev
Dry	5.3	0.5	5.6	0.3	6.2	0.3	6.3	0.4
Wet	5.4	0.3	5.3	0.4	6.3	0.5	6.3	0.4
[1] Mean of six replicates		[2] Std Dev: Standard deviation						

Results of Tensile Strength Retained (TSR) tests are listed in Table D.6 in Appendix D and summarized for each mix in Table 6.8. A plot of the average results is shown in Figure 6.23. The results indicate that:

- The Control mix dry and wet strengths were higher than those of the warm mixes.
- The dry strengths of the warm mixes were similar, but the wet strengths showed more variation.
- The recorded TSR values for all mixes were all higher than the minimum tentative criteria of 70 percent for low environmental risk regions in the Caltrans Testing and Treatment Matrix to ensure moisture resistance. The Control, Evotherm, and Cecabase mixes also all had TSR values higher than the minimum 75 percent for medium and high environmental risk regions. However, the Gencor mix did not meet this criterion. The reason for this is unclear from the results, given that the Gencor specimen's air-void contents were similar to the Control, lower than the other warm mixes, and lower than the standard test requirement of seven percent. Consequently, treatment would typically be required to raise the test results for this mix up to the minimum to reduce the risk of moisture damage in the pavement in these regions.

The results showed similar trends to the Hamburg Wheel-Track test results.

Table 6.8: Summary of Tensile Strength Retained Test Results

Parameter	Indirect Tensile Strength (kPa)							
	Control		Gencor		Evotherm		Cecabase	
	Mean[1]	Std Dev[2]	Mean	Std Dev	Mean	Std Dev	Mean	Std Dev
Dry Test	1,018	778	903	658	901	728	881	712
Wet Test	47	22	39	25	16	104	42	40
TSR	77.2		72.5		78.1		81.6	
Damage	-	Yes	-	Yes	-	Yes	-	Yes
[1] Mean of six replicates			[2] Std Dev: Standard deviation					
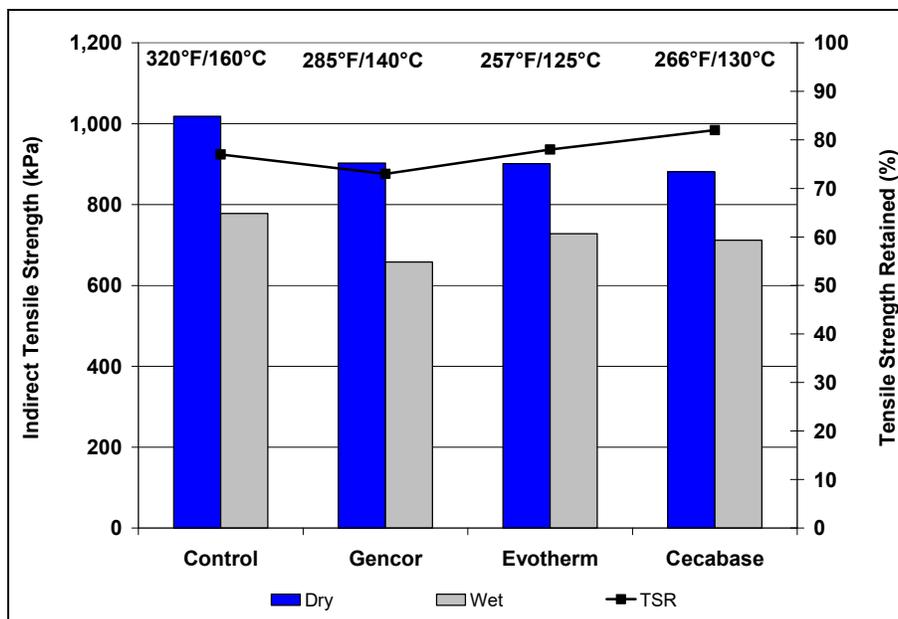
Figure 6.23: Average tensile strength retained for each mix.

Observation of the split faces of the cores revealed very little internal stripping (loss of adhesion between asphalt and aggregate evidenced by clean aggregate on the broken face) after moisture conditioning.

6.3   Summary of Laboratory Testing Results

The laboratory test results indicate that use of the warm-mix technologies assessed in this study, produced and compacted at lower temperatures, did not significantly influence the performance of the asphalt concrete when compared to control mixes produced and compacted at conventional hot-mix asphalt temperatures. Specific observations include:

- Shear performance of the Evotherm and Cecabase mixes did appear to be influenced in part by the lower mix production and construction temperatures, which would have resulted in less oxidation of the binder and consequent lower stiffness of the mix. However, the differences were not statistically significant. Rutting performance under accelerated load testing did not appear to be affected, however. Fatigue performance and moisture sensitivity also did not appear to be affected.
- The Gencor (water injection technology) mix appeared to have lower moisture resistance compared to the other three mixes in all the moisture sensitivity tests, and did not meet the Caltrans-specified performance requirements for medium and high environmental risk regions. This mix was produced at a higher temperature than the other two warm mixes and contained no moisture.
- Test results were influenced by mix production temperatures, actual binder content, specimen air-void content, actual stress and strain levels, and actual test temperature. These parameters need to be taken into consideration when comparing performance between the different mixes.

7. CONCLUSIONS AND PRELIMINARY RECOMMENDATIONS

7.1   Conclusions

This first-level report describes part of the third phase of a warm-mix asphalt study, which compares the performance of a gap-graded rubberized asphalt control mix, produced and constructed at conventional hot-mix asphalt temperatures (320°F [160°C]), with three warm mixes produced at between 36°F (20°C) and 63°F (35°C) lower than the control. The technologies tested included water injection (*Gencor Ultrafoam GX®*, produced at 284°F [140°C]) and two chemical surfactants (*Evotherm DAT™*, produced at 248°F [125°C] and *Cecabase®*, produced at 266°F [130°C]). The test track layout and design, mix design and production, and test track construction are discussed, as are results of Heavy Vehicle Simulator (HVS) and laboratory testing.

Key findings from the study include the following:
- A consistent subgrade was prepared and consistent base-course and underlying dense-graded hot-mix asphalt concrete layers were constructed on the test track using materials sourced from a nearby quarry and asphalt plant. Thickness and compaction of the base and bottom layer of asphalt were consistent across the test track.
- Minimal asphalt plant modifications were required to accommodate the warm-mix technologies, and the delivery systems were approved under the Caltrans Material Plant Quality Program.
- No problems were noted with producing the asphalt mixes at the lower temperatures. Target mix production temperatures (320°F, 284°F, 248°F, and 266°F [160°C, 125°C, 140°C, and 130°C] for the Control, Gencor, Evotherm, and Cecabase mixes, respectively), set by the warm-mix technology providers, were all achieved. There was very little variation in mix properties among the four mixes. Hveem stabilities, determined at three different curing regimes, exceeded the minimum requirement by a considerable margin. Curing did not appear to influence the stability. No moisture was measured in the mixes after production.
- Compaction temperatures differed considerably between the mixes and were consistent with production temperatures. The Evotherm and Cecabase mixes, produced at 248°F and 266°F (140°C and 130°C), respectively, lost heat at a slower rate during transport and placement than the Control and Gencor mixes, produced at the higher temperatures. The lower temperatures in the three warm-mixes did not appear to influence the paving or compaction operations, and interviews with the paving crew after construction revealed that no problems were experienced at the lower temperatures. Improved working conditions were identified as an advantage.
- Smoke and odors were significantly more severe on the Control section compared to the Gencor section. No smoke or odors were noted on the Evotherm and Cecabase sections.
- Mix workability of the mix, determined through observation of and interviews with the paving crew, was considerably better on the warm-mix sections compared to the Control.
- Average thicknesses of the top (rubberized) and bottom asphalt layers across the four sections were 0.22 ft. (66 mm) and 0.23 ft. (74 mm), respectively. The average thickness of the combined two

layers was 0.45 ft. (137 mm), 0.05 ft. (17 mm) thicker than the design thickness of 0.4 ft. (120 mm). General consistency of thickness across the track was considered satisfactory and representative of typical construction projects.

- Nuclear gauge–determined density measurements were inconsistent with core-determined air-void contents. The core determined air-void contents indicated that slightly higher density was achieved on the Control section (95 percent of the RICE specific gravity) compared to the warm-mix sections (94 percent). Compaction across the test track appeared to be consistent and it was concluded that adequate compaction can be achieved on rubberized warm-mixes at lower temperatures. Based on observations from the test track construction and interviews with roller operators, optimal compaction temperatures will differ among the different warm-mix technologies, but adequate compaction can be achieved on warm-mixes at the lower temperatures. Roller operators will, however, need to consider that there might be differences in roller response between warm-mix and conventional hot-mixes, and that rolling operations and patterns may need to be adjusted to ensure that optimal compaction is always achieved.

- HVS trafficking on each of the four sections revealed that the duration of the embedment phases on all sections were similar; however, the depth of the ruts at the end of the embedment phases differed slightly between sections, with the Gencor (6.5 mm [0.26 in.]) and Cecabase (5.5 mm [0.22 in.]) having less embedment than the Control and Evotherm sections, which had similar embedment (7.9 mm [0.31 in.]). This is opposite to the early rutting performance in the Phase 1 study.

- Rut rate (increase in rut depth per load repetition) after the embedment phase on the Control and Evotherm sections was almost identical. On the Gencor and Cecabase sections, rut rate was considerably slower than the Control after the embedment phase. The difference in performance between the three warm-mix sections is attributed in part to the lower production and paving temperatures of the Evotherm mix compared to the other warm mixes, as well as to the thickness of the asphalt layers (the Evotherm section had thinner asphalt layers than the Control and Cecabase sections).

- The laboratory test results indicate that use of the warm-mix technologies assessed in this study, produced and compacted at lower temperatures, did not significantly influence the performance of the asphalt concrete when compared to control specimens produced and compacted at conventional hot-mix asphalt temperatures. Specific observations include the following:
  + Shear performance of the Evotherm and Cecabase mixes did appear to be influenced in part by the lower mix production and construction temperatures, which would have resulted in less oxidation of the binder and consequent lower stiffness of the mix. Rutting performance under accelerated load testing did not appear to be affected, however. Fatigue performance and moisture sensitivity also did not appear to be affected.
  + The Gencor (water injection technology) mix appeared to have lower moisture resistance compared to the other three mixes in all the moisture sensitivity tests. This mix was produced at a higher temperature than the other two warm mixes and contained no moisture.
  + Laboratory test results were influenced by mix production temperatures, actual binder content, specimen air-void content, actual stress and strain levels, and actual test temperature. These parameters need to be taken into consideration when comparing performance between the different mixes.

The findings of the study are also summarized below in the form of answers to the questions identified in Section 1.3.

7.1.1　Comparative Energy Usage

Comparative energy usage could not be assessed in this study due to the very small quantities produced. These studies will need to be carried out during larger full-scale pilot studies on in-service pavements when large quantities of mix are produced (i.e., more than 5,000 tonnes).

7.1.2　Achieving Compaction Density at Lower Temperatures

Compaction measurements during construction indicated that average air-void contents on the warm-mix sections were marginally higher than on the Control sections, but were typical of full-scale construction projects. Based on these observations it is concluded that adequate compaction can be achieved on warm-mixes at lower temperatures. Optimal compaction temperatures will differ among the different warm-mix technologies. Roller operators will need to consider that there might be differences in roller response between warm-mix and conventional hot mixes, and that rolling operations and patterns may need to be adjusted to ensure that optimal compaction is always achieved. Contractors will need to determine mix production temperatures based on required compaction temperatures, and take loss of temperature during silo storage and transportation into consideration.

7.1.3　Optimal Temperature Ranges for Warm-Mixes

Optimal compaction temperatures will differ between the different warm-mix technologies. This study has shown that temperatures of at least 35°C (60°F) lower than conventional temperatures are appropriate for producing and compacting the modified mixes.

7.1.4　Cost Implications

The cost benefits of using the warm-mix technologies could not be assessed in this study due to the very small quantities produced.

7.1.5　Rutting Performance

Based on the results of HVS testing, it is concluded that the use of any of the three warm-mix asphalt technologies used in this experiment will not significantly influence the rutting performance of the mix.

7.1.6　Moisture Sensitivity

Laboratory moisture sensitivity testing indicated that the water injection technology (Gencor) showed lower moisture resistance compared to the other mixes, but still met Caltrans-specified performance requirements in most instances. No moisture sensitivity was noted during accelerated pavement testing.

7.1.7 Fatigue Performance

Laboratory fatigue testing indicated that the warm-mix technologies used in this study will not influence the fatigue performance of a mix.

7.1.8 Other Effects

Smoke and odors were significantly reduced during construction of the warm-mix sections compared to the Control. The workability of the warm-mixes in terms of raking and shoveling was also considerably better than the Control mix.

7.2 Preliminary Recommendations

The HVS and laboratory testing completed in this phase have provided no results to suggest that warm-mix technologies should not be used in gap-graded rubberized mixes in California, provided that standard specified construction and performance limits for hot-mix asphalt are met. Significant reductions in smoke and odors and improved workability of the warm mixes also support wider use of these technologies. Consideration should be given to further study into the effects of warm-mix asphalt technologies and production and placement of warm-mixes at lower temperatures on binder oxidation/aging rates. The effects that these may have on performance over the life of the asphalt surfacing should also be investigated. Research in this study has shown differences in early rutting performance between conventional and rubber mixes, between mixes tested after different curing periods, and between pavements subjected to mostly shade and mostly sun, respectively.

8. REFERENCES

1. JONES, D. and Harvey, J. 2007. **Warm-Mix Asphalt Study: Workplan for Comparison of Conventional and Warm-Mix Asphalt Performance Using HVS and Laboratory Testing.** Davis and Berkeley, CA: University of California Pavement Research Center. (UCPRC-WP-2007-01).

2. JONES, D., Wu, R., Tsai, B., Lu, Q. and Harvey, J. 2008. **Warm-Mix Asphalt Study: Test Track Construction and First-level Analysis of Phase 1 HVS and Laboratory Testing.** Davis and Berkeley, CA: University of California Pavement Research Center. (RR-2008-11).

3. JONES, D., Wu, R., Tsai, B., Lu, Q. and Harvey, J. 2008. **Warm-Mix Asphalt Study: First-Level Analysis of Phase 2 HVS and Laboratory Testing, and Phase 1 and Phase 2 Forensic Assessments.** Davis and Berkeley, CA: University of California Pavement Research Center. (RR-2009-02).

4. JONES, D. and Tsai, B. 2012. **Warm-Mix Asphalt Study: First-Level Analysis of Phase 2b Laboratory Testing on Laboratory Prepared Specimens.** Davis and Berkeley, CA: University of California Pavement Research Center. (RR-2012-07).

5. JONES, D., Wu, R., Tsai, B. and Harvey, J. 2011. **Warm-Mix Asphalt Study: Test Track Construction and First-Level Analysis of Phase 3b HVS and Laboratory Testing (Rubberized Asphalt, Mix Design #2).** Davis and Berkeley, CA: University of California Pavement Research Center. (RR-2011-03).

6. JONES, D. 2012. **Warm-Mix Asphalt Study: Field Test Performance Evaluation.** Davis and Berkeley, CA: University of California Pavement Research Center. (RR-2012-08).

7. **Standard Specifications.** 2006. Sacramento, CA: State of California Department of Transportation.

8. JONES, D. 2005. **Quality Management System for Site Establishment, Daily Operations, Instrumentation, Data Collection and Data Storage for APT Experiments.** Pretoria, South Africa: CSIR Transportek. (Contract Report CR-2004/67-v2).

APPENDIX A: MIX DESIGN

A.1   Mix Design

The mix design, developed by Granite Construction and used for the production of the four mixes (control plus three warm-mixes) at the Granite Construction Bradshaw Asphalt Plant is provided in Figure A.1.

December 6, 2012

Granite Construction

4001 Bradshaw Road

Sacramento, CA 95827

Attention: Stacy Merola

Subject: Submittal of 12.5 mm (½") RHMA-GG Type 2

Project: 205572- Oak Avenue Rehab

Pursuant to Section 39-2.01, 39-2.02, and 39-3.03 of the State of California, Department of Transportation Standard Specifications, July 1999, and the project special provisions the following is submitted:

GRANITE PRODUCT CODE 2033

GRADATION			
Sieve Size	Submittal	Caltrans Specifications	Contract Compliance
19 mm (3/4")	100	100	100
12.5 mm (1/2")	98	90 - 100	90 - 100
9.5 mm (3/8")	X = 83	77 – 89	76 - 90
4.75 mm (No. 4)	X = 40	33 - 47	30 - 44
2.36 mm (No. 8)	X = 23	18 – 28	6 - 26
600 µm (No. 30)	X = 12		
75 µm (No. 200)	5	3 - 7	0 - 8
Bitumen Ratio: 7.0%	Asphalt/Rubber Ratio: 82/18	PG 64-16: 79.9%	
Raffex 120 / Tricor: 2.5% (By Wt. Asphalt)	CRM Scrap Tire Rubber: 77%	CRM High Natural Rubber: 23%	

Source: Bradshaw Plant

If you require any additional information, please do not hesitate to call.
Respectfully,
GRANITE CONSTRUCTION COMPANY

Drew Walkenbach
Quality Control Engineer

Figure A.1: Mix design.

GRANITE CONSTRUCTION COMPANY SINCE 1922

Plant	Bradshaw
Product Code	2033 (09BA)
Date Completed	09/24/09
Paramount PG 64-16	

1/2 inch - RHMA-G

HOT MIX ASPHALT LABORATORY TEST RESULTS*

% AC (DWA)	% Air Voids (CT 309)	% Air Voids (CT 367)	Corrected Stability CT 366	VMA LP-2	VFA LP-3	Film Thickness MS-2	Dust Proportion LP-4
6.50	5.3	NA	41	18.7	71.7	11.6	0.76
7.00	4.6	NA	35	19.0	75.7	12.6	0.70
7.50	3.5	NA	32	19.0	81.5	13.6	0.65
8.00	3.2	NA	33	19.6	83.9	14.5	0.61

* Each Result Represents the Average of Three Replicate Samples (See Page 3 of 3 for graphs)

HOT MIX ASPHALT PROPERTIES

MIXTURE PROPERTIES AT OPTIMUM OIL CONTENT		SPECS.
OPTIMUM TOTAL OIL CONTENT (DWA), %	7.0	N/A
OPT. VIRGIN OIL CONTENT IF RAP MIX (DWA), %	NA	N/A
LAB COMPACTED UNIT WEIGHT (CT308), pcf	148.6	N/A
AIR VOIDS (CT367), %	4.5	4 ± 2 %
MAXIMUM THEORETICAL DENSITY (CT367), pcf		N/A
AIR VOIDS (CT 367 utilizing CT309), %		N/A
MAXIMUM THEO. DENSITY (CT309), pcf	2.492	N/A
HVEEM STABILITY, Min. (CT366)	35	23
VMA (LP-2), % , Min.	18.9	18
VFA (LP-3), %	76.5	65 - 75
FILM THICKNESS, μm (MS-2)	NA	N/A
DUST PROPORTION (LP-4)	0.7	N/A
SWELL (CT 305), Inch, Max.	-	0.03

RAP PROPERTIES	
A.C. CONTENT (DWA) %	4.0
GRADATION*, SEE PAGE 1 OF 4	

* GRADATION PERFORMED AFTER CHEMICAL EXTRACTION

Mixing Temperature	230
Compaction Temp.	230
Compaction Method	CT

AGGREGATE PROPERTIES

FINE AGGREGATE PROPERTIES		SPECS.
Bulk Specific Gravity (CT 206)	2.665	-
Absorption (%) (CT 206)	1.70	-
Apparent Specific Gravity (CT 208)	2.772	-
Sand Equivalent (CT 217)	71	47 min.
Fine Aggregate Angularity (AASHTO T304, A)	46.3	45 min.
Percent Crushed Particles (CT 205)	0	70 min.
K_f Factor	1.1	1.7 max.
Plasticity Index	-	-
Liquid Limit	-	-

COARSE AGGREGATE PROPERTIES		SPECS.
Bulk Specific Gravity (CT 206)	2.796	-
Absorption (%) (CT 206)	0.57	-
Loss Angeles Abrasion (CT 211)		
Loss @ 100 Revs	3	10 max.
Loss @ 500 Revs	15	45 max.
Percent Crushed Particles (CT 205)		
1 Face	100	90 min.
2 Faces	100	-
Flat and Elongated Particles (ASTM D4791)		
% max. by weight	5.6	5:1 max.
K_c Factor	0.4	1.7 max.

COMBINED AGG. PROPERTIES		SPECS.
Sodium Sulfate Soundness (CT 214)		
Loss After 5 Cycles	-	-
Bulk Specific Gravity (CT 367)	2.787	-
Bulk Specific Gravity (LP - 2)	2.743	-

Reviewed by: Dan Ridolfi
9/24/2009

GRANITE *Engineering Services*

Page 1 of 4

Figure A.1: Mix design (*continued*).

Figure A.1: Mix design (*continued*).

APPENDIX B: TEST PIT PROFILES

B.1   Dynamic Cone Penetrometer

Dynamic cone penetrometer (DCP) profiles taken outside and within the wheelpath are shown in Figure B.1 through Figure B.4. Profiles were taken after removal of the asphalt concrete during excavation of the test pits. DCP profile details are as follows:

- Figure B.1: 620HA: Phase 3a Control
- Figure B.2: 621HA: Phase 3a Gencor
- Figure B.3: 622HA: Phase 3a Evotherm
- Figure B.4: 623HA: Phase 3a Cecabase

B.2   Layer Thickness and Rutting

Test pit profiles for each test section are shown in Figure B.5 through Figure B.8. All test pits were excavated between Station 9 and Station 11. All profiles show the test pit face at Station 9. Test pit details are as follows:

- Figure B.5: 620HA: Phase 3a Control after 74,000 repetitions
- Figure B.6: 621HA: Phase 3a Gencor after 159,000 repetitions
- Figure B.7: 622HA: Phase 3a Evotherm after 200,000 repetitions
- Figure B.8: 623HA: Phase 3a Cecabase after 224,000 repetitions

Figure B.1: 620HA: Control DCP profile (untrafficked [left] and wheelpath [right]).

Figure B.2: 621HA: Gencor DCP profile (untrafficked [left] and wheelpath [right]).

Figure B.3: 622HA: Evotherm DCP profile (untrafficked [left] and wheelpath [right]).

Figure B.4: 623HA: Cecabase DCP profile (untrafficked [left] and wheelpath [right]).
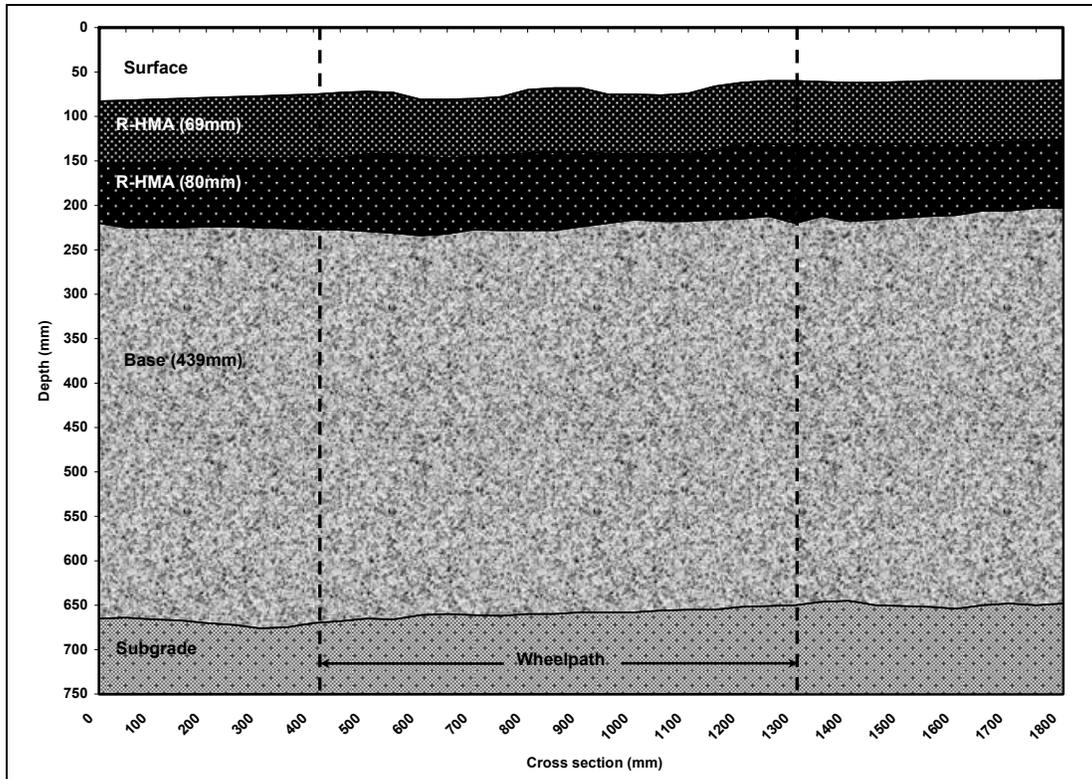
Figure B.5: 620HA: Control test pit profile (after 74,000 load repetitions).
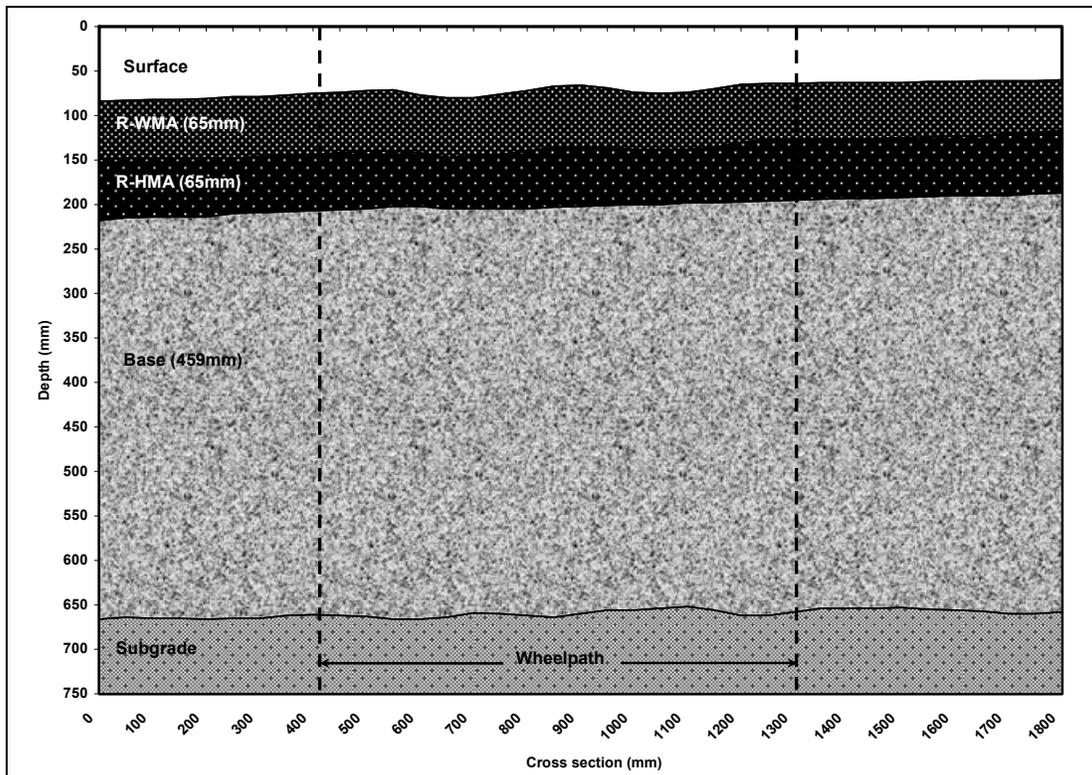
Figure B.6: 621HA: Gencor test pit profile (after 159,000 load repetitions).
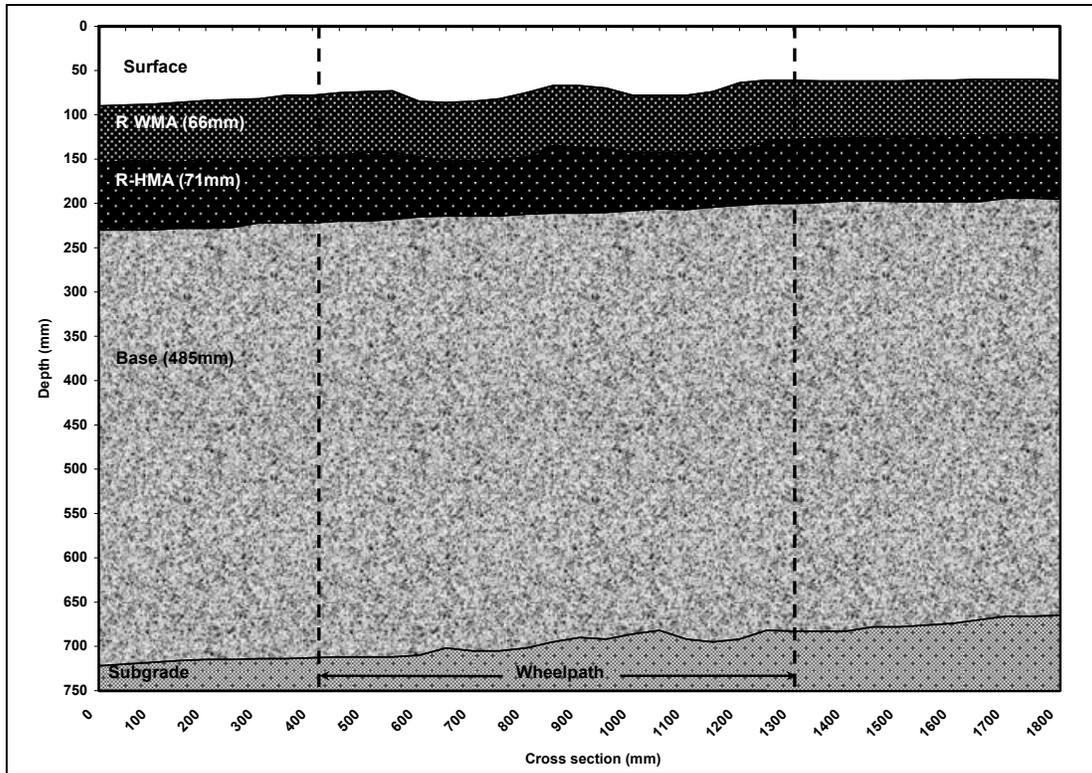
Figure B.7: 622HA: Evotherm test pit profile (after 200,000 load repetitions).
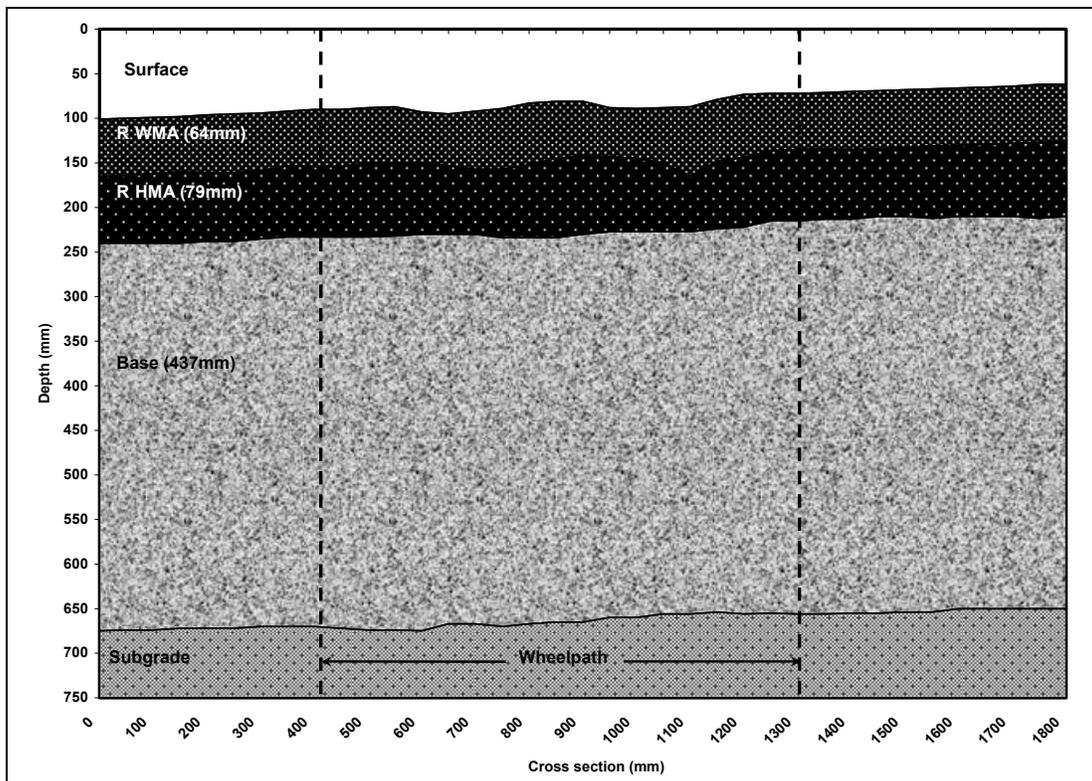
Figure B.8: 623HA: Cecabase test pit profile (after 224,000 load repetitions).

APPENDIX C: BEAM FATIGUE SOAKING PROCEDURE

C.1   Preparation of Specimens

Prepare the specimens as follows:

1. Measure and record the bulk specific gravity, width, and height of each beam.

2. Dry each beam is dried at room temperature (around 30°C) in a forced draft oven or in a concrete conditioning room to constant mass (defined as the mass at which further drying does not alter the mass by more than 0.05 percent at two-hour drying intervals). Record the final dry mass. Note: Place beams on a rigid and flat surface during drying.

3. Using epoxy resin, bond a nut to be used for supporting the LVDT to the beam. Record the mass of the beam with the nut.

C.2   Conditioning of Specimens

1. Place the beam in the vacuum container supported above the container bottom by a spacer. Fill the container with water so that the beam is totally submerged. Apply a vacuum of 635 mm (25 in.) of mercury for 30 minutes. Remove the vacuum and determine the saturated surface dry mass according to AASHTO T-166. Calculate the volume of absorbed water and determine the degree of saturation. If the saturation level is less than 70 percent, vacuum saturate the beam for a longer time and determine the saturated surface dry mass again.

2. Place the vacuum-saturated beam in a water bath with the water temperature pre-set at 60°C. The beam should be supported on a rigid, flat (steel or wood) plate to prevent deformation of the beam during conditioning. The top surface of the beam should be about 25 mm below the water surface.

3. After 24 hours, drain the water bath and refill it with cold tap water. Set the water bath temperature to 20°C. Wait for two hours for temperature equilibrium.

4. Remove the beam from the water bath, and determine its saturated surface dry mass.

5. Wrap the beam with Parafilm to ensure no water leakage.

6. Check the bonded nut. If it becomes loose, remove it and rebond it with epoxy resin.

7. Apply a layer of scotch tape to the areas where the beam contacts the clamps of the fatigue machine. This will prevent adhesion between the Parafilm and the clamps.

8. Start the fatigue test of the conditioned beam within 24 hours.

APPENDIX D: LABORATORY TEST RESULTS

D.1   Shear Test Results

Shear test results are summarized in Table D.1 through Table D.4.

D.2   Beam Fatigue Test Results

Beam fatigue test results are summarized in Table D.5.

D.3   Tensile Strength Retained Test Results

Tensile strength retained test results are summarized in Table D.6.

Table D.1: Summary of Shear Test Results for Control Mix

Specimen Designation	Air-Void Content (%)	Test Temp. (°C)	Test Shear Stress Level (kPa)	Initial Resilient Shear Modulus (kPa)	Percent Permanent Shear Strain at 5,000 Cycles	Cycles to 5% Permanent Shear Strain
G1-16-ST-7045	5.4	41.97	74.37	191.99	0.034445	29,386
G1-19-ST-7045	4.4	44.95	71.26	112.66	0.044573	8,465
G1-29-ST-7045	4.8	44.96	74.70	137.23	0.041492	12,824
G1-23-ST-10045	4.3	44.80	99.53	141.56	0.065968	2,304
G1-34-ST-10045	4.5	44.94	101.79	150.88	0.047113	6,482
G1-51-MT-10045	5.5	44.80	104.16	167.41	0.038856	15,140
G1-12-ST-13045	4.3	44.98	130.78	145.76	0.065331	1,995
G1-46-MT-13045	4.7	44.94	134.69	150.87	0.044655	7,527
G1-47-MT-13045	4.9	44.82	132.32	175.04	0.045206	7,262
G1-25-ST-7055	4.5	54.95	73.99	96.87	0.051323	4,558
G1-33-ST-7055	4.2	54.73	69.98	75.33	0.061190	2,440
G1-48-MT-7055	5.5	54.94	74.41	84.96	0.043692	8,614
G1-22-ST-10055	5.1	48.29	94.30	70.04	0.084843*	828
G1-49-MT-10055	4.9	54.59	97.29	85.63	0.069226	1,712
G1-50-MT-10055	5.5	55.05	101.10	92.67	0.067358	2,067
G1-15-ST-13055	4.5	55.43	124.98	73.82	0.157429*	414
G1-31-ST-13055	5.2	54.90	126.45	80.10	0.148309*	384
G1-52-MT-13055	4.8	54.94	124.80	69.69	0.128241*	455
*: Extrapolated results						

Table D.2: Summary of Shear Test Results for Gencor Mix

Specimen Designation	Air-Void Content (%)	Test Temp. (°C)	Test Shear Stress Level (kPa)	Initial Resilient Shear Modulus (kPa)	Percent Permanent Shear Strain at 5,000 Cycles	Cycles to 5% Permanent Shear Strain
G2-17-ST-7045	8.3	45.37	72.44	159.84	0.041769	10,906
G2-22-ST-7045	5.0	45.00	74.01	194.70	0.037447	27,723
G2-37-ST-7045	5.1	45.04	71.17	144.13	0.050822	4,632
G2-14-ST-10045	5.9	45.00	98.05	159.08	0.051678	4,212
G2-21-ST-10045	8.1	45.02	102.45	167.15	0.040777	11,401
G2-48-ST-10045	5.2	44.94	101.78	176.22	0.063027	2,199
G2-15-ST-13045	9.3	44.94	133.67	190.00	0.060155	2,498
G2-19-ST-13045	9.0	44.75	134.28	163.83	0.073473	1,488
G2-27-ST-13045	7.6	44.88	132.95	158.61	0.060855	2,640
G2-12-ST-7055	5.5	55.06	70.63	79.62	0.063320	2,112
G2-29-ST-7055	4.0	54.64	69.67	76.38	0.083635	860
G2-36-ST-7055	5.4	54.87	66.11	69.23	0.081743	1,106
G2-13-ST-10055	9.0	54.95	78.81	84.23	0.080246	1,110
G2-18-ST-10055	4.8	54.90	94.74	74.07	0.078200	1,359
G2-34-ST-10055	4.9	54.89	95.56	68.18	0.108993*	463
G2-16-ST-13055	5.0	54.97	128.37	78.92	0.135867*	316
G2-26-ST-13055	5.0	55.00	125.06	73.21	0.153997*	218
G2-33-ST-13055	4.6	54.54	129.26	85.16	0.128837*	318
*: Extrapolated results						

Table D.3: Summary of Shear Test Results for Evotherm Mix

Specimen Designation	Air-Void Content (%)	Test Temp. (C)	Test Shear Stress Level (kPa)	Initial Resilient Shear Modulus (kPa)	Percent Permanent Shear Strain at 5,000 Cycles	Cycles to 5% Permanent Shear Strain
G3-17-ST-7045	6.0	44.82	72.90	141.80	0.053803	3,536
G3-21-ST-7045	5.5	44.91	73.02	152.53	0.053297	3,905
G3-30-ST-7045	6.4	44.87	73.01	172.33	0.048798	5,657
G3-24-ST-10045	5.8	45.10	103.91	203.27	0.053267	3,718
G3-32-ST-10045	6.2	45.15	103.86	170.81	0.062158	2,516
G3-35-ST-10045	6.3	44.87	100.97	141.61	0.062525	2,212
G3-12-ST-13045	6.3	44.88	135.82	178.51	0.092844	1,072
G3-19-ST-13045	6.2	45.21	134.35	148.10	0.087085	955
G3-20-ST-13045	5.8	44.97	135.12	157.10	0.082564	1,152
G3-25-ST-7055	5.4	55.00	70.56	202.40	0.038043	10,727
G3-34-ST-7055	5.8	54.76	71.12	80.01	0.071155	1,367
G3-36-ST-7055	6.2	55.20	70.07	69.77	0.057152	2,996
G3-13-ST-10055	5.7	54.95	102.59	250.48	0.040067	10,079
G3-15-ST-10055	5.6	55.02	103.64	159.67	0.053620	3,949
G3-29-ST-10055	5.9	54.74	101.33	76.59	0.133879*	358
G3-31-ST-13055	5.9	54.90	129.36	72.30	0.116150*	354
G3-33-ST-13055	5.6	54.91	123.84	54.31	0.161348*	157
G3-37-ST-13055	5.7	54.98	132.82	90.17	0.146410*	656
*: Extrapolated results						

Table D.4: Summary of Shear Test Results for Cecabase Mix

Specimen Designation	Air-Void Content (%)	Test Temp. (C)	Test Shear Stress Level (kPa)	Initial Resilient Shear Modulus (kPa)	Percent Permanent Shear Strain at 5,000 Cycles	Cycles to 5% Permanent Shear Strain
G4-19-ST-7045	5.2	44.60	69.98	156.89	0.045850	6,937
G4-22-ST-7045	6.1	44.73	72.55	180.11	0.047605	6,202
G4-32-ST-7045	5.7	44.64	70.36	151.02	0.050567	4,738
G4-15-ST-10045	5.5	44.89	100.06	144.36	0.063009	1,651
G4-17-ST-10045	5.9	44.80	100.80	179.24	0.061758	2,203
G4-31-ST-10045	5.9	44.76	101.44	152.49	0.061130	2,461
G4-21-ST-13045	6.3	44.92	128.74	166.80	0.063638	1,709
G4-27-ST-13045	5.0	45.17	137.26	157.24	0.081656	631
G4-48-MT-13045	5.2	45.25	135.00	160.63	0.079591	1,137
G4-23-ST-7055	4.5	54.54	69.65	75.72	0.071848	1,043
G4-33-ST-7055	5.9	54.92	72.95	69.25	0.072313	854
G4-37-ST-7055	5.1	54.66	70.81	72.22	0.078510*	823
G4-16-ST-10055	5.4	55.10	93.21	71.07	0.087514	486
G4-25-ST-10055	6.9	54.97	96.08	79.87	0.094599	629
G4-50-MT-10055	5.4	54.92	93.43	69.39	0.092451	513
G4-12-ST-13055	4.7	55.05	127.74	80.95	0.135345*	201
G4-20-ST-13055	5.2	55.24	128.96	91.16	0.119414*	289
G4-36-ST-13055	5.8	54.91	128.65	59.92	0.133603*	383
*: Extrapolated results						

Table D.5: Summary of Beam Fatigue Test Results

Mix	Cond.	Specimen	Air-Void Content[1] (%)	Test Temp. (°C)	Test Strain Level (μstrain)	Initial Phase Angle (Deg.)	Initial Stiffness (MPa)	Fatigue Life (Nf)
Control	Dry	G1-04-B1	3.78	19.76	0.000204	25.11	5,822	29,121,863*
		G1-13-B2	4.63	19.77	0.000205	25.07	5,630	30,889,886*
		G1-14-B3	5.21	19.79	0.000206	24.67	5,421	31,263,809*
		G1-10-B3	4.13	19.92	0.000399	19.98	6,054	498,596
		G1-11-B3	3.90	19.81	0.000403	28.44	5,576	488,640
		G1-14-B2	5.67	20.19	0.000416	28.27	4,426	321,255
	Wet	G1-05-B2	3.71	20.08	0.000206	27.40	5,396	12,426,049*
		G1-09-B2	3.97	20.03	0.000207	25.58	5,573	17,263,849*
		G1-15-B2	5.26	20.03	0.000200	25.03	5,050	16,424,590*
		G1-05-B1	3.99	20.19	0.000402	28.27	5,003	175,550
		G1-09-B3	5.07	20.09	0.000401	26.07	5,110	108,681
		G1-13-B1	4.63	20.05	0.000398	26.72	4,736	180,723
Gencor	Dry	G2-04-B1	6.49	19.78	0.000205	25.41	5,225	30,364,428*
		G2-08-B1	6.72	19.77	0.000206	23.88	5,721	17,814,777*
		G2-09-B3	6.95	19.78	0.000205	20.33	6,842	7,119,470*
		G2-06-B2	7.42	19.81	0.000407	26.66	4,754	224,635
		G2-07-B1	6.40	19.88	0.000401	18.62	5,384	144,114
		G2-07-B2	7.17	19.78	0.000403	25.25	5,187	201,888
	Wet	G2-01-B3	7.21	21.11	0.000203	25.88	4,474	1,469,612*
		G2-02-B2	6.37	20.12	0.000208	26.31	4,556	3,810,683
		G2-12-B1	6.15	20.13	0.000208	25.16	4,615	4,342,136
		G2-02-B1	7.35	19.97	0.000416	27.73	3,804	54,805
		G2-03-B3	7.14	20.16	0.000411	26.00	3,969	29,691
		G2-12-B2	6.17	20.30	0.000405	27.03	4,198	24,123
Evotherm	Dry	G3-05-B2	5.87	20.38	0.000208	23.75	6,058	10,208,217*
		G3-07-B2	6.36	20.14	0.000206	22.91	6,084	10,792,051*
		G3-08-B1	6.09	19.98	0.000206	16.77	5,898	58,850,271*
		G3-07-B1	6.02	19.94	0.000405	17.68	5,863	73,863
		G3-08-B2	5.71	20.00	0.000406	19.66	5,599	330,563
		G3-09-B2	6.34	19.77	0.000403	24.99	5,425	108,871
	Wet	G3-03-B2	5.79	20.12	0.000208	24.95	5,177	12,092,693*
		G3-06-B2	7.15	19.13	0.000201	23.64	5,047	3,618,056
		G3-09-B1	5.70	19.98	0.000208	25.09	5,102	6,166,944*
		G3-01-B3	6.84	19.98	0.000417	21.36	6,090	35,922
		G3-02-B1	6.63	20.17	0.000408	21.97	5,737	43,294
		G3-03-B3	5.88	21.08	0.000400	22.33	5,848	57,832
Cecabase	Dry	G4-02-B3	7.13	21.06	0.000201	24.06	5,516	14,799,268*
		G4-03-B3	7.75	19.91	0.000204	17.88	5,356	52,120,468*
		G4-09-B1	6.38	20.33	0.000209	19.56	7,238	3,614,010
		G4-01-B1	7.72	20.16	0.000406	25.82	5,187	133,149
		G4-06-B2	7.21	21.12	0.000396	25.16	5,399	144,856
		G4-08-B2	6.24	21.23	0.000398	25.26	5,592	74,501
	Wet	G4-01-B2	7.02	20.01	0.000210	27.75	4,431	16,308,611*
		G4-07-B2	6.23	20.71	0.000202	28.42	4,732	12,705,336*
		G4-07-B3	6.37	20.17	0.000207	27.34	4,701	16,392,610*
		G4-05-B2	7.09	20.78	0.000402	23.88	5,167	64,692
		G4-07-B1	6.13	20.13	0.000405	25.09	5,235	148,694
		G4-08-B3	6.54	19.85	0.000422	25.96	4,991	50,026

* Extrapolated results   [1] Air-void content was measured with the CoreLok method.

Table D.6: Summary of Tensile Strength Retained Test Results

Mix	Condition	Specimen	Air-Void (%)	Strength (kPa)	Average Strength (kPa)	Std. Dev.	TSR (%)
Control	Dry	G1-54-T	5.65	961	1,017	47	77.2
		G1-58-T	5.36	1,016			
		G1-60-T	5.85	1,086			
		G1-63-T	4.46	1,014			
		G1-65-T	5.61	1,052			
		G1-68-T	4.95	974			
	Wet	G1-55-T	5.72	798	778	21	
		G1-53-T	5.60	786			
		G1-59-T	5.39	735			
		G1-61-T	5.14	781			
		G1-62-T	4.96	775			
		G1-67-T	5.67	788			
Gencor	Dry	G2-64-T	5.81	873	903	39	72.5
		G2-56-T	5.19	918			
		G2-58-T	5.30	968			
		G2-65-T	5.66	917			
		G2-63-T	6.11	876			
		G2-66-T	5.51	864			
	Wet	G2-53-T	5.05	708	658	25	
		G2-59-T	5.75	643			
		G2-67-T	5.63	641			
		G2-57-T	4.93	658			
		G2-55-T	5.18	647			
		G2-54-T	4.96	651			
Evotherm	Dry	G3-61-T	6.27	928	901	16	78.1
		G3-62-T	5.89	882			
		G3-55-T	6.35	893			
		G3-60-T	6.56	910			
		G3-57-T	5.83	894			
		G3-65-T	6.24	897			
	Wet	G3-53-T	7.01	748	728	104	
		G3-64-T	6.36	926			
		G3-54-T	6.04	631			
		G3-68-T	6.42	689			
		G3-56-T	5.68	669			
		G3-58-T	6.58	701			
Cecabase	Dry	G4-58-T	5.72	903	881	42	81.6
		G4-54-T	6.80	865			
		G4-65-T	6.71	842			
		G4-68-T	6.25	862			
		G4-57-T	6.17	855			
		G4-66-T	5.93	956			
	Wet	G4-60-T	6.11	713	712	40	
		G4-56-T	6.64	697			
		G4-65-T	5.84	774			
		G4-67-T	6.38	706			
		G4-55-T	6.96	651			
		G4-59-T	6.04	728			